Functional Determinants of Hepatocellular Organic Anion Transporters: Evolutionary Comparison and Domain Analysis of Two Paralogs

---

Dissertation

zur

Erlangung der naturwissenschaftlichen Doktorwürde (Dr. sc. nat.)

vorgelegt der

Mathematisch-naturwissenschaftlichen Fakultät

der

Universität Zürich

von

Anya Beate Hammann-Hänni

von

Wald BE

Promotionskomitee

Prof. Dr. Markus Grütter (Vorsitz)

Prof. Dr. Peter Meier-Abt (Leitung der Dissertation)

Prof. Dr. Raimund Dutzler

Zürich 2007

Table of contents

Abbreviations

ABC	ATP-binding cassette
ACE	angiotensin converting enzyme
APD-ajmalinium	*N*-(4,4-Azo-n-pentyl)-21-deoxy-ajmalinium
ATP	adenosine triphosphate
Bamet-R2	antitumoral compound *cis*-diamine-chloro-cholylglycinate-platinum(II)
Bamet-UD2	antitumoral compound *cis*-diamine-bisursodeoxycholate-platinum(II)
BBB	blood-brain barrier
BCA	bicinchoninic acid (protein assay)
blLPM	basolateral liver plasma membranes
BQ-123	endothelin-A receptor-selective antagonist, a cyclo [D-Trp-D-Asp-Pro-D-Val-Leu]
BSP	bromosulfophthalein
CHAPS	[3-(3-cholamidopropyl)-dimethylammonio]-1-propane sulfonate
CCK-8	cholecystokinin-octapeptide
CDCA	chenodeoxycholate
CHO	chinese hamster ovary (cell line)
CMC	Critical micelllear concentration
CNS	central nervous system
Cos-1	CV-1 origin, SV40, transformed African green monkey kidney fibroblast cell line
CRC 220	trivial name of 4-methoxy-2,3,6-trimethylphenylsulfonyl-L-aspartyl-D-amidinophenylalanine-piperidide
Cyclo A	cyclosporin A
DDM	n-dodecyl-β-D-maltopyranoside
DHEAS	dehydroepiandrosterone sulfate
DNP-SG	[S-(2,4-dinitrophenyl)-glutathione
DPDPE	[D-penicillamine^{2,5}]-enkephalin
$E_2$17βG	estradiol-17β-glucuronide
E3S	estrone-3-sulfate
FOS-16	FOS-choline-16
GCDCA	glycochenodeoxycholic acid
Gd-B20790	trivial name of gadolonium-18-((3-(2-carboxylbutyl)-2,4,6-triiodophenyl)amino)-3,6,9-tris(carboxymethyl)-11,18-dioxo-3,6,9,12-tetrazaoctadecanoic acid
GSH	(reduced) glutathione

GUDCA	glycoursodeoxycholic acid
HEK	human embryonic kidney (cell line)
HeLa	cancerous cervical cell line after Henrietta Lacks who donated the cells
HepG2	human hepatoma G2 (cell line)
HMG-CoA	hydroxy-3-methyl-glutaryl coenzyme A
LLCPK	Lewis lung carcinoma pig kidney (cell line)
LTC_4	leukotriene C4
MDCK	Madin-Darby canine kidney (epithelial cell line)
MDR	multidrug resistance protein
MFS	major facilitator superfamily
MOI	multiplicity of infection
MRP	multidrug resistance-associated protein
Na^+	sodium
Ntcp/NTCP	Na^+/taurocholate cotransporting polypeptide
OAT	organic anion transporter
Oatp/OATP	organic anion transporting polypeptide
OCT	organic cation transporter
OG	n-octyl-β-D-glucopyranoside
ORF	open reading frame
PBS	phosphate buffered saline
PEPT	peptide transporter
P-gp	P-glycoprotein
PGT	prostaglandin transporter
QSAR	quantitative structure-activity relationship
rT_3	reverse triiodothyronine
Sf9	*Spodoptera frugiperda* 9 (cell line)
SLC (O)	solute carrier (of Oatps/OATPs)
SN-38	trivial name of 7-ethyl-10-hydroxycamptothecin
T_3	triiodothyronine
T_4	thyroxine
TC	taurocholic acid
TCDCA	taurochenodeoxycholic acid
TMH	transmembrane α helix
TUDCA	tauroursodeoxycholic acid

Summary

Drug disposition profoundly affects pharmacological effects in tissues and hence therapeutic efficacy. Absorption, tissue distribution and elimination of drugs and other xenobiotics occur because cellular barriers in an organism are conquerable due to the presence of membrane transport proteins. Members of the Organic Anion Transporting Polypeptide superfamily (animals: Oatp/*Slco*, human: OATP/*SLCO*) represent membrane solute carrier proteins. They are responsible for the cellular entry of a wide range of endogenous and exogenous amphipathic organic compounds. Hence, they allow the passage of drugs across the cellular barriers. Oatps/OATPs are found not only in mammals, but also in a big variety of non-mammalian species, of which many are representatives of animal evolution. No proteins with significant homologies have been found in plants, yeast and bacteria. This suggests the emergence of an ancient Oatp protein in an early ancestor of the animal kingdom. The 36 human, rat and mouse Oatps/OATPs have been divided into six families, which are subdivided into subfamilies. The present study focuses on members of the OATP1 family, which is a subclass extensively investigated in the past.

Compared to other Oatps/OATPs, which are expressed in multiple tissues, OATP1 family members exhibit a more restricted expression pattern. The majority of the members of the OATP1 family are expressed in the liver, where they are presumably involved in the hepatic clearance of albumin-bound compounds from portal blood. With reference to the transport mechanism of Oatps/OATPs very little is known. It is generally believed that Oatps/OATPs act in a sodium-independent manner and are capable to mediate anion exchange. There are several studies reporting a pH-gradient dependent substrate transport. In terms of protein structure, only theoretical approaches have been under consideration. However, there are several conserved structural features which are believed to be important for transport function of Oatps/OATPs.

The Na^+/bile salt cotransporter Ntcp/NTCP is responsible for sodium-dependent hepatocellular uptake of bile salts. Its transport mechanism is well-described, in contrary to Oatps/OATPs.

The research presented with this PhD thesis includes evolutionary comparisons and identification of structural determinants of OATP1 family members. Three aims were persued: 1) The functional characterization of the evolutionarily ancient skate Oatp1d1 in terms of toxic cyclopeptide uptake compared to mammalian liver Oatps/OATPs, 2) the identification of distinct amino acids sequences and/or individual amino acid residues essential for Oatp1a4-mediated substrate recognition and/or transport and 3) a high-yield expression system for direct solubilization of the bile salt cotransporter rat Ntcp was established. After subsequent Ntcp reconstitution we aimed at proof of transport function.

In the first part of this work Oatp1d1, expressed in the liver of the little skate *Leucoraja erinacea*, was identified as an uptake system for oligopeptide toxins: high affinity uptake for phalloidin (Km ~2.2 μM) and low affinity microcystin uptake (Km ~27 μM) were determined. The alternative skate liver organic anion transporter, the dimeric Ostα/β, exhibited no phalloidin and only minor microcystin transport. Because the same toxins are also transported by liver specific Oatps/OATPs in rodents and human, the data support the notion that Oatp1d1 represents an evolutionarily ancient precursor of mammalian Oatps/OATPs. The closest mammalian OATP orthologue, the human brain and testis OATP1C1, did not show any phalloidin transport activity. Hence, Oatp1d1 can be closely associated with certain forms of toxic liver injury such as for example protein phosphatase inhibition by the water borne toxin microcystin.

In the second part two rat paralogs of 77% amino acids sequence identity, which are members of the well-characterized OATP1A subfamily, were investigated. Oatp1a4 is a high affinity digoxin transporter while Oatp1a1 does not transport digoxin. Transport studies with digoxin in combination with chimeric constructs between the two Oatps and point mutations were performed. Consequently, three amino acid residues were identified in Oatp1a4, which are essential for transport function. As substrates transported by both, Oatp1a4 and Oatp1a1, were affected as well by the three Oatp1a4 mutants described, the three amino acids mutated are suggested to be important for overall Oatp1a4-mediated transport. It remains unanswered whether these three amino acid residues are directly involved in substrate binding or whether they affect the 3D structure of the transport protein.

The results obtained in the last section are of interest for future isolation of a purified organic anion transport protein. In this third part the baculovirus/Sf9 cell-based high-yield expression system was used for rat Ntcp and Oatp1a1. Functional expression in Sf9 cells was proven for both transport proteins. Measured bile salt transport into membrane vesicles isolated from Ntcp-expressing Sf9 cells could associated with Ntcp. However, transport into membrane vesicles isolated from Oatp1a1-expressing Sf9 cells was not diffrent from transport into wildtype Sf9 membrane vesicles. The signal could not be associated with the presence of Oatp1a1. Therfore experiments were continued with the cotransporter Ntcp. Ntcp Sf9 membrane vesicles were used for successful solubilization of functional Ntcp. Prove of Ntcp function was given after reconstitution. Na^+/taurocholate cotransport with Ntcp in artificial liposomes could be determined. For isolation of purified Ntcp at a later date this system will enable analyses required to confirm the transport-competent conformation of Ntcp.

Taken together this work has identified: 1) Skate Oatp1d1, an evolutionarily ancient precursor of mammalian liver Oatps/OATPs, as a hepatocellular uptake system for the toxins phalloidin and microcystin. 2) Three amino acid residues of rat Oatp1a4, which are essential for over-all transport function, possibly, they are important for substrate recognition or for retaining the protein structure in a transport-competent form. And 3) we established an expression system suitable for direct solubilization and subsequent functional reconstitution of rat Ntcp.

Zusammenfassung

Pharmakologische Effekte im Gewebe und so die therapeutische Wirkung werden stark von der Arzneimittelverteilung beeinflusst. Absorption, Gewebeverteilung und Elimination von Arzneimitteln und anderen Xenobiotika finden statt, da Zellbarrieren in einem Organismus, dank vorhandenen Membrantransportproteinen, überwindbar sind. Mitglieder der Organische Anionen-Transport-Polypeptide (Tiere: Oatp/*Slco*; Mensch OATP/*SLCO*) vertreten Membrantransportproteine. Sie sind verantwortlich für die zelluläre Aufnahme zahlreicher endogener und exogener amphipathischer, organischer Verbindungen. Sie ermöglichen folglich die Passage von Azneimitteln durch die Zellbarrieren hindurch. Oatps/OATPs finden sich nicht nur in Säugetieren, sondern auch in einer grossen Auswahl von Nicht-Säugern, darunter auch manche Vertreter der Tierevolution. In Pflanzen, Hefen und Bakterien sind keine Proteine mit bedeutender Homologie gefunden worden. Dies lässt vermuten, dass die Entstehung eines in Bezug auf die Entwicklung alten Oatps in einem Vorfahre des Tierreiches liegt. Die 36 Menschen-, Ratten- und Maus-Oatps/OATPs sind in sechs Familien unterteilt, welche wiederum in Unterfamilien eingeteilt sind. Die gegenwärtige Untersuchung konzentriert sich auf Mitglieder der OATP1 Familie, eine Unterklasse, die in der Vergangenheit umfangreich untersucht worden ist.

Verglichen mit anderen Oatps/OATPs, die in verschiedenen Geweben exprimiert werden, weisen die Mitglieder der OATP1 Familie eine begrenzte Gewebeexpression auf. Die meisten Mitglieder der OATP1 Familie sind in der Leber exprimiert, wo sie vermutlich für die hepatische Clearance von albumin-gebundenen Verbindungen aus dem Portalblut verantwortlich sind. Über den Transportmechanismus der Oatps/OATPs ist sehr wenig bekannt. Grundsätzlich wird angenommen, dass Oatps/OATPs in natriumabhängiger Weise arbeiten, und dass sie Anionen-Austausch ermöglichen. Es gibt einige Untersuchungen, die von einer Abhängigkeit des Transportes vom pH-Gradienten berichten. In Bezug auf die Proteinstruktur stehen nur theoretische Ansätze zur Diskussion. Allerdings wird von einigen konservierten strukturellen Eigenschaften angenommen, dass sie für die Transporterfunktion von Oatps/OATPs wichtig sind.

Der Natrium/Gallensalz-Cotransporter Ntcp/NTCP ist verantwortlich für die hepatozelluläre Aufnahme von Gallensalzen. Dessen Transportmechanismus ist genau beschrieben, im Gegensatz zu den Oatps/OATPs.

Die mit dieser Dissertation vorgelegten Forschungsarbeit beinhaltet Evolutionsvergleiche und die Identifizierung von Strukturdeterminanten bei Mitgliedern der OATP1 Familie. Drei Hauptziele wurden verfolgt: 1) Die funktionelle Charakterisierung des in Bezug auf die Entwicklung alten Rochen-Oatp1d1 betreffend den Transport von toxischen Oligopeptiden, verglichen mit Säugetier Leber-Oatps/OATPs, 2) die Identifizierung von genau festgelegten Aminosäure Sequenzen und/oder einzelnen Aminosäuren, die für die Substraterkennung und/oder den Transport von Oatp1a4 unentbehrlich sind und 3) wurde ein *high-yield* Expressionssystem zur direkten Solubilisierung vom Gallensalz Cotransporter Ratten-Ntcp ermittelt. Nach anschliessender Ntcp-Rekonstitution wurde der Nachweis für die Transportfunktion erzielt.

Im ersten Teil dieser Arbeit wurde Oatp1d1 - exprimiert in der Leber des kleinen Rochen *Leucoraja erniacea* - als Aufnahmesystem für Oligopeptid-Toxine identifiziert: hoch-affiner Phalloidin-Transport (Km ~ 2.2 μM) und niedrig-affiner Microcystin-Transport (Km ~ 27μM) wurden nachgewiesen. Der alternative Rochenleber-Transporter für organische Anionen, der dimere Ostα/β, weist keinen Phalloidin und nur geringfügigen Microcystin Transport auf. Da dieselben Toxine ebenfalls von den leberspezifischen Oatps/OATPs in Nagern und Mensch transportiert werden, bestärken diese Resultate die Annahme, dass Oatp1d1 ein Evolutionsvorläufer der Säugetier-Oatps/OATPs ist. Der nächstverwandte Säugetier-OATP-Ortholog, der menschliche Hirn- und Testis- OATP1C1, wies keine Phalloidin-Transportaktivität auf. Oatp1d1 kann also mit einigen Formen der toxinvermittelten Leberschäden in Verbindung gebracht werden, wie zum Beispiel die durch Trinkwasser übertragen Protein-Phosphatase-Hemmung mittels Microcystin.

Im zweiten Teil wurden zwei Ratten-Paraloge mit 77% identischen Aminosäurensequenzen untersucht, welche Mitglieder der eingehend beschriebenen OATP1A Subfamile sind. Oatp1a4 ist ein hoch-affiner Digoxin Transporter, während Oatp1a1 kein Digoxin transportiert. Es wurden Transportstudien mit Digoxin in Kombination mit chimären Konstrukten zwischen den beiden Oatps und Punktmutationen durchgeführt. In Oatp1a4 wurden folglich drei Aminosäuren identifiziert, welche für die Transportfunktion unentbehrlich sind. Da Substrate, die

von beiden, Oatp1a4 und Oatp1a1, transportiert werden, ebenfalls von den drei beschriebenen Oatp1a4-Mutanten beeinflusst worden sind, können die mutierten Aminosäuren als wichtig für allumfassenden Oatp1a4 Transport gedeutet werden. Es bleibt unbeantwortet, ob die drei Aminosäuren direkt in die Substratbindung involviert sind, oder ob sie die 3D Struktur des Transportproteins beeinträchtigen.

Die Resultate des letzten Teils sind von Interesse für eine zukünftige Isolierung eines aufgereinigten Organische Anionen-Transporters. In diesem dritten Teil wurde das Baculovirus/Sf9 Zellen *high-yield* Expressionsystem für Ratten-Ntcp und Oatp1a1 angewendet. Für beide Transportproteine wurde funktionelle Expression in Sf9 Zellen nachgewiesen. Gallensalztransport in Membranvesikel, welche von Ntcp-exprimierenden Sf9 Zellen isoliert worden sind, konnte Ntcp zugewiesen werden. Transport in Membranvesikel, welche von Oatp1a1-exprimierenden Sf9 Zellen isoliert worden sind, war allerdings gleich wie Transport in wildtyp Sf9 Membranvesikeln. Das Signal konnte nicht Oatp1a1 zugeordnet werden. Daher wurden Experimente mit dem Cotransporter Ntcp weitergeführt. Ntcp Sf9 Membranevesikel wurden für eine erfolgreiche Solubilisierung von funktionellem Ntcp eingesetzt. Nach der Rekonstitution konnte Ntcp-Funktion nachgewiesen werden. In künstlichen Liposomen konnte Natrium/Taurocholat-Cotransport mit Ntcp bestimmt werden. Dieses System wird Untersuchungen ermöglichen, die für die Bestätigung der transportfähigen Konformation von Ntcp während einer späteren Isolierung von aufgereinigtem Ntcp nötig sind.

Zusammenfassend hat diese Arbeit folgendes nachgewiesen: 1) Rochen-Oatp1d1, ein Entwicklungsvorläufer von Säugetier Leber-Oatps/OATPs wurde als heptozelluläres Aufnahmesystem für die Toxine Phalloidin und Microcystin beschrieben. 2) Drei Aminosäuren des Ratten-Oatp1a4 wurden identifiziert, welche für die Transportfunktion unentbehrlich sind, die möglicherweise für Substraterkennung oder für die Beibehaltung der transportfähigen Proteinstruktur wichtig sind. Und 3) haben wir ein Expressionsystem ermittelt, das für die direkte Solubilisierung und anschliessende Rekonstitution von Ntcp geeignet ist.

CHAPTER 1

Introduction

1 Introduction

1.1 The role of membrane transport proteins in absorption, tissue-selective distribution and elimination of drugs and other xenobiotics

Absorption, tissue distribution and elimination of drugs and xenobiotics exposed to an organism can be resumed as drug disposition. Drug disposition profoundly affects pharmacological effects in tissues and hence therapeutic efficacy. After oral administration, drug disposition starts with absorption into the gut followed by the entry into blood-circulation via the portal system. The drug is carried through the hepatic portal vein into the liver. Besides being responsible for detoxification, the liver eliminates metabolites or unchanged compounds back into the blood circulation or via bile into feces. Besides the liver the kidney is the second important organ for elimination of drugs and other xenobiotics. Back in the blood circulation, the compound may be distributed into tissues and other organs, usually to differing extents, where it can exert its pharmacological effect.

The gastrointestinal tract, the liver, the kidney and the blood-brain-barrier (BBB) of the central nervous system provide efficient barriers to the permeability of various compounds. These cellular barriers are only conquerable due to the presence of membrane transport proteins. Comprehensive *in vivo* and *in vitro* studies demonstrate that membrane transport proteins are not only essential for the selective permeability of endogenous compounds, but are also determining factors regarding the exposure of an organism to drugs and other xenobiotics. The physicochemical properties (size, charge) and/or lipophilicity of a compound determine the molecular interaction with the membrane transport protein and therefore the extent of uptake.
Hence, tissue distribution of drugs is controlled by permeability as a result of membrane transport across the cellular barriers mentioned above. At the intestinal membrane absorption from the lumen into the portal bloodstream occurs, however the membrane transport proteins involved and their exact mode of transport are not well defined up to date. Conversely, there are other membrane transport proteins responsible for the efflux of xenobiotics from the gut epithelial cells back into the gastrointestinal lumen which can be limiting for drug absorption. The liver is reached with uptake transport proteins at the basolateral membrane of hepatocytes. There

compounds are extracted from the blood and are transported to the metabolizing enzymes for biotransformation. This first-pass metabolism is a determinant factor for bioavailability of drugs. Later elimination back into the blood circulation or into bile occurs with canalicular membrane transporters. In addition to the liver, the kidney is the second important organ for drug clearance. Several transport proteins have been identified in the renal proximal tubules, which allow the vectorial transport of drugs from the blood into to tubular lumen. Reabsorption of substances from the lumen back into the renal proximal tubular cells is also sometimes mediated by transporters, although many drugs are reabsorbed only by passive diffusion depending on a high drug concentration gradient across the renal brush border membrane [1, 2]. Central nervous system (CNS) penetration of drugs can be of vital importance when treating diseases such as meningitis, seizure disorders and psychiatric illnesses. On the other hand, drug transport across the BBB can be unfavorable if the drug causes adverse effects after reaching the central nervous system. In general, BBB penetration increases with increasing lipophilicity, although some transport proteins have been found to facilitate transport of many poorly lipophilic compounds across the BBB. BBB penetration of lipophilic drugs can also be unexpectedly poor as a result of drug transport efflux proteins found in this region [3].

Inter-individual expression levels of transport proteins can be a determinant factor for transport or efflux. Investigations have shown that certain drugs can induce expression levels of membrane transport proteins, as well as inhibit the absorption of other compounds as they interact with transport proteins at the molecular level [1, 4]. So a considerable number of transporter-based clinically important drug-drug interactions, associated with polymedication, and drug-food interactions have been documented [5]. Understanding of the possible implications of these interaction mechanisms and of the consequences of genetic variations should help to provide better and safer drug therapy. Accordingly, treatments involving drugs that are substrates of the respective transporters could be optimized and individualized.

Knowledge concerning drug transport across cell membranes [1, 4, 6, 7] makes it evident that there is great interest in having a more detailed understanding of the numerous membrane transport proteins at the molecular level. Moreover, malfunction of transport across cell membranes is known to cause disorders in different systems in an organism, emphasizing the importance of comprehending the working mechanisms behind these transport proteins. Therefore, investigations are essential not only in basic biomedical research, but also in the applied sciences of future therapeutic drug discovery and development using rational drug design. The molecular basis of substrate selectivity has to be investigated not only with human membrane transport proteins, but also with those found in rodents and other animals used in research and development of drugs. Understanding substrate-transport protein recognition and binding is a requirement for better assessment of transporter-mediated drug interaction, emphasizing the clinical relevance of transporter research.

Membrane transport proteins responsible for gastrointestinal, renal, hepatobiliary and CNS transport are members of two large protein families: the adenosine-triphosphate (ATP)-binding cassette (ABC) transporter superfamily and the solute carrier family of proteins. At present, there are 48 known ABC-transporters in humans, including the well-investigated P-glycoprotein (P-gp) and multidrug resistance-associated proteins (MRPs) [1, 8]. The solute carrier family includes the organic cation transporters (OCTs) [9], peptide transporters (PEPTs) [10], organic anion transporters (OATs) [11] and organic anion transporting polypeptides (OATPs), which will be the focus of this chapter, as well as further characterized in this thesis. These membrane transport proteins differ with respect to substrate specificity and mode of transport. However, they are all expressed in tissues relevant for disposition of drugs and other xenobiotics. Moreover, they transport not only exogenous, but also endogenous organic compounds such as bile salts and hormones. In terms of hepatobiliary transport, there is overlapping substrate specificity of OATPs (Na^+-independent hepatocellular uptake) with the sodium-taurocholate cotransporting polypeptide, NTCP, (Na^+-dependent hepatocellular uptake) for the bile salt taurocholate [12, 13]. Overlapping substrate specificity indicates a degree of coordination of transport of endogenous compounds between the membrane transporters NTCP and OATPs. NTCP will be discussed further at the end of this chapter.

1.2 The Organic Anion Transporting Polypeptide (OATP) superfamily

Organic anion transporting polypeptides of the OATP superfamily transmembrane solute carriers (denoted OATPs in human and Oatps in all other species; gene symbol = *SLCO/Slco* for solute carrier OATP) are responsible for transport of a wide spectrum of amphipathic substrates. In the early 90's, rat Oatp1a1 was identified by expression cloning as the first member of the OATP superfamily, and was shown to have properties of a sodium-independent organic anion transporter [14]. Subsequently, additional human and rodent members have been discovered. Using homology screening either by hybridization experiments or with *in silico* alignments, the availability of genome sequences accelerated the identification of Oatps/OATPs even more. To date the superfamily includes 36 human, rat and mouse Oatps/OATPs (Fig.1). Further Oatps have been identified in non-mammalian species such as chicken, zebra fish, little skate, frog, fruit fly and worm [15-17]. These species are representatives of animal evolution implying the presence of an ancestral Oatp. However, no proteins with significant homologies have been found in plants, yeast or in bacteria [16, 18].

A new species-independent classification system based on the divergent evolution system has been implemented to ease matters (HUGO gene nomenclature committee website, www.gene.ucl.ac.uk/nomenclature/) [15]. The overall amino acid sequence identity between all Oatp/OATP-related proteins varies between 24% and 97% [18, 19]. The whole OATP superfamily is classified into six families, which are subsequently divided into subfamilies. An individual family contains proteins with amino acid sequence identities of ≥ 40% and is indicated by different numbers (e.g. OATP**1**, OATP**2**, OATP**3**). Subfamilies contain proteins with amino acid sequence identities of ≥ 60% and are denoted by letters (e.g. OATP1**A**, OATP1**B**, OATP1**C**). Individual paralogs within a subfamily are indicated by different numbers applied after the nominated letter (e.g. Oatp1a**1**, OATP1A**2**), while the same end number is assigned to orthologs (e.g. OATP1C**1** and Oatp1c**1**) [15].

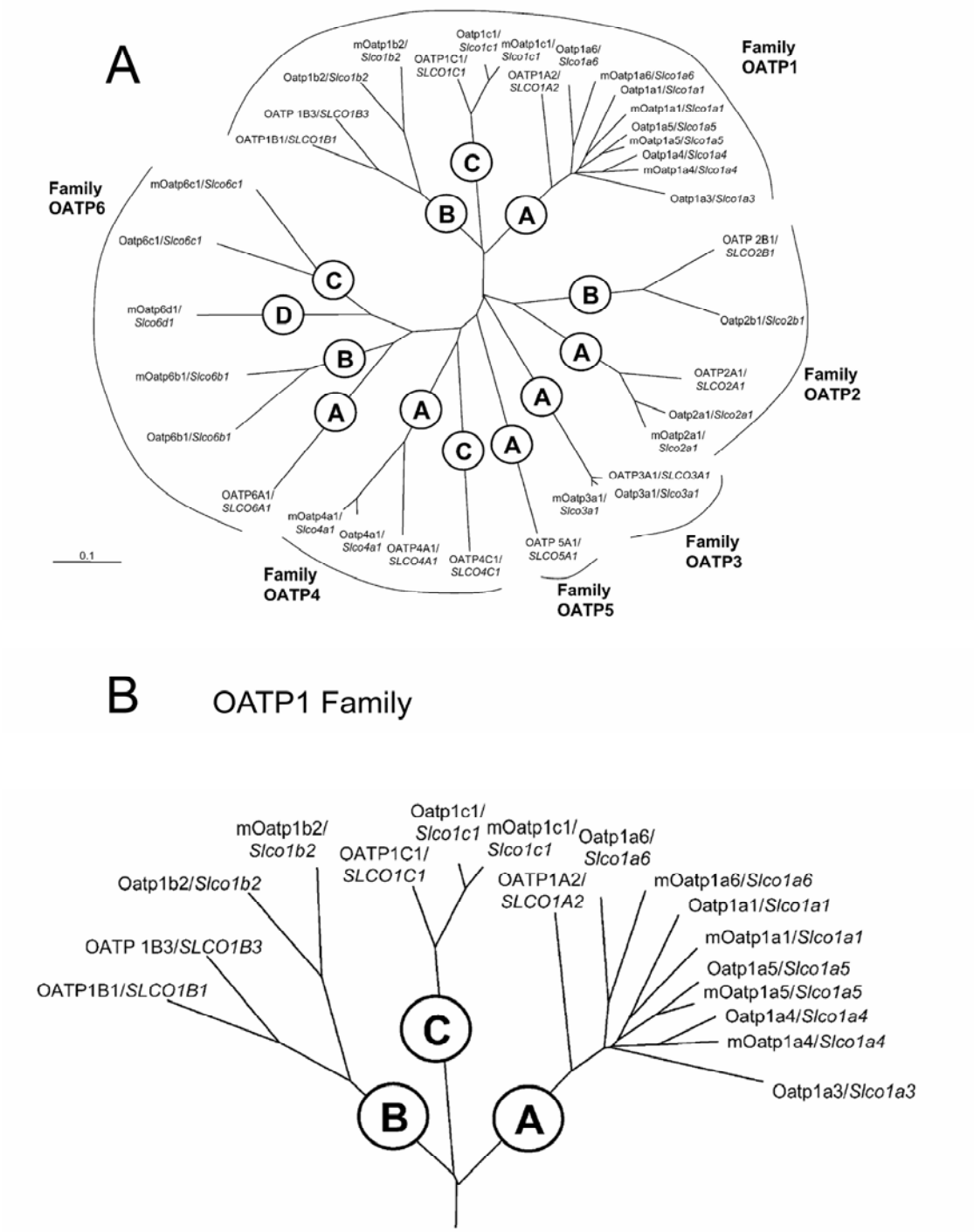

Fig. 1

Phylogenetic classification of the OATP superfamily I (A) Phylogenetic classification of human and rodent (rat, mouse) members of the OATP/SLCO superfamily. Families contain Oatps/OATPs with amino acid sequence identities of more than 40 %; subfamilies contain members with amino acid sequence identities of more than 60 %. (B) Enlargement of the evolutionary relationship among members of the OATP1 family. The tree was originally calculated using the clustalW program (http://www.ebi.ac.uk/clustalw/) and visualized with the program TREEVIEW [20].

Interestingly, there is a well-conserved stretch of 13 amino acids between human, rat and mouse Oatps/OATPs. This sequence has been proposed as a so-called “superfamily signature” by Hagenbuch and co-workers [18]. Moreover, conserved amino acids have been found within the OATP1 and the OATP2 family. Some of these residues are also conserved in several other multimember families; however, none of them were found to be fully conserved throughout the OATP/*SLCO* superfamily and no “family-specific” residues have been identified so far [16].

The evolutionary relationship among Oatps/OATPs is not completely characterized. In some families such as OATP3, there is a strict 1:1 relationship between proteins found in human, rat and mouse; this is not the case in other families. The subfamily OATP1A, for example, has only one human member but five rat members. OATP1B contains two human members but only one rat and one mouse member. Such inequalities are believed to be a result of gene duplication events after species divergence of human and rodents. Not surprisingly, the conservation level is much higher within the OATP3 family compared to that of OATP1. There are several independent analysis [16, 21, 22] suggesting an evolutionary relationship between Oatps/OATPs and the major facilitator superfamily (MFS), which underlie further studies leading to a first 3D model of two human OATPs [16]. This aspect will be addressed further later in this chapter.

Because many OATP families, including OATP1 and OATP2, have partially overlapping substrate specificities, some active residues are expected to be conserved across more than one family. Whether there are evolutionarily conserved structural determinants that account for overlapping substrate profiles is unknown. In order to bridge the knowledge about the evolutionary relationship and the known transport properties of individual Oatps/OATPs, comprehensive investigation is needed.

Not all Oatps/OATPs have been functionally well-characterized and very little is known about their transport mechanism(s). Moreover, the physiological role(s) of most Oatps/OATPs remains unclear and require further investigation. Although some members of the OATP superfamily are selectively expressed in the liver at the basolateral membrane of hepatocytes, most Oatps/OATPs are present in multiple tissues including BBB, choroid plexus, intestine, kidney, placenta, testis, lung and heart [18, 23].

The following sections will focus mainly on Oatps/OATPs of the OATP1 family, a subclass most often investigated from this superfamily, and on which a particular focus will be placed in this thesis. The current knowledge regarding functional characteristics, driving force, tissue distribution and structural properties will be discussed.

1.2.1 Functional characteristics of OATP1 family members

As mentioned before, it is well accepted that Oatps/OATPs represent sodium-independent bile salt and organic anion transporters [14, 24, 25]. Oatp1a1 was initially cloned as a sodium-independent bromosulfophthalein (BSP) and taurocholate uptake system in rat liver [14, 26]. Later, it could be shown that Oatp1a1 mediated transmembrane transport of a wide range of amphipathic organic compounds [27-29]. All OATP1A and OATP1B subfamily members show a very broad substrate spectrum, in contrast to the OATP1C subfamily with a rather narrow spectrum. However, a characteristic found throughout the OATP1 family is the overlapping substrate specificity. The amphipathic organic compounds include not only bile salts like taurocholate (TC), cholate, glycocholate, taurochenodeoxycholate (TCDCA) and tauroursodeoxycholate (TUDCA), but also steroid hormones and their conjugates like dehydroepiandrosterone (DHEAS), estrone-3-sulfate (E3S) and estradiol-17β-glucuronide ($E_2$17βG), the thyroid hormones thyroxine (T_4), triiodothyronine (T_3) and reverse triiodothyronine (rT_3), as well as eicosanoids like prostaglandins and leukotrienes.

In addition to endogenous substrates, members of the OATP1 family mediate uptake of numerous drugs such as the cardiac glycosides digoxin and ouabain, various 3-hydroxy-3-methyl-glutaryl coenzyme A (HMG-CoA) reductase inhibitors like pravastatin and rosuvastatin, the antibiotic benzylpenicillin, the angiotensin converting enzyme (ACE) inhibitors enalapril and temocaprilat, the chemotherapeutic agents methotrexate, the antihistamine fexofenadine, the thrombin inhibitor CRC220, the opioid receptor agonist [D-penicillamine^{2,5}]-enkephalin (DPDPE) and deltorphin II and even some organic cationic drugs, such as *N*-methyl quinine and *N*-methyl quinidine. Moreover, OATP1 family members transport toxins such as phalloidin (*Amanita phalloides*), microcystin (cyanobacteria) and ochratoxin A (mycotoxin). Table 1 summarizes the substrate specificities for individual rat and human OATP1 family members with the appropriate publications. Little is known about the mouse

OATP1 family members and their individual transport properties, so they have not been included.

Despite their multispecific character, selective compounds have been identified for some members of the OATP1 family. For example, gadoxetate and dinitrophenyl-glutathione (DNP-SG) are transported only by Oatp1a1, cholecystokinin-octapeptide (CCK-8), however, is taken up by OATP1B3 and Oatp1b2 and bilirubin plus bisglucuronosyl bilirubin are substrates found exclusively for OATP1B1. Differences in substrate transport have been documented with respect to apparent affinities, namely characterized by the Km value. OATP1C1 is an example of a high affinity T_4 and rT_3 transporter (Km 0.09 µM and 0.13 µM, respectively). A second example of high affinity transporter is Oatp1a4, which mediates digoxin transport (Km 0.24 µM), however the same carrier protein transports BQ-123 with an apparent affinity of approximately 600 µM.

Table 1
Substrate specificities of rat and human OATP1 family members, if available expressed with apparent affinity Km otherwise with ratios[1].

Oatp/OATP	Substrate	Km [μM]	Expression System	Ratio[1]	References
Oatp1a1	b[2]:				
	Taurocholate	19-50	Oocytes CHO cells		[14, 27, 28]
	Cholate	54	Oocytes CHO cells		[14, 28, 29]
	Glycocholate	54	Oocytes CHO cells		[28, 29]
	TUDCA	13	Oocytes		[29]
	TCDCA	7	Oocytes CHO cells		[28, 29]
	Sulfotaurolithocholate	6	Oocytes		[29]
	h[3]:				
	Aldosterone	0.015	Oocytes		[39]
	$E_2$17βG	3-20	Oocytes CHO cells Cos-7 cells		[28, 39-41]
	DHEAS	5	Oocytes CHO cells		[28, 29]
	E3S	5-12	Oocytes CHO cells		[28, 29]
	Cortisol	13	Oocytes		[39]
	T_4		Oocytes	22.7	[42]
	rT_3		Oocytes	21.3	[42]
	T_3		Oocytes	16.3	[42]
	e[4]:				
	LTC_4	0.27	Oocytes		[29, 30]
	p[5]:				
	CRC 220	30-57	Oocytes CHO cells		[28, 43]
	DPDPE	48	Oocytes		[44]
	Deltorphin II	137	Oocytes		[44]
	BQ-123	600	Oocytes		[29]
	GSH		HeLa cells	n.a.[9]	[45]
	d[6]:				
	Cerivastatin	6	HEK293 cells		[46]
	Pravastatin	30	HEK293 cells		[47]
	Rosuvastatin		HeLa cells	57.0	[48]
	Fexofenadine	32	HeLa cells		[49]
	Temocaprilat	47	Cos-7 cells		[40]
	Enalapril	214	HeLa cells		[50]
	Ouabain	1700-3000	Oocytes CHO cells		[28, 39]
	Gadoxetate	3300	Oocytes		[51]
	Dexamethasone		Oocytes	2.5	[39]
	Bamet-R2		CHO cells	6.0	[52]
	Bamet-UD2		CHO cells	6.0	[52]
	o[7]:				
	BSP	1-3	Oocytes CHO cells HeLa cells		[14, 27, 28, 33]
	DNP-SG	408	Oocytes		[29, 30]
	APD-ajmalinium		Oocytes	3.0	[53]
	N-methylquinidine		Oocytes	1.8	[54]
	Rocuronium		Oocytes	1.7	[54]
	Monoglucuronosyl bilirubin		Oocytes	2.7	[29]
	t[8] :				
	Ochratoxin A	17-29	Oocytes CHO cells		[28, 55]

Table 1 (continued)

Oatp/OATP	Substrate	Km [μM]	Expression System	Ratio	References
OATP1A2	b:				
	Taurocholate	60	Oocytes		[24, 56]
	Cholate	93	Oocytes		[24]
	TUDCA	19	Oocytes		[24, 53]
	TCDCA		Oocytes	9.3	[24]
	Glycocholate		Oocytes	2.8	[24]
	h:				
	DHEAS	7	Oocytes		[56]
	T_3	7	Oocytes		[56, 57]
	T_4	8	Oocytes		[56, 57]
	E3S	59	Oocytes		[53, 56, 58]
	$E_2$17βG		Oocytes	1.6	[56, 58, 59]
	rT_3		Oocytes	3.1	[57]
	e:				
	Prostaglandin E_2		Oocytes	4.3	[56]
	p:				
	DPDPE	202	Oocytes		[44, 56]
	Deltorphin II	330	Oocytes		[44, 56]
	BQ-123		Oocytes	3.7	[56]
	CRC 220		Oocytes	n.a.	[53]
	d:				
	Rosuvastatin	3	HeLa cells		[48]
	Fexofenadine	6	HeLa cells		[49]
	Saquinavir	36	HepG2 cells		[60]
	Unoprostone metabolite	93	Oocytes		[61]
	Methotrexate	457	Oocytes		[62]
	Ouabain	5500	Oocytes		[39, 56]
	Chlorambuciltaurocholate		Oocytes	3.2	[63]
	Bamet-R2		Oocytes	2.6	[52]
	Bamet-UD2		Oocytes	3.3	[52]
	o:				
	N-methylquinidine	5	Oocytes		[54]
	BSP	20	Oocytes		[24, 56]
	N-methylquinine	26	Oocytes		[54]
	Recuronium		Oocytes	1.6	[54]
	APD-ajmalinium		Oocytes	14.9	[39, 53, 54]
	Unconjugated bilirubin		Oocytes	1.4	[59]
	Gd-B20790		Oocytes	2.1	[64]
	t:				
	Microcystin-LR	20	Oocytes		[65]
Oatp1a3_v1	b:				
Oatp1a3_v2	Taurocholate	10 / 31	Oocytes		[66, 67]
			MDCK II cells		
	h:				
	DHEAS	8 / 8	MDCK II cells		[67]
	E3S	12 / 15	MDCK II cells		[67]
	T_4	20 / 12	MDCK II cells		[67]
	$E_2$17βG	35 / 45	MDCK II cells		[67]
	T_3	44 / 25	MDCK II cells		[67]
	e:				[66]
	Prostaglandin E_2		Oocytes	n.a. / 1.9	
	d:				
	Methotrexate	1-2	Oocytes		[66-69]
			MDCK II cells		
			LLCPK cells		
	Zidovudine	64 / 76	MDCK II cells		[67]
	o:				
	Folate		Oocytes	1.9	[66, 68]
	t:				
	Ochratoxin A	6 / 17	MDCK II cells		[67]

Table 1 (continued)

Oatp/OATP	Substrate	Km [μM]	Expression System	Ratio	References
Oatp1a4	b:				
	Taurocholate	35	Oocytes		[25, 70, 71]
	Cholate	46	Oocytes		[25]
	Glycocholate	40	Oocytes		[29]
	TUDCA	17	Oocytes		[29]
	TCDCA	12	Oocytes		[29]
	h:				
	$E_2$17βG	3	Oocytes		[25, 70]
	T_3	6	Oocytes		[71]
	T_4	7	Oocytes		[70, 71]
	E3S	11	Oocytes		[25, 70]
	DHEAS	17	Oocytes		[29, 70]
	p:				
	DPDPE	19	Oocytes		[44, 70]
	BQ-123	30	Oocytes		[29]
	Leu-Enkephalin		Oocytes	1.4	[70]
	d:				
	Digoxin	0.24	Oocytes		[25, 70]
	Atorvastatin	22	HEK293 cells		[72]
	Pravastatin	38	Oocytes		[73]
	Cerivastatin		HEK293 cells	n.a.	[46]
	Rosuvastatin		HeLa cells	26.0	[48]
	Biotin		Oocytes	1.7	[70]
	Ouabain	470	Oocytes		[25]
	Fexofenadine	6	HeLa cells		[49]
	o:				
	APD-ajmalinium		Oocytes	8.0	[54]
	Rocuronium		Oocytes	2.6	[54]
Oatp1a5	b:				
	Taurocholate	18-30	Oocytes COS-1 cells		[34, 71]
	Cholate	9	COS-1 cells		[34]
	Glycocholate	15	COS-1 cells		[34]
	GUDCA	5	COS-1 cells		[34]
	GCDCA	6	COS-1 cells		[34]
	Glycodeoxycholate	4	COS-1 cells		[34]
	Taurodeoxycholate	6	COS-1 cells		[34]
	TCDCA	7	COS-1 cells		[34]
	h:				
	T_4	5	Oocytes		[71]
	T_3	7	Oocytes		[71]
	$E_2$17βG	39	Oocytes		[74]
	DHEAS	162	Oocytes		[74]
	E3S	268	Oocytes		[74]
	e:				
	Prostaglandin E_2	35	Oocytes		[74]
	LTC_4		Oocytes	n.a.	[74]
	p:				
	DPDPE	137	Oocytes		[74]
	BQ-123	417	Oocytes		[74]
	d:				
	Ouabain	1600	Oocytes		[74]
	Fexofenadine	58	Oocytes HeLa cells	 n.a.	[75, 76]
	Digoxin		Oocytes	n.a.	[74]
	Rosuvastatin		HeLa cells	34.0	[48]
	o:				
	BSP	8	Oocytes		[74]
Oatp1a6	n.a.				

Table 1 (continued)

Oatp/OATP	Substrate	Km [μM]	Expression System	Ratio	References
OATP1B1	b:	10-34	Oocytes		[56, 71, 77-79]
	Taurocholate		HEK293 cells		
	Cholate	11	Oocytes		[56, 64]
	TUDC	7	HEK293 cells		[80]
	GUDC	5	HEK293 cells		[80]
	Glycocholate		Oocytes	3.8	[56]
	h:				
	T_3	3	Oocytes		[56, 78, 81]
	T_4	3	Oocytes		[56, 78]
	$E_2$17βG	8-10	Oocytes		[23, 56, 77-79, 82-84]
			HEK293 cells		
	E3S	0.23-45	Oocytes		[23, 56, 77, 78, 83, 85,
			HEK293 cells		86]
			CHO cells		
	DHEAS	22	Oocytes		[56, 77, 78, 81]
			HEK293 cells		
	e:				
	Prostaglandin E_2		Oocytes	4.7- 8.4	[23, 56, 78]
			HEK293 cells		
	LTE_4		Oocytes	1.5	[78]
	LTC_4		Oocytes	2.7-16.2	[56, 78]
	Thromboxane B_2		Oocytes	3.8	[78]
	p:				
	DPDPE		Oocytes	3.5	[56, 81]
	BQ-123		Oocytes	12.0	[56]
	d:				
	Valsartan	1	HEK293 cells		[87]
	Olmesartan	43	Oocytes		[88]
	Pitavastatin	3	HEK293 cells		[84]
	Rosuvastatin	4-9	Oocytes		[48, 89, 90]
			HeLa cells		
	Pravastatin	14-35	Oocytes		[47, 79]
			HEK293 cells		
	Cerivastatin		HEK293 cells	3.1	[84, 91]
			MDCK II cells	n.a.	
	Fluvastatin	1.4-3.5	CHO cells		[86, 92]
	Atorvastatin		HEK293 cells	4	[72]
	Rifampicin	13	Oocytes		[93]
	Bamet-R2	10	Oocytes		[52]
	Bamet-UD2	10	Oocytes		[52]
	Troglitazone sulphate		Oocytes	6.2	[85]
	Methotrexate		Oocytes	3.0	[81]
	Benzylpenicilin		HEK293 cells	n.a.	[23]
	SN-38		Oocytes	1.6	[83]
			HEK293 cells	n.a.	
	Caspofungin		HeLa cells	n.a.	[94]
	Bosentan		CHO cells	n.a.	[95]
	o:				[59]
	Unconjugated bilirubin	0.01	Oocytes		
	Monoglucurosyl bilirubin	0.1	HEK293 cells		[77]
	BSP	0.1-0.3	Oocytes		[56, 77]
			HEK203 cells		
	Bisglucuronosyl bilirubin				
		0.3	HEK293 cells		[77]
	Bilirubin	8.0	Oocytes	n.a.	[59, 77, 93]
			HEK293 cells		
	t:				
	Microcystin-LR	7	Oocytes		[65]
	Phalloidin	17-39	Oocytes		[96, 97]
			HEK293 cells		
	Arsenic		HEK293 cells	n.a.	[98]

Table 1 (continued)

Oatp/OATP	Substrate	Km [μM]	Expression System	Ratio	References
Oatp1b2	b:				
	Taurocholate	27	Oocytes		[99]
	h :				
	DHEAS	5	Oocytes		[74, 99]
	$E_2$17βG	32	Oocytes		[74, 99]
	E3S	37	Oocytes		[74, 99]
	T_3		Oocytes	1.9	[99]
	T_4		Oocytes	2.3	[99]
	e:				
	LTC_4	7	Oocytes		[74]
	Prostaglandin E_2	13	Oocytes		[74, 99]
	p:				
	BQ-123	14	Oocytes		[74]
	CCK-8	15	Oocytes		[100]
	DPDPE	22	Oocytes		[74]
	d:				
	Atorvastatin	7	HEK293 cells		[72]
	Rosuvastain		HeLa cells	39.5	[48]
	Pravastatin		MDCK II cells	n.a.	[101]
	Cerivastatin		HEK293	n.a.	[46]
	o:				
	BSP	1	Oocytes		[99]
	t :				
	Phalloidin	6	Oocytes		[96]
	Microcystin		Oocytes	2.3	[65]
OATP1B3	b:				
	Taurocholate	6-42	Oocytes		[36, 56, 81]
	Glycocholate	43	Oocytes	3.3	[36, 56]
	Cholate	42	Oocytes		[36]
	TUDC	16	HEK293 cells		[80]
	GUDC	25	HEK293 cells		[80]
	TDCA		Oocytes	1.9	[36]
	TCDCA		Oocytes	1.8	[36]
	h:				
	$E_2$17βG	5	Oocytes		[56, 77, 102]
			HEK293 cells	7.4	
	T_3	6	Oocytes		[56, 81]
	DHEAS		Oocytes	7.1	[56, 102]
			HEK293 cells	5.2	
	T_4		Oocytes	1.7	[56]
	E-3-S		Oocytes	2.3	[56]
	e:				
	LTC_4		Oocytes	2.3	[56, 102]
			HEK293 cells	2.3	
	p:				
	CCK-8	11	Oocytes		[56, 84, 100]
		4	HEK293 cells		
	GSH	4651	Oocytes		[36]
	Deltorphin II		Oocytes	1.4	[56]
	BQ-123		Oocytes	12.0	[56]
	DPDPE		Oocytes	10.3	[56]

Table 1 (continued)

Oatp/OATP	Substrate	Km [μM]	Expression System	Ratio	References
OATP1B3	d:				
(continued)	Telmisartan	1	HEK293 cells		[103]
	Olmesartan	72	Oocytes		[88]
	Rifampicin	2	Oocytes		[93, 104]
	Pitavastatin	3	HEK293 cells		[84]
	Paclitaxel	7	Oocytes		[105]
	Valsartan	18	HEK293 cells		[87]
	Methotrexate	25	Oocytes		[81]
	Rosuvastatin		HeLa cells	4.5	[48]
	Ouabain		Oocytes	5.9	[56]
	Digoxin		Oocytes	2.4	[56]
	Fexofenadine	108	HEK293 cells		[106, 107]
	Bosentan		CHO cells	n.a.	[95]
	o:				
	Unconjugated bilirubin	0. 039	Oocytes		[59]
	BSP	0.3-3	Oocytes		[56, 77, 102]
			HEK293 cells		
	Monoglucuronosyl bilirubin	0.5	HEK293 cells		[77]
	t:				
	Amanitin	4	MDCK II cells		[108]
	Phalloidin	8	Oocytes		[96]
	Microcystin-LR	9	Oocytes		[65]
Oatp1c1	h:				
	T_4	0.2	HEK293 cells		[109]
	$E_2$17βG	10	HEK293 cells		[109]
	E3S		HEK293 cells	1.7	[109]
	rT_3		HEK293 cells	19.7	[109]
	d:				
	Cerivastatin	1	HEK293 cells		[109]
	Pravastatin		HEK293 cells	1.6	[109]
	t:				
	Ochratoxin A		HEK293 cells	1.5	[109]
OATP1C1	h:				
	T_4	0.09	Oocytes		[110]
			CHO cells	10.8	
	rT_3	0.13	CHO cells		[110]
	T_3		CHO cells	1.7	[110]
	E3S		CHO cells	1.8	[110]
	$E_2$17βG		CHO cells	2.3	[110]
	o :				[110]
	BSP		Oocytes	2.1	
			CHO cells	2.3	

[1]Ratios correspond to uptake of Oatp/OATP cRNA injected oocytes or transfected cells devided by uptake in control oocytes or cells, respectively.

[2]b: bile salts, [3]h: hormones, [4]e: eicosanoids, [5]p: peptides, [6]d: drugs, [7]o: other organic ions, [8]t: toxins
[9]n.a.: not available

1.2.2 Driving force(s) investigated with OATP1 family members

In spite of the important and rapid advances made in understanding individual transport properties of members of the OATP1 family, the mechanisms involved in the functional regulation under normal and pathological circumstances, namely the driving force of these membrane transport proteins, are poorly understood. Oatp/OATP-mediated transport is agreed on at large to be independent of sodium, chloride and potassium gradients, membrane potential and ATP-levels and is generally believed to occur by electroneutral exchange, in which the cell uptake of organic anions is coupled to the efflux of anions such as HCO_3^-, GSH and/or glutathione-S-conjugates [14, 24, 25, 30-34].

Satlin and co-workers have suggested electroneutral and pH-dependent anion exchange studying Oatp1a1-mediated transport. Studies with HeLa cells expressing Oatp1a1 proposed HCO_3^- to be exported in exchange for taurocholate; uptake of this bile salt was accelerated by coupling an outwardly directed pH-gradient with extra cellular taurocholate-stimulated HCO_3^- extrusion, this in alkali-loaded cells [32]. The other solute GSH has been reported to function as an intracellular substrate for Oatp1a1 as well as for Oatp1a4. In oocytes expressing Oatp1a1, a 1:1 stoichiometric GSH/taurocholate exchange was shown [30]. Similar studies with Oatp1a4 could not prove Oatp1a4 as a GSH exchanger, but rather suggested Oatp1a4 as a primary export carrier. These observations indicate that an outwardly directed GSH electrochemical gradient can be described as a driving force only for Oatp1a1 [31].

Human OATPs that have thus far been examined for their ability to transport GSH are OATP2B1, OAT1B1 and OATP1B3 [35-37]. A recent study focused mainly on OATP1B1 and OATP1B3 and reported, amongst others, new findings regarding the transport mode [36]. OATP1B1 was found to behave similarly to what has been shown for Oatp1a1. In the studies of Briz et al OATP1B1 behaves as a GSH/organic anion exchanger and is involved in uptake processes. The published results concerning GSH transport by OATP1B3 are controversial. Ballatori and co-workers [35, 37] showed up to date with two studies that GSH is not required for transport activity, i.e. has no effect on uptake nor on efflux with OATP1B1 and OATP1B3. However, the group of Briz and co-workers [36] found that OATP1B3 appeared to accept GSH as a low affinity substrate. The notion was made that OATP1B3 mediates extrusion of organic anions by symporting with GSH. The most probable stoichiometry found for this cotransport of GSH and bile acids was 2:1. Consequently,

the transport mechanism of OATP1B1 and OATP1B3 were not described being the same, as it has been demonstrated for Oatp1a1 and Oatp1a4. GSH is synthesized in every mammalian cell and is essential for a multitude of biochemical processes. There are several members of the multidrug resistance-associated protein family of ABC transporters, which have also been found to be responsible for GSH transport, indicating a wide range of export mechanisms for endogenous GSH [35].

Further studies have focused on a pH-sensitivity reported to be responsible for functional regulation of Oatps/OATPs. Intracellular acidification in CHO and HepG2 cells affected glycocholate uptake mediated by Oatp1a1. It was concluded that low intracellular pH might modify the driving forces or that the protonation of the intracellular domain of the membrane protein might trigger the changes observed [38]. Taken together, the driving force(s) of Oatps/OATPs is far from being well understood. Nevertheless, the pH sensitivity of Oatps/OATPs appears to be an important factor that needs to be pursued further.

1.2.3 Tissue distribution of OATP1 family members

For some, but not all Oatps/OATPs, tissue distribution has been studied using different techniques (e.g. Northern and Western blots and immunohistochemistry). Consistent with their potential role in detoxification processes, Oatps/OATPs are present in various tissues such as the BBB, choroid plexus, intestine, liver, kidney, testis, placenta, lung and heart [15]. Members of the OATP1 family show a more restricted tissue expression pattern, compared to Oatps/OATPs from other families, which can be detected in almost every tissue that has been investigated [15]. This indicates that certain Oatps/OATPs have organ-specific functions, while others might be involved in house-keeping functions. Tissue distribution at protein level published so far for members of the OATP1 family is summarized in Table 2.

The subfamily OATP1A comprises 1 single human member, namely OATP1A2 (Fig. 1, Table 2). OATP1A2 was originally cloned from a human liver cDNA library, but its strongest expression is in the brain [24]. In addition, OATP1A2 could be localized in the kidney [111] and ciliary body epithelium of the eye [61]. Further studies showed expression in liver and colon cancer cells, as well as in a human hepatoma cell line [23, 47, 102]. OATP1A2 has 5 rat (i.e. Oatp1a1, Oatp1a3, Oatp1a4, Oatp1a5 and Oatp1a6) and 4 mouse (i.e. Oatp1a1, Oatp1a4, Oatp1a5 and Oatp1a6) homologues within the subfamily (Figure 2). Except for Oatp1a6, which so far seems to be an

orphan transporter, all members of the OATP1A-subfamily have been characterized thoroughly regarding their expression profile, as documented in Table 2.

The subfamily OATP1B has two human members OATP1B1 and OATP1B3, which share a similar expression pattern with the paralogue Oatp1b2 (Fig. 1, Table 2). OATP1B1 was cloned from human liver [23, 47, 78, 102]. Localization of OATP1B1 appears restricted to the basolateral plasma membrane of hepatocytes [23, 47, 78, 102]. Its apparent exclusive expression in human liver suggests that OATP1B1 plays a crucial role in the hepatic clearance of albumin-bound amphipathic organic compounds, including drugs. In addition, OATP1B3 was cloned from human liver [81, 102]. Under normal physiological conditions, OATP1B3 is predominantly expressed at the basolateral plasma membrane of hepatocytes [81, 102]. Even though OATP1B3 was first thought to be a selective liver carrier, expanded studies showed expression in various human cancer tissues, as well as in different tumor cell lines derived from gastric, colon, pancreas, gallbladder, lung and brain cancers [81]. The pathobiological significance of OATP1B3 present in human cancer tissues remains to be investigated. For the two human OATP1B subfamily members in rat the single orthologue Oatp1b2 has been identified. Oatp1b2 is mainly expressed in the liver [74], but also found in the ciliary body epithelium of the eye [61].

The subfamily OATP1C contains human OATP1C1, which has been isolated from a human brain library [110]. OATP1C1 differs from most other OATP superfamily members, because of its selective distribution in brain and testis. In testis, OATP1C1 localizes to sterogenic Leydig cells [110]. The rat orthologue Oatp1c1 has been isolated from a cDNA library enriched in mRNAs specific to the BBB [112].

Table 2
Tissue distribution of human and rat members of the OATP1 family determined at protein level by Western blotting and immunohistochemical analysis

Oatp/OATP	Length (amino acids)	Tissue distribution and cellular/subcellular Expression	References
Oatp1a1	670	Liver (bl[1]) Kidney (proximal tubules, ap[2]) Choroid plexus (ap)	[28, 29, 113-116]
OATP1A2	670	Liver (bl) Brain (frontal cortex) Eye (ciliary body)	[44, 53, 61]
Oatp1a3_v1 Oatp1a3_v2	669	Kidney (proximal tubules, bl)	[66, 68, 69]
Oatp1a4	661	Liver (bl) Brain (BBB) Choroid plexus (bl) Eye (ciliary body, retina)	[29, 44, 70, 115, 117]
Oatp1a5	670	Jejunum Choroid plexus	[34, 118]
Oatp1a6	670	n.a.[3]	
OATP1B1	691	Liver (bl)	[78, 102, 119]
Oatp1b2	687	Liver (bl) Eye (ciliary body)	[61, 74]
OATP1B3	702	Liver (bl) Cancer cell lines	[81, 102]
Oatp1c1	716	Brain	[112]
OATP1C1	712	Brain Eye (ciliary body) Testis (Leydig cells)	[61, 110]

[1] bl : basolateral
[2] ap: apical
[3] n.a.: not available

1.2.4 Structural properties of OATP1 family members

In order to understand drug transport and for design of drugs with optimized biodistribution and elimination, it is important to elucidate the structure of the substrate binding regions of the *SLCO* superfamily multispecific transporters. There is also a great interest from the biomedical perspective in comprehending how various substrates bind to these regions, whether more than one substrate can bind simultaneously and how substrate binding initiates the translocation process. Finally, these questions can only be solved by crystallization of ligand-transporter complexes, in combination with functional characterization of critical residue point mutations. Accordingly, many studies have contributed to certain knowledge about the structural properties of Oatps/OATPs which can be applied to OATP1 family members.

Members of the OATP superfamily identified so far consist of 643 (Oatp2A1) to 848 (OATP5A1) amino acids [18] with molecular masses of 60 to 90 kDa. Several conserved structural features are believed to be important for the transport function of Oatps/OATPs. These features include the number of transmembrane-spanning α helices (TMH), the large extra cellular region between TMH 9 and 10 and the so-called “superfamily signature” with the consensus sequence D-X-RW-(I,V)-GAWW-X-G-(F,L)-L [18] (Fig. 2B). According to hydropathy analysis, all Oatps/OATPs are thought to have 12 TMHs [18, 23, 24], with their C- and N-termini localized at the intracellular side (Fig. 2A). However, it has not yet been proven experimentally for any Oatp/OATP and very little is known about the arrangement of the TMHs relative to each other. The large extra cellular region features many conserved cysteines and resembles the zinc finger domains of DNA binding proteins [120]. Moreover, there are *N*-glycosylation sites in common among Oatps/OATPs in the extra cellular loop 2 and 5 (Fig.2A).[14]

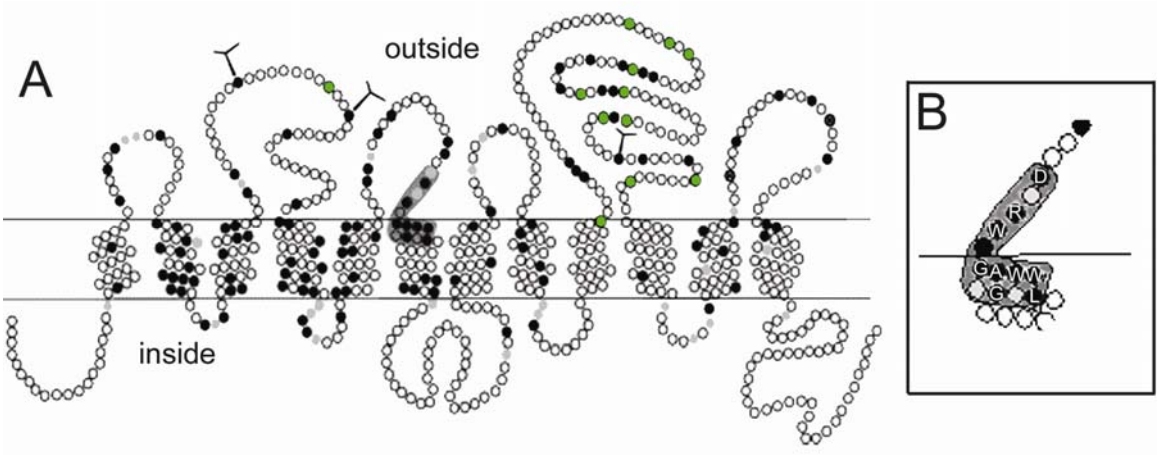

Fig. 2

Predicted 12 transmembrane helices model of rat Oatp1a1 (A) and enlargement of the OATP superfamily signature (B) I Within the theoretical Oatp1a1-model conserved amino acids are indicated in black. Conserved and charged amino acids are given in grey and conserved Cysteins are marked in green. Potential *N*-glycosilation sites (Y) are present on extra cellular loops (adapted from [18]).

Recent investigations aiming at the elucidation of the structure-function relationship of the cysteine-rich extra cellular loop yielded results with an OATP2 family member, which may also apply to Oatps/OATPs from the OATP1 family. Firstly, truncated OATP2B1 lacking this large extra cellular loop showed intracellular accumulation of the protein, indicating the importance of this loop for surface expression. The studies were extended by investigating the effects of mutations of 10 conserved extra cellular cysteines to alanines. It could be shown that the cysteines were necessary for targeting of OATP2B1 to the cell surface and that the majority of the 10 mutants impair transport function. Furthermore, all 10 extra cellular cysteines are likely to be involved in disulfide linkage. In conclusion, several indices exist that the cysteines are essential for a mature protein and therefore for proper cell surface expression [121].

The distant relationship of Oatps/OATPs with the major facilitator superfamily (MFS) of transport proteins, of which almost all members feature also 12 TMHs [22], underlies a study [16] in which bioinformatic tools helped to identify 2 MFS transport proteins with significant sequence structure homology to Oatps/OATPs. Both proteins feature a single substrate-binding site and operate by an alternating-access mechanism through a rocker-switch type of movement. They were initially used as templates for modeling a 3D model of two human OATPs. The results include a noteworthy theoretical model of an OATP1 family member, namely OATP1B3 (Fig. 3A), as well as of OATP2B1. Analysis of the conservation pattern identified the presence of a central pseudo twofold symmetry axis, perpendicular to the membrane plane, and a central pore that might be functionally significant. Measuring the electrostatic potential on the surface of the protein showed that the putative pore was positive. This is consistent with a pore that is exposed to the aqueous phase and binding and transporting negatively charged compounds. This conforms also to the anionic nature of the majority of Oatp/OATP substrates (Fig. 3B). Additionally, the pore was large enough to accommodate typical Oatp/OATP substrates. The lateral side of the model was shown to be neutral, as it is required for its interposition with the lipid bilayer.

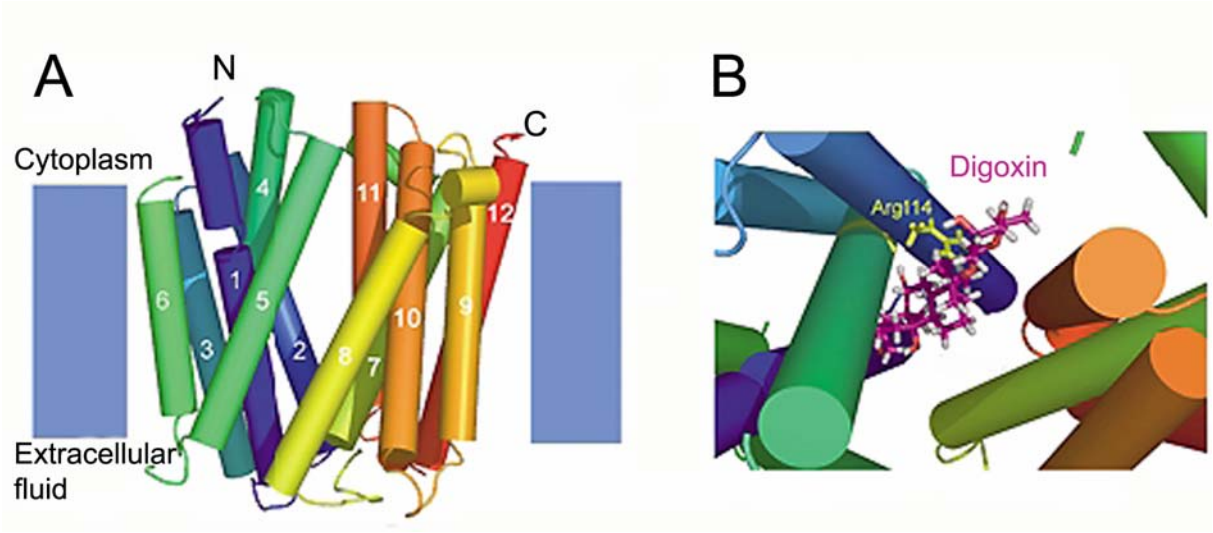

Fig. 3

Cartoon representation of the theoretical structural model of OATP1B3 I Transmembrane helices of the OATP1B3 structural model [16] are shown in colors. The approximate positions of the membrane bilayer and the N- and C- termini are indicated (A). OATP1B3 substrate digoxin (shown in cyan as stick model) was fitted into the pore, viewed from the intracellular side. The docking was performed by GOLD [122]. The figure was generated by PyMOL (www.pymol.org).

Other conserved features of Oatps/OATPs are the amino acids, which are preferentially in TMH 2 to 6, in the extra cellular loops 1, 3, 5 and in the intracellular loops 1, 2, 4 und 5 [18]. The study of Meier-Abt and co-workers [16] confirmed that the conserved amino acid residues within the OATP1 and OATP2 family may characterize their function. In the 3D models, they were predicted to be solvent-exposed and facing the pore, which would therefore be responsible for the positive potential of the pore, or they were predicted to play a key role in stabilizing the α helices. Surprisingly, a structure-based alignment of the large extra cellular region model showed no positive electrostatic potential. This indicates that this region is probably not involved in the attraction of the substrate to the transporters. It can be speculated that the large extra cellular region may cover the pore in the absence of a substrate, moving away upon substrate binding. While this *in silico* work is a theoretical study, it so far remains the most advanced investigation of structural properties of Oatps/OATPs.

Extended functional studies on OATP1B1 brought up an unexpected characteristic of the membrane transport protein. OATP1B1-mediated concentration dependent transport of estrone-3-sulfate was characterized by biphasic kinetics using

transfected HEK293 cells [123]. Confirmation was given by using a different expression system, *Xenopus laevis* oocytes. Km values were found for a high- and a low-affinity component of estrone-3-sulfate. Accordingly, the studies revealed that two functional sites were apparently involved on one single OATP transporter. Recent work could reassure this finding of multiple substrate binding for estrone-3-sulfate on OATP1B1 [86].

The broad substrate specificity of many Oatps/OATPs raises the question as to the common chemical and/or structural denominators of Oatp/OATP substrates. It can very well be that certain common features determine the molecular basis of the multispecificity of Oatps/OATPs. Two research groups worked with different approaches to generate pharmacophore models in order to understand the structural requirements of Oatps/OATPs. The group of Yarim et al based their model on knowledge concerning Oatp1a5 [124], which has a broad substrate specificity and is well investigated regarding transport properties. Apparent affinity (Km) values of Oatp1a5 substrates were used to perform 2D/3D-quantitative structure-activity relationships (QSAR) to yield a predictive description of global structural requirements for interaction between the substrates and Oatp1a5. The ligand-based approach was extrapolated for known Oatp/OATP substrates. This hypothetical pharmacophore model comprises the following topological information on the substrate binding site: firstly, a negatively charged group, secondly, a relatively extended hydrophobic region and thirdly, a hydrogen bond donor (Fig. 4).

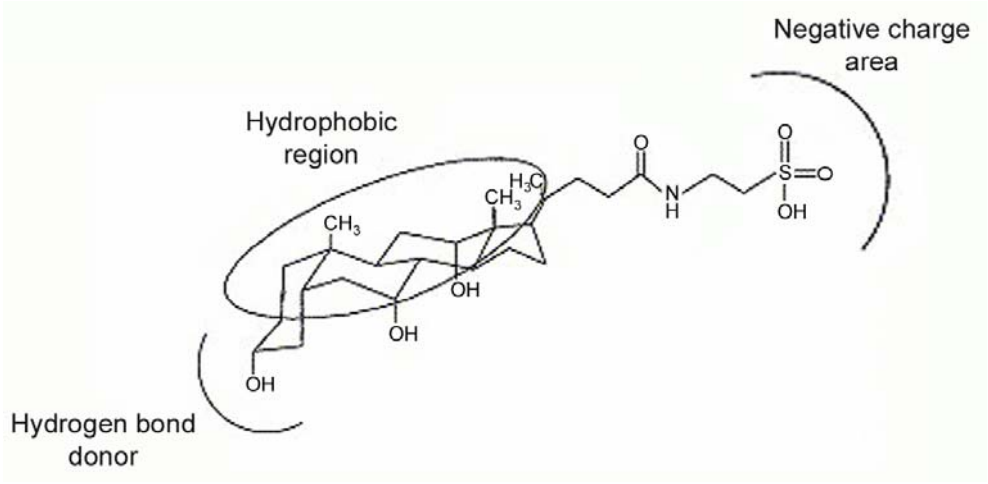

Fig. 4
Hypothetical pharmacophore features exemplified by taurocholate I (adapted from [124])

Within the second study aiming at the elucidation of the molecular mechanisms of multispecificity, Chang and co-workers performed a combination of pharmacophore building and meta-analysis [125]. The meta-analysis was based on literature data on two extensively studied OATP1 family members, rat Oatp1a1 and human OATP1B1. From these combined datasets a meta-pharmacophore was generated, speculating on the essential features responsible for recognition at the membrane transport protein and enabling transport across the plasma membrane. The pharmacophore models for Oatp1a1 and OATP1B1 consist of 2 hydrogen acceptors and 2 or 3 hydrophobic features. Both studies have one key feature of their generated pharmacophores in common, namely the hydrophobic bulky and relatively extended region. Additionally, Yarim et al found a negatively charged group. Considering hydrogen bond donors or acceptors, the two research groups remain in discordance.

Altogether, a reasonable amount of work has been achieved towards the elucidation of structure-function relationship of Oatps/OATPs. The knowledge regarding some important physiological roles stimulates ongoing investigation and will hopefully climax in the crystallization of an Oatp/OATP.

1.3 The bile acid transporter Na^+/taurocholate cotransporting polypeptide (Ntcp/NTCP)

As mentioned before, not only xenobiotics are transported into the liver but also many endogenous compounds important for intact liver physiology and metabolism. Endogenous compounds like conjugated and unconjugated bile acids are translocated across the basolateral membrane into hepatocytes. This uptake of bile acids is mediated mainly by sodium-dependent cotransport. In addition, several members of the OATP superfamily mediate sodium-independent bile acid/organic anion exchange. Bile acids are the predominant organic solutes in bile and are subject to the enterohepatic circulation. Bile formation itself is essential for normal intestinal and lipid digestions and absorption, cholesterol homeostasis and for hepatic excretion of lipid-soluble drugs, xenobiotics and heavy metals. Bile acids are thus found in a continuous flow which is restricted to hepatocytes, the biliary tree, the intestine and the portal blood [126]. Accordingly, the enterohepatic circulation is dependent on several transport systems, among which the two sodium-dependent bile acid cotransporters of the *SLC10* family play a crucial role. Na^+/taurocholate cotransporting polypeptide located at the basolateral membrane of hepatocytes is in charge of extracting bile acids efficiently from the portal blood for resecretion across the canalicular membrane into the bile. In parallel the apical sodium-dependent bile salt transporter (ASBT) expressed in ileocytes, actively removes bile acid from the intestinal lumen and allows their return to the liver via the portal circulation [13, 127].

1.3.1 Functional characteristics and expression pattern of Ntcp/NTCP

Ntcp/NTCP (animals: Ntcp; human: NTCP) belongs to the sodium bile salt cotransport family *SLC10*. Rat Ntcp was isolated first by expression cloning using the *Xenopus laevis* expression system [128]. Subsequently further orthologs were identified in human [129], mouse [130] and rabbit [131].

As pointed out, Ntcp/NTCP represents the predominant uptake system for conjugated and unconjugated bile acids in hepatocytes. Substrate specificity summarized in [12, 132] comprises cholate, taurocholate (Km 6-34μM), glycocholate (Km 27μM), taurochenodeoxy cholate (Km 5μM), taurodeoxycholate (Km 14μM) taurohydroxycholate (Km 7μM), tauromurocholate and the bile salt sulfate

chenodeoxycholate-3-sulfate. Non-bile salt substrates identified so far are estrone-3-sulfate (Km 27-60μM), DHEAS, BSP (Km ≤4μM) and drugs covalently bound to taurocholate (e.g. chlorambucil). Up to date no drug has been described being mediated by Ntcp. Overlapping substrate specificity with OATP1 family members also found at the basolateral membranes of hepatocytes is evident when comparing with substrates mentioned in Table 1.

The driving force for Ntcp/NTCP is provided by the inwardly directed electrochemical Na^+-gradient maintained by the basoateral Na^+/K^+-ATPase as well as the negative intracellular potential. Detailed analysis have revealed that transport is electrogenic with a Na^+: taurocholate stoichometry of at least 2:1 [133, 134].

More recently, expression of rat Ntcp was also detected in the luminal membranes of pancreatic acinar cells [135]. This is a counter evidence for Ntcp/NTCP representing a liver-specific expressed membrane transport polypeptide as assumed for a long time.

1.3.2 Structural properties of Ntcp/NTCP

Currently there is only limited information about the structural properties of Ntcp/NTCP as disclosed before also for Oatps/OATPs. Rat/mouse and human Ntcp/NTCP consist of 362 and 349 amino acids, respectively. They show an overall sequence identity of > 73% and 5 possible *N*-linked glycosilation sites have been suggested [128]. Molecular mass determinations of native rat Ntcp in isolated basolateral liver plasma membranes (blLPM) showed an apparent molecular mass of 51 ± 3 kD (mean ± SD). Deglycosilation experiments decreased the apparent molecular mass from 51 to 33.5 kD, which demonstrates that native Ntcp is extensively glycosilated in intact rat hepatocytes. This was suggested also because of a consistent broad band for Ntcp in blLPM with Western blot analysis [136].

The ligand-binding sites have not been localized and the exact transport mechanism remains unknown. Bioinformatic predictions and experimental evidence have shown that Ntcp/NTCP has an external N-terminus, an odd number of TMHs (7 or 9) and a cytoplasmic C-terminus [137, 138]. Ultimately, an approach such as X-ray crystallography will be required to determine topology.

1.4 References

1. Beringer, P.M. and R.L. Slaughter, *Transporters and their impact on drug disposition.* Ann Pharmacother, 2005. 39(6): p. 1097-108.
2. Lee, W. and R.B. Kim, *Transporters and renal drug elimination.* Annu Rev Pharmacol Toxicol, 2004. 44: p. 137-66.
3. Tamai, I. and A. Tsuji, *Transporter-mediated permeation of drugs across the blood-brain barrier.* J Pharm Sci, 2000. 89(11): p. 1371-88.
4. Ayrton, A. and P. Morgan, *Role of transport proteins in drug absorption, distribution and excretion.* Xenobiotica, 2001. 31(8-9): p. 469-97.
5. Zhang, L., et al., *Scientific perspectives on drug transporters and their role in drug interactionst.* Mol Pharm, 2006. 3(1): p. 62-9.
6. Kusuhara, H. and Y. Sugiyama, *Role of transporters in the tissue-selective distribution and elimination of drugs: transporters in the liver, small intestine, brain and kidney.* J Control Release, 2002. 78(1-3): p. 43-54.
7. Mizuno, N., et al., *Impact of drug transporter studies on drug discovery and development.* Pharmacol Rev, 2003. 55(3): p. 425-61.
8. Stefkova, J., R. Poledne, and J.A. Hubacek, *ATP-binding cassette (ABC) transporters in human metabolism and diseases.* Physiol Res, 2004. 53(3): p. 235-43.
9. Koepsell, H., *Organic cation transporters in intestine, kidney, liver, and brain.* Annu Rev Physiol, 1998. 60: p. 243-66.
10. Daniel, H. and G. Kottra, *The proton oligopeptide cotransporter family SLC15 in physiology and pharmacology.* Pflugers Arch, 2004. 447(5): p. 610-8.
11. You, G., *The role of organic ion transporters in drug disposition: an update.* Curr Drug Metab, 2004. 5(1): p. 55-62.
12. Geyer, J., T. Wilke, and E. Petzinger, *The solute carrier family SLC10: more than a family of bile acid transporters regarding function and phylogenetic relationships.* Naunyn Schmiedebergs Arch Pharmacol, 2006. 372(6): p. 413-31.
13. Hagenbuch, B. and P. Dawson, *The sodium bile salt cotransport family SLC10.* Pflugers Arch, 2004. 447(5): p. 566-70.
14. Jacquemin, E., et al., *Expression cloning of a rat liver Na(+)-independent organic anion transporter.* Proc Natl Acad Sci U S A, 1994. 91(1): p. 133-7.
15. Hagenbuch, B. and P.J. Meier, *Organic anion transporting polypeptides of the OATP/ SLC21 family: phylogenetic classification as OATP/ SLCO superfamily, new nomenclature and molecular/functional properties.* Pflugers Arch, 2004. 447(5): p. 653-65.
16. Meier-Abt, F., Y. Mokrab, and K. Mizuguchi, *Organic anion transporting polypeptides of the OATP/SLCO superfamily: identification of new members in nonmammalian species, comparative modeling and a potential transport mode.* J Membr Biol, 2005. 208(3): p. 213-27.
17. Cai, S.Y., et al., *An evolutionarily ancient Oatp: insights into conserved functional domains of these proteins.* Am J Physiol Gastrointest Liver Physiol, 2002. 282(4): p. G702-10.
18. Hagenbuch, B. and P.J. Meier, *The superfamily of organic anion transporting polypeptides.* Biochim Biophys Acta, 2003. 1609(1): p. 1-18.
19. Huber, R.D., et al., *Characterization of two splice variants of human organic anion transporting polypeptide 3A1 isolated from human brain.* Am J Physiol Cell Physiol, 2007. 292(2): p. C795-806.
20. Page, R.D., *TreeView: an application to display phylogenetic trees on personal computers.* Comput Appl Biosci, 1996. 12(4): p. 357-8.
21. Bateman, A., et al., *The Pfam protein families database.* Nucleic Acids Res, 2004. 32(Database issue): p. D138-41.
22. Chang, A.B., et al., *Phylogeny as a guide to structure and function of membrane transport proteins.* Mol Membr Biol, 2004. 21(3): p. 171-81.
23. Tamai, I., et al., *Molecular identification and characterization of novel members of the human organic anion transporter (OATP) family.* Biochem Biophys Res Commun, 2000. 273(1): p. 251-60.
24. Kullak-Ublick, G.A., et al., *Molecular and functional characterization of an organic anion transporting polypeptide cloned from human liver.* Gastroenterology, 1995. 109(4): p. 1274-82.
25. Noe, B., et al., *Isolation of a multispecific organic anion and cardiac glycoside transporter from rat brain.* Proc Natl Acad Sci U S A, 1997. 94(19): p. 10346-50.
26. Jacquemin, E., et al., *Expression of the hepatocellular chloride-dependent sulfobromophthalein uptake system in Xenopus laevis oocytes.* J Clin Invest, 1991. 88(6): p. 2146-9.

27. Kullak-Ublick, G.A., et al., *Functional characterization of the basolateral rat liver organic anion transporting polypeptide.* Hepatology, 1994. 20(2): p. 411-6.
28. Eckhardt, U., et al., *Polyspecific substrate uptake by the hepatic organic anion transporter Oatp1 in stably transfected CHO cells.* Am J Physiol, 1999. 276(4 Pt 1): p. G1037-42.
29. Reichel, C., et al., *Localization and function of the organic anion-transporting polypeptide Oatp2 in rat liver.* Gastroenterology, 1999. 117(3): p. 688-95.
30. Li, L., et al., *Identification of glutathione as a driving force and leukotriene C4 as a substrate for oatp1, the hepatic sinusoidal organic solute transporter.* J Biol Chem, 1998. 273(26): p. 16184-91.
31. Li, L., P.J. Meier, and N. Ballatori, *Oatp2 mediates bidirectional organic solute transport: a role for intracellular glutathione.* Mol Pharmacol, 2000. 58(2): p. 335-40.
32. Satlin, L.M., V. Amin, and A.W. Wolkoff, *Organic anion transporting polypeptide mediates organic anion/HCO3- exchange.* J Biol Chem, 1997. 272(42): p. 26340-5.
33. Shi, X., et al., *Stable inducible expression of a functional rat liver organic anion transport protein in HeLa cells.* J Biol Chem, 1995. 270(43): p. 25591-5.
34. Walters, H.C., et al., *Expression, transport properties, and chromosomal location of organic anion transporter subtype 3.* Am J Physiol Gastrointest Liver Physiol, 2000. 279(6): p. G1188-200.
35. Ballatori, N., et al., *Molecular mechanisms of reduced glutathione transport: role of the MRP/CFTR/ABCC and OATP/SLC21A families of membrane proteins.* Toxicol Appl Pharmacol, 2005. 204(3): p. 238-55.
36. Briz, O., et al., *Oatp8/1B3-mediated cotransport of bile acids and glutathione. An export pathway for organic anions from hepatocytes?* J Biol Chem, 2006.
37. Mahagita, C., et al., *Human organic anion transporter 1B1 and 1B3 function as bidirectional carriers and do not mediate GSH-bile acid cotransport.* Am J Physiol Gastrointest Liver Physiol, 2007. 293(1): p. G271-8.
38. Marin, J.J., et al., *Sensitivity of bile acid transport by organic anion-transporting polypeptides to intracellular pH.* Biochim Biophys Acta, 2003. 1611(1-2): p. 249-57.
39. Bossuyt, X., et al., *Polyspecific drug and steroid clearance by an organic anion transporter of mammalian liver.* J Pharmacol Exp Ther, 1996. 276(3): p. 891-6.
40. Ishizuka, H., et al., *Transport of temocaprilat into rat hepatocytes: role of organic anion transporting polypeptide.* J Pharmacol Exp Ther, 1998. 287(1): p. 37-42.
41. Kouzuki, H., et al., *Contribution of organic anion transporting polypeptide to uptake of its possible substrates into rat hepatocytes.* J Pharmacol Exp Ther, 1999. 288(2): p. 627-34.
42. Friesema, E.C., et al., *Identification of thyroid hormone transporters.* Biochem Biophys Res Commun, 1999. 254(2): p. 497-501.
43. Eckhardt, U., et al., *The peptide-based thrombin inhibitor CRC 220 is a new substrate of the basolateral rat liver organic anion-transporting polypeptide.* Hepatology, 1996. 24(2): p. 380-4.
44. Gao, B., et al., *Organic anion-transporting polypeptides mediate transport of opioid peptides across blood-brain barrier.* J Pharmacol Exp Ther, 2000. 294(1): p. 73-9.
45. Mittur, A., A.W. Wolkoff, and N. Kaplowitz, *The thiol sensitivity of glutathione transport in sidedness-sorted basolateral liver plasma membrane and in Oatp1-expressing HeLa cell membrane.* Mol Pharmacol, 2002. 61(2): p. 425-35.
46. Shitara, Y., et al., *In vitro and in vivo correlation of the inhibitory effect of cyclosporin A on the transporter-mediated hepatic uptake of cerivastatin in rats.* Drug Metab Dispos, 2004. 32(12): p. 1468-75.
47. Hsiang, B., et al., *A novel human hepatic organic anion transporting polypeptide (OATP2). Identification of a liver-specific human organic anion transporting polypeptide and identification of rat and human hydroxymethylglutaryl-CoA reductase inhibitor transporters.* J Biol Chem, 1999. 274(52): p. 37161-8.
48. Ho, R.H., et al., *Drug and bile acid transporters in rosuvastatin hepatic uptake: function, expression, and pharmacogenetics.* Gastroenterology, 2006. 130(6): p. 1793-806.
49. Cvetkovic, M., et al., *OATP and P-glycoprotein transporters mediate the cellular uptake and excretion of fexofenadine.* Drug Metab Dispos, 1999. 27(8): p. 866-71.
50. Pang, K.S., et al., *The modified dipeptide, enalapril, an angiotensin-converting enzyme inhibitor, is transported by the rat liver organic anion transport protein.* Hepatology, 1998. 28(5): p. 1341-6.
51. van Montfoort, J.E., et al., *Hepatic uptake of the magnetic resonance imaging contrast agent gadoxetate by the organic anion transporting polypeptide Oatp1.* J Pharmacol Exp Ther, 1999. 290(1): p. 153-7.
52. Briz, O., et al., *Carriers involved in targeting the cytostatic bile acid-cisplatin derivatives cis-diammine-chloro-cholylglycinate-platinum(II) and cis-diammine-bisursodeoxycholate-platinum(II) toward liver cells.* Mol Pharmacol, 2002. 61(4): p. 853-60.

53. Meier, P.J., et al., *Substrate specificity of sinusoidal bile acid and organic anion uptake systems in rat and human liver.* Hepatology, 1997. 26(6): p. 1667-77.
54. van Montfoort, J.E., et al., *Polyspecific organic anion transporting polypeptides mediate hepatic uptake of amphipathic type II organic cations.* J Pharmacol Exp Ther, 1999. 291(1): p. 147-52.
55. Kontaxi, M., et al., *Uptake of the mycotoxin ochratoxin A in liver cells occurs via the cloned organic anion transporting polypeptide.* J Pharmacol Exp Ther, 1996. 279(3): p. 1507-13.
56. Kullak-Ublick, G.A., et al., *Organic anion-transporting polypeptide B (OATP-B) and its functional comparison with three other OATPs of human liver.* Gastroenterology, 2001. 120(2): p. 525-33.
57. Fujiwara, K., et al., *Identification of thyroid hormone transporters in humans: different molecules are involved in a tissue-specific manner.* Endocrinology, 2001. 142(5): p. 2005-12.
58. Kullak-Ublick, G.A., et al., *Dehydroepiandrosterone sulfate (DHEAS): identification of a carrier protein in human liver and brain.* FEBS Lett, 1998. 424(3): p. 173-6.
59. Briz, O., et al., *Role of organic anion-transporting polypeptides, OATP-A, OATP-C and OATP-8, in the human placenta-maternal liver tandem excretory pathway for foetal bilirubin.* Biochem J, 2003. 371(Pt 3): p. 897-905.
60. Su, Y., X. Zhang, and P.J. Sinko, *Human organic anion-transporting polypeptide OATP-A (SLC21A3) acts in concert with P-glycoprotein and multidrug resistance protein 2 in the vectorial transport of Saquinavir in Hep G2 cells.* Mol Pharm, 2004. 1(1): p. 49-56.
61. Gao, B., et al., *Localization of organic anion transporting polypeptides in the rat and human ciliary body epithelium.* Exp Eye Res, 2005. 80(1): p. 61-72.
62. Badagnani, I., et al., *Interaction of methotrexate with organic-anion transporting polypeptide 1A2 and its genetic variants.* J Pharmacol Exp Ther, 2006. 318(2): p. 521-9.
63. Kullak-Ublick, G.A., et al., *Chlorambucil-taurocholate is transported by bile acid carriers expressed in human hepatocellular carcinomas.* Gastroenterology, 1997. 113(4): p. 1295-305.
64. Pascolo, L., et al., *Molecular mechanisms for the hepatic uptake of magnetic resonance imaging contrast agents.* Biochem Biophys Res Commun, 1999. 257(3): p. 746-52.
65. Fischer, W.J., et al., *Organic anion transporting polypeptides expressed in liver and brain mediate uptake of microcystin.* Toxicol Appl Pharmacol, 2005. 203(3): p. 257-63.
66. Masuda, S., et al., *Cloning and functional characterization of a new multispecific organic anion transporter, OAT-K2, in rat kidney.* Mol Pharmacol, 1999. 55(4): p. 743-52.
67. Takeuchi, A., et al., *Multispecific substrate recognition of kidney-specific organic anion transporters OAT-K1 and OAT-K2.* J Pharmacol Exp Ther, 2001. 299(1): p. 261-7.
68. Masuda, S., et al., *Functional analysis of rat renal organic anion transporter OAT-K1: bidirectional methotrexate transport in apical membrane.* FEBS Lett, 1999. 459(1): p. 128-32.
69. Saito, H., S. Masuda, and K. Inui, *Cloning and functional characterization of a novel rat organic anion transporter mediating basolateral uptake of methotrexate in the kidney.* J Biol Chem, 1996. 271(34): p. 20719-25.
70. Kakyo, M., et al., *Immunohistochemical distribution and functional characterization of an organic anion transporting polypeptide 2 (oatp2).* FEBS Lett, 1999. 445(2-3): p. 343-6.
71. Abe, T., et al., *Molecular characterization and tissue distribution of a new organic anion transporter subtype (oatp3) that transports thyroid hormones and taurocholate and comparison with oatp2.* J Biol Chem, 1998. 273(35): p. 22395-401.
72. Lau, Y.Y., et al., *Multiple transporters affect the disposition of atorvastatin and its two active hydroxy metabolites: application of in vitro and ex situ systems.* J Pharmacol Exp Ther, 2006. 316(2): p. 762-71.
73. Tokui, T., et al., *Pravastatin, an HMG-CoA reductase inhibitor, is transported by rat organic anion transporting polypeptide, oatp2.* Pharm Res, 1999. 16(6): p. 904-8.
74. Cattori, V., et al., *Localization of organic anion transporting polypeptide 4 (Oatp4) in rat liver and comparison of its substrate specificity with Oatp1, Oatp2 and Oatp3.* Pflugers Arch, 2001. 443(2): p. 188-95.
75. Kikuchi, A., et al., *Transporter-mediated intestinal absorption of fexofenadine in rats.* Drug Metab Pharmacokinet, 2006. 21(4): p. 308-14.
76. Dresser, G.K., et al., *Fruit juices inhibit organic anion transporting polypeptide-mediated drug uptake to decrease the oral availability of fexofenadine.* Clin Pharmacol Ther, 2002. 71(1): p. 11-20.
77. Cui, Y., et al., *Hepatic uptake of bilirubin and its conjugates by the human organic anion transporter SLC21A6.* J Biol Chem, 2001. 276(13): p. 9626-30.
78. Abe, T., et al., *Identification of a novel gene family encoding human liver-specific organic anion transporter LST-1.* J Biol Chem, 1999. 274(24): p. 17159-63.
79. Nakai, D., et al., *Human liver-specific organic anion transporter, LST-1, mediates uptake of pravastatin by human hepatocytes.* J Pharmacol Exp Ther, 2001. 297(3): p. 861-7.

80. Maeda, K., et al., *Uptake of ursodeoxycholate and its conjugates by human hepatocytes: role of Na(+)-taurocholate cotransporting polypeptide (NTCP), organic anion transporting polypeptide (OATP) 1B1 (OATP-C), and oatp1B3 (OATP8).* Mol Pharm, 2006. 3(1): p. 70-7.
81. Abe, T., et al., *LST-2, a human liver-specific organic anion transporter, determines methotrexate sensitivity in gastrointestinal cancers.* Gastroenterology, 2001. 120(7): p. 1689-99.
82. Campbell, S.D., S.M. de Morais, and J.J. Xu, *Inhibition of human organic anion transporting polypeptide OATP 1B1 as a mechanism of drug-induced hyperbilirubinemia.* Chem Biol Interact, 2004. 150(2): p. 179-87.
83. Nozawa, T., et al., *Role of organic anion transporter OATP1B1 (OATP-C) in hepatic uptake of irinotecan and its active metabolite, 7-ethyl-10-hydroxycamptothecin: in vitro evidence and effect of single nucleotide polymorphisms.* Drug Metab Dispos, 2005. 33(3): p. 434-9.
84. Hirano, M., et al., *Contribution of OATP2 (OATP1B1) and OATP8 (OATP1B3) to the hepatic uptake of pitavastatin in humans.* J Pharmacol Exp Ther, 2004. 311(1): p. 139-46.
85. Nozawa, T., et al., *Involvement of organic anion transporting polypeptides in the transport of troglitazone sulfate: implications for understanding troglitazone hepatotoxicity.* Drug Metab Dispos, 2004. 32(3): p. 291-4.
86. Noe, J., et al., *Substrate-Dependent Drug-Drug Interactions between Gemfibrozil, Fluvastatin and Other Organic Anion-Transporting Peptide (OATP) Substrates on OATP1B1, OATP2B1, and OATP1B3.* Drug Metab Dispos, 2007. 35(8): p. 1308-14.
87. Yamashiro, W., et al., *Involvement of transporters in the hepatic uptake and biliary excretion of valsartan, a selective antagonist of the angiotensin II AT1-receptor, in humans.* Drug Metab Dispos, 2006. 34(7): p. 1247-54.
88. Nakagomi-Hagihara, R., et al., *OATP1B1, OATP1B3, and mrp2 are involved in hepatobiliary transport of olmesartan, a novel angiotensin II blocker.* Drug Metab Dispos, 2006. 34(5): p. 862-9.
89. Simonson, S.G., et al., *Rosuvastatin pharmacokinetics in heart transplant recipients administered an antirejection regimen including cyclosporine.* Clin Pharmacol Ther, 2004. 76(2): p. 167-77.
90. Schneck, D.W., et al., *The effect of gemfibrozil on the pharmacokinetics of rosuvastatin.* Clin Pharmacol Ther, 2004. 75(5): p. 455-63.
91. Shitara, Y., H. Sato, and Y. Sugiyama, *Evaluation of drug-drug interaction in the hepatobiliary and renal transport of drugs.* Annu Rev Pharmacol Toxicol, 2005. 45: p. 689-723.
92. Kopplow, K., et al., *Human hepatobiliary transport of organic anions analyzed by quadruple-transfected cells.* Mol Pharmacol, 2005. 68(4): p. 1031-8.
93. Vavricka, S.R., et al., *Interactions of rifamycin SV and rifampicin with organic anion uptake systems of human liver.* Hepatology, 2002. 36(1): p. 164-72.
94. Sandhu, P., et al., *Hepatic uptake of the novel antifungal agent caspofungin.* Drug Metab Dispos, 2005. 33(5): p. 676-82.
95. van Giersbergen, P.L., et al., *Inhibitory and inductive effects of rifampin on the pharmacokinetics of bosentan in healthy subjects.* Clin Pharmacol Ther, 2007. 81(3): p. 414-9.
96. Meier-Abt, F., H. Faulstich, and B. Hagenbuch, *Identification of phalloidin uptake systems of rat and human liver.* Biochim Biophys Acta, 2004. 1664(1): p. 64-9.
97. Fehrenbach, T., et al., *Characterization of the transport of the bicyclic peptide phalloidin by human hepatic transport proteins.* Naunyn Schmiedebergs Arch Pharmacol, 2003. 368(5): p. 415-20.
98. Lu, W.J., et al., *Organic anion transporting polypeptide-C mediates arsenic uptake in HEK-293 cells.* J Biomed Sci, 2006. 13(4): p. 525-33.
99. Cattori, V., et al., *Identification of organic anion transporting polypeptide 4 (Oatp4) as a major full-length isoform of the liver-specific transporter-1 (rlst-1) in rat liver.* FEBS Lett, 2000. 474(2-3): p. 242-5.
100. Ismair, M.G., et al., *Hepatic uptake of cholecystokinin octapeptide by organic anion-transporting polypeptides OATP4 and OATP8 of rat and human liver.* Gastroenterology, 2001. 121(5): p. 1185-90.
101. Sasaki, M., et al., *Prediction of in vivo biliary clearance from the in vitro transcellular transport of organic anions across a double-transfected Madin-Darby canine kidney II monolayer expressing both rat organic anion transporting polypeptide 4 and multidrug resistance associated protein 2.* Mol Pharmacol, 2004. 66(3): p. 450-9.
102. Konig, J., et al., *Localization and genomic organization of a new hepatocellular organic anion transporting polypeptide.* J Biol Chem, 2000. 275(30): p. 23161-8.
103. Ishiguro, N., et al., *Predominant contribution of OATP1B3 to the hepatic uptake of telmisartan, an angiotensin II receptor antagonist, in humans.* Drug Metab Dispos, 2006. 34(7): p. 1109-15.

104. Tirona, R.G., et al., *Human organic anion transporting polypeptide-C (SLC21A6) is a major determinant of rifampin-mediated pregnane X receptor activation.* J Pharmacol Exp Ther, 2003. 304(1): p. 223-8.
105. Smith, N.F., et al., *Identification of OATP1B3 as a high-affinity hepatocellular transporter of paclitaxel.* Cancer Biol Ther, 2005. 4(8): p. 815-8.
106. Niemi, M., et al., *Fexofenadine pharmacokinetics are associated with a polymorphism of the SLCO1B1 gene (encoding OATP1B1).* Br J Clin Pharmacol, 2005. 59(5): p. 602-4.
107. Shimizu, M., et al., *Contribution of OATP (organic anion-transporting polypeptide) family transporters to the hepatic uptake of fexofenadine in humans.* Drug Metab Dispos, 2005. 33(10): p. 1477-81.
108. Letschert, K., et al., *Molecular characterization and inhibition of amanitin uptake into human hepatocytes.* Toxicol Sci, 2006. 91(1): p. 140-9.
109. Sugiyama, D., et al., *Functional characterization of rat brain-specific organic anion transporter (Oatp14) at the blood-brain barrier: high affinity transporter for thyroxine.* J Biol Chem, 2003. 278(44): p. 43489-95.
110. Pizzagalli, F., et al., *Identification of a novel human organic anion transporting polypeptide as a high affinity thyroxine transporter.* Mol Endocrinol, 2002. 16(10): p. 2283-96.
111. Sekine, T., H. Miyazaki, and H. Endou, *Molecular physiology of renal organic anion transporters.* Am J Physiol Renal Physiol, 2006. 290(2): p. F251-61.
112. Li, J.Y., R.J. Boado, and W.M. Pardridge, *Blood-brain barrier genomics.* J Cereb Blood Flow Metab, 2001. 21(1): p. 61-8.
113. Angeletti, R.H., et al., *Dichotomous development of the organic anion transport protein in liver and choroid plexus.* Am J Physiol, 1998. 275(3 Pt 1): p. C882-7.
114. Angeletti, R.H., et al., *The choroid plexus epithelium is the site of the organic anion transport protein in the brain.* Proc Natl Acad Sci U S A, 1997. 94(1): p. 283-6.
115. Gao, B., et al., *Localization of the organic anion transporting polypeptide 2 (Oatp2) in capillary endothelium and choroid plexus epithelium of rat brain.* J Histochem Cytochem, 1999. 47(10): p. 1255-64.
116. Bergwerk, A.J., et al., *Immunologic distribution of an organic anion transport protein in rat liver and kidney.* Am J Physiol, 1996. 271(2 Pt 1): p. G231-8.
117. Gao, B., et al., *Localization of organic anion transport protein 2 in the apical region of rat retinal pigment epithelium.* Invest Ophthalmol Vis Sci, 2002. 43(2): p. 510-4.
118. Ohtsuki, S., et al., *In vitro study of the functional expression of organic anion transporting polypeptide 3 at rat choroid plexus epithelial cells and its involvement in the cerebrospinal fluid-to-blood transport of estrone-3-sulfate.* Mol Pharmacol, 2003. 63(3): p. 532-7.
119. Keppler, D., J. Konig, and Y. Cui, *The human hepatocyte-specific organic anion transporter encoded by the SLC21A8 gene.* Gastroenterology, 2002. 122(5): p. 1545-6; author reply 1546.
120. Hakes, D.J. and R. Berezney, *Molecular cloning of matrin F/G: A DNA binding protein of the nuclear matrix that contains putative zinc finger motifs.* Proc Natl Acad Sci U S A, 1991. 88(14): p. 6186-90.
121. Hanggi, E., et al., *Functional analysis of the extracellular cysteine residues in the human organic anion transporting polypeptide, OATP2B1.* Mol Pharmacol, 2006. 70(3): p. 806-17.
122. Verdonk, M.L., et al., *Improved protein-ligand docking using GOLD.* Proteins, 2003. 52(4): p. 609-23.
123. Tamai, I., et al., *Functional characterization of human organic anion transporting polypeptide B (OATP-B) in comparison with liver-specific OATP-C.* Pharm Res, 2001. 18(9): p. 1262-9.
124. Yarim, M., et al., *Application of QSAR analysis to organic anion transporting polypeptide 1a5 (Oatp1a5) substrates.* Bioorg Med Chem, 2005. 13(2): p. 463-71.
125. Chang, C., et al., *Comparative pharmacophore modeling of organic anion transporting polypeptides: a meta-analysis of rat Oatp1a1 and human OATP1B1.* J Pharmacol Exp Ther, 2005. 314(2): p. 533-41.
126. Meier, P.J. and B. Stieger, *Bile salt transporters.* Annu Rev Physiol, 2002. 64: p. 635-61.
127. Hallen, S., et al., *Identification of a region of the ileal-type sodium/bile acid cotransporter interacting with a competitive bile acid transport inhibitor.* Biochemistry, 2002. 41(50): p. 14916-24.
128. Hagenbuch, B., et al., *Functional expression cloning and characterization of the hepatocyte Na+/bile acid cotransport system.* Proc Natl Acad Sci U S A, 1991. 88(23): p. 10629-33.
129. Hagenbuch, B. and P.J. Meier, *Molecular cloning, chromosomal localization, and functional characterization of a human liver Na+/bile acid cotransporter.* J Clin Invest, 1994. 93(3): p. 1326-31.

130. Cattori, V., U. Eckhardt, and B. Hagenbuch, *Molecular cloning and functional characterization of two alternatively spliced Ntcp isoforms from mouse liver1.* Biochim Biophys Acta, 1999. 1445(1): p. 154-9.
131. Kramer, W., et al., *Substrate specificity of the ileal and the hepatic Na(+)/bile acid cotransporters of the rabbit. I. Transport studies with membrane vesicles and cell lines expressing the cloned transporters.* J Lipid Res, 1999. 40(9): p. 1604-17.
132. Schroeder, A., et al., *Substrate specificity of the rat liver Na(+)-bile salt cotransporter in Xenopus laevis oocytes and in CHO cells.* Am J Physiol, 1998. 274(2 Pt 1): p. G370-5.
133. Hagenbuch, B. and P.J. Meier, *Sinusoidal (basolateral) bile salt uptake systems of hepatocytes.* Semin Liver Dis, 1996. 16(2): p. 129-36.
134. Weinman, S.A., M.W. Carruth, and P.A. Dawson, *Bile acid uptake via the human apical sodium-bile acid cotransporter is electrogenic.* J Biol Chem, 1998. 273(52): p. 34691-5.
135. Kim, J.Y., et al., *Transporter-mediated bile acid uptake causes Ca2+-dependent cell death in rat pancreatic acinar cells.* Gastroenterology, 2002. 122(7): p. 1941-53.
136. Stieger, B., et al., *In situ localization of the hepatocytic Na+/Taurocholate cotransporting polypeptide in rat liver.* Gastroenterology, 1994. 107(6): p. 1781-7.
137. Hallen, S., et al., *Membrane insertion scanning of the human ileal sodium/bile acid co-transporter.* Biochemistry, 1999. 38(35): p. 11379-88.
138. Hallen, S., et al., *Organization of the membrane domain of the human liver sodium/bile acid cotransporter.* Biochemistry, 2002. 41(23): p. 7253-66.

CHAPTER 2

Aims of the Presented Work

As mentioned before, investigations on substrate specificity of individual members of the OATP superfamily have been extensive. In terms of structure-function relationship, specific structural determinants required for Oatp/OATP transport activity have not been specified yet.

The current work focuses on members of the well-investigated OATP1 family. The **first aim** was to examine whether an evolutionarily ancient Oatp, namely Oatp1d1 from skate liver, shares the transport properties with the more evolved mammalian liver Oatps/OATPs. This was examined with transport studies using the toxins phalloidin and microcystin as substrates. The **second aim** was to identify distinct amino acid sequences and/or individual amino acid residues that are essential for substrate binding and/or transport of rat Oatp1a4. Because Oatp1a4 is a digoxin-transporter and Oatp1a1 does not transport digoxin, the cardiac glycoside was used as a model substrate. Transport studies were performed with chimeric constructs and mutated Oatp1a4.

Investigations towards complete molecular description of specific structural properties and future purification of an organic anion transporter require a solubilized and isolated membrane transport protein. The **third aim** was to establish a high-yield expression system for functional characterization and functional reconstitution of organic anion transporters. For this purpose the baculovirus/Sf9 cell-based expression system was used.

CHAPTER 3

The Organic Anion Transport Polypeptide 1d1 (Oatp1d1) Mediates Hepatocellular Uptake of Phalloidin and Microcystin into Skate Liver

F. Meier-Abt*[1], A. Hammann-Hänni*[2], B. Stieger[2], N. Ballatori[1,4] and J.L. Boyer[1,3]

[1)] Mount Desert Island Biological Laboratories (MDIBL), Salsbury Cove, Maine 04672

[2)] Institute of Clinical Pharmacology and Toxicology, University Hospital Zurich, Switzerland

[3)] Department of Medicine and Liver Centre, Yale University School of Medicine, New Haven, CT 06520

[4)] Department of Environmental Medicine, University of Rochester School of Medicine, Rochester, New York 14642

[*)] These co-authors contributed similarly to this work

Published: Toxicol Appl Pharmacol. 2007 Feb 1;218(3):274-9. Epub 2006 Nov 21

3. 1 Abstract

Organic anion transporting polypeptides (animals: Oatps; human: OATPs) mediate cellular uptake of numerous organic compounds including xenobiotic toxins into mammalian hepatocytes. In the little skate *Leucoraja erinacea* a liver specific Oatp (Oatp1d1, also called sOatp) has been identified and suggested to represent an evolutionarily ancient precursor of the mammalian liver OATP1B1 (human), Oatp1b2 (rat), and OATP1B3 (human). The present study tested whether Oatp1d1 shares functional transport activity of the xenobiotic oligopeptide toxins phalloidin and microcystin with the mammalian liver Oatps/OATPs. The phalloidin analogue [^{3}H]-demethylphalloin was taken up into skate hepatocytes with high affinity (Km ~ 0.4 μM), and uptake could be inhibited by phalloidin and a variety of typical Oatp/OATP substrates such as bromosulfophthalein, bile salts, estrone-3-sulfate, cyclosporine A and high concentrations of microcystin-LR (Ki ~ 150 μM). When expressed in *Xenopus laevis* oocytes Oatp1d1 increased uptake of (Km ~ 2.2 μM) and microcystin-LR (Km ~ 27 μM) 2 to 3-fold over water-injected oocytes, whereas the alternative skate liver organic anion transporter, the dimeric Ostα/β, exhibited no phalloidin and only minor microcystin-LR transport. Also, the closest mammalian Oatp1d1 orthologue, the human brain and testis OATP1C1, did not show any phalloidin transport activity. These results demonstrate that the evolutionarily ancient Oatp1d1 is able to mediate uptake of cyclic oligopeptide toxins into skate liver. These findings support the notion that Oatp1d1 is a precursor of the liver specific mammalian Oatps/OATPs and that its transport properties are closely associated with certain forms of toxic liver injury such as for example protein phosphatase inhibition by the water borne toxin microcystin.

3. 2 Introduction

Organic anion transporting polypeptides (animals: Oatps; human: OATPs) of the OATP/*SLCO* superfamily of solute carriers mediate multispecific substrate uptake in various organs of vertebrate animal species [1]. In mammalian liver, members of the OATP1 family (i.e. mouse and rat liver: Oatp1a1, Oatp1a4, Oatp1b2; human liver: OATP1A2, OATP1B1, OATP1B3) mediate sodium-independent uptake of bile salts, organic dyes (e.g. bromosulfophthalein), steroids and steroid conjugates, thyroid hormones, prostaglandins, various oligopeptides and numerous drugs [2]. Interestingly, the substrate spectrum of the hepatic Oatps/OATPs also include endogenous and exogenous linear and cyclic oligopeptides such as the endothelin receptor antagonist BQ-123, the thrombin inhibitor CRC220, the opioid receptor agonists DPDPE and deltorphin II and the enterohepatic hormone cholecystokinin 8 (CCK) [1, 2]. More recently, the hepatic Oatps/OATPs have also been shown to be responsible for the uptake of the hepatotoxic exogenous cyclic peptides phalloidin, α-amanitin and microcystin into rat and/or human livers [3-5]. These findings explain the observations of prevention of amatoxin and microcystin induced liver injury by concomitant administration of typical Oatp substrates [6, 7].

In the liver of the little skate *Leucoraja erinacea* an evolutionarily ancient Oatp has been identified at the basolateral (sinusoidal) plasma membrane domain of hepatocytes [8]. This sOatp or Oatp1d1/*Slco1d1* (for classification and nomenclature see [1]) shares 41.2-43.3% amino acid sequence identities with the rat liver Oatp1b2 (also called Oatp4) and the human liver OATP1B1 (also called OATP-C, OATP2, LST-1) and OATP1B3 (also called OATP8) [8]. Furthermore, Oatp1d1 exerts the highest degree of homology (50.4% amino acid sequence identity) with the most ancient OATP1 family member, i.e. OATP1C1 (or OATP-F) [1, 9]. Because the mammalian liver Oatps/OATPs have most probably arisen from gene duplication after species divergence [1, 2], it was of interest to examine whether the ancient skate Oatp1d1 shares the phalloidin and microcystin transport properties with the mammalian liver Oatps/OATPs. For this purpose, transport of radioactively labelled phalloidin was measured in isolated skate hepatocytes, and its transport was characterized by kinetic and inhibition studies. Furthermore, Oatp1d1 was expressed in *Xenopus laevis* oocytes in order to elucidate its suggested transport functions for phalloidin and the water-borne hepatotoxin microcystin.

3. 3 Material and Methods

Animals I Male skates (~ 1 kg) were caught by net in Frenchman's Bay off of Bar Harbor, ME, USA. They were maintained in large aerated tanks supplied with continuously flowing 15°C seawater and were used within 1-3 days of capture. Animals were anesthetized prior to hepatectomy with sodium pentobarbital (2.5 mg/kg) injected via a caudal vein. Female *Xenopus laevis* were purchased from Xenopus I, Inc., (Dexter, MI, USA) and from the African Xenopus facility c.c., Noordoek, South Africa. The frogs were maintained and treated according to NIH guidelines.

Materials I Radiolabeled [^{3}H]-taurocholate (3.47 Ci/mmol) and [^{3}H]-estrone-3-sulfate (53 Ci/mmol) were purchased from NEN Life Science Products AG (Boston, MA, USA) and Perkin Elmer Life Sciences (Boston, MA). [^{3}H]-Demethylphalloin (8.9 GBq/mmol) was synthesized as described [10]. For all transport experiments demethylphalloin was used as labeled substrate. It is structurally very similar to phalloidin and has been shown to be a biological equivalent of phalloidin and to be transported by the same Oatps/OATPs as phalloidin in mammalian liver [3, 11-13] . [^{3}H]-Dihydromicrocystin-LR (1.1x 10^8 Bq/mol) was prepared as described [14]. All chemicals were obtained from commercial sources and were of the highest degree of purification available.

Isolation of skate hepatocytes I Skate hepatocytes were prepared by collagenase perfusion of isolated livers as previously described [15]. Cells were then maintained on ice in an elasmobranch Ringer buffer (270 mM NaCl, 4 mM KCl, 2 mM $CaCl_2$, 3 mM $MgCl_2$, 8 mM $NaHCO_3$, 1 mM KH_2PO_4, 0.5 mM Na_2SO_4, and 350 mM urea) [15]. For transport experiments cell suspensions were prewarmed in a 15 °C water bath. Cells were normally used for transport experiments within 3 hours after isolation.

Functional characterization in skate hepatocytes I Hepatocyte suspensions (15 °C) were diluted in elasmobranch Ringer buffer [16] to approximately 45 mg cells (wet weight) per milliliter. All transport studies were conducted at 15 °C. They were initiated by adding cell suspension (1.9 – 2.08 ml) to incubation solution (0.02 – 0.2 ml), resulting in a total assay volume of 2.1 ml per data point (2 zero points, 4 uptake points, 3 standards). The incubation solution consisted of elasmobranch Ringer

buffer supplemented with the radioactively labeled compounds and the inhibitor concentrations as given in the figure legends. Unspecific binding of isotopes was accounted for by subtracting zero time point values from the timed transport values. Standards were used to transform cell-associated radioactivity into molar amounts of tracer uptake. Unless stated otherwise, all transport studies were performed in quadruplicates in at least two separate cell preparations.

Functional characterization in *Xenopus laevis* oocytes I For *in vitro* synthesis of cRNA, the cDNA clones of Oatp1d1 [8], Ostα/β [17] and OATP1C1 [9] were linearized with XhoI and NotI, respectively. Capped cRNA was synthesized using the mMESSAGE mMACHINE T3 and T7 Kit (Ambion, Austin, TX, U.S.A.). *Xenopus laevis* oocytes were prepared and handled as described previously [3]. After an overnight incubation at 18 °C healthy oocytes were injected with 50 nl water or with 5 ng Oatp1d1-cRNA, 2 ng Ostα/β-cRNA or 5 ng OATP1C1-cRNA. After 3 days in culture, transport of [^{3}H]-demethylphalloin, [^{3}H]-estrone-3-sulfate, [^{3}H]-dihydromicrocystin-LR or [125I]-L-thyroxine was measured at 25 °C in a medium containing 100 mM NaCl, 2 mM KCl, 1 mM $CaCl_2$, 1 mM $MgCl_2$ and 10 mM HEPES/Tris, pH 7.5 as described previously [3].
Kinetic studies with phalloidin and microcystin-LR were determined at 30 min which was within the initial linear uptake range (not shown). The obtained values were corrected for the values measured in water-injected oocytes and were fitted to the Michaelis-Menten equation using nonlinear regression analysis to obtain the kinetic parameters.

Statistical analysis I *Cis*-inhibition of phalloidin transport into skate hepatocytes was analyzed using ANOVA (analysis of variances) for one-way analysis. As a post test, Dunnett's test was performed if overall $p<0.05$, which was considered to be statistically significant.
Substrate specificities of Oatp1d1, Ostα/β and OATP1C1 were compared with transport in water-injected control oocytes by the unpaired Student's t test. Statistical significance was indicated by $p<0.05$.

3. 4 Results

Phalloidin transport into skate hepatocytes I To determine whether phalloidin is taken up into skate hepatocytes, the structural phalloidin analogue demethylphalloin was used. As a control for transport competent skate hepatocytes, taurocholate uptake was determined in parallel. As illustrated in Fig. 1, isolated skate hepatocytes demonstrated predominant sodium-independent taurocholate uptake as previously shown [16]. Approximately 60 % of total taurocholate uptake at 60 min were observed within the first 10 min of incubation (Fig. 1A). Similar sodium-independent uptake was also seen for phalloidin although its uptake into skate hepatocytes was slower (uptake at 10 min: ~ 40% of uptake at 60 min) as compared to taurocholate (Fig. 1B). Furthermore, after an initial rapid uptake phase time-dependent phalloidin did not level of, but continued to rise steadily up to 60 min. However, initial linear uptake rates (1 min uptake values) showed clear saturability with increasing substrate concentrations (Fig. 2) with an apparent Km-value of 0.4 $\pm$ 0.1 μM and a Vmax-value of 10.1 $\pm$ 0.3 fmol/mg protein x min^{-1}. These data strongly indicate carrier-mediated uptake of phalloidin into skate hepatocytes.

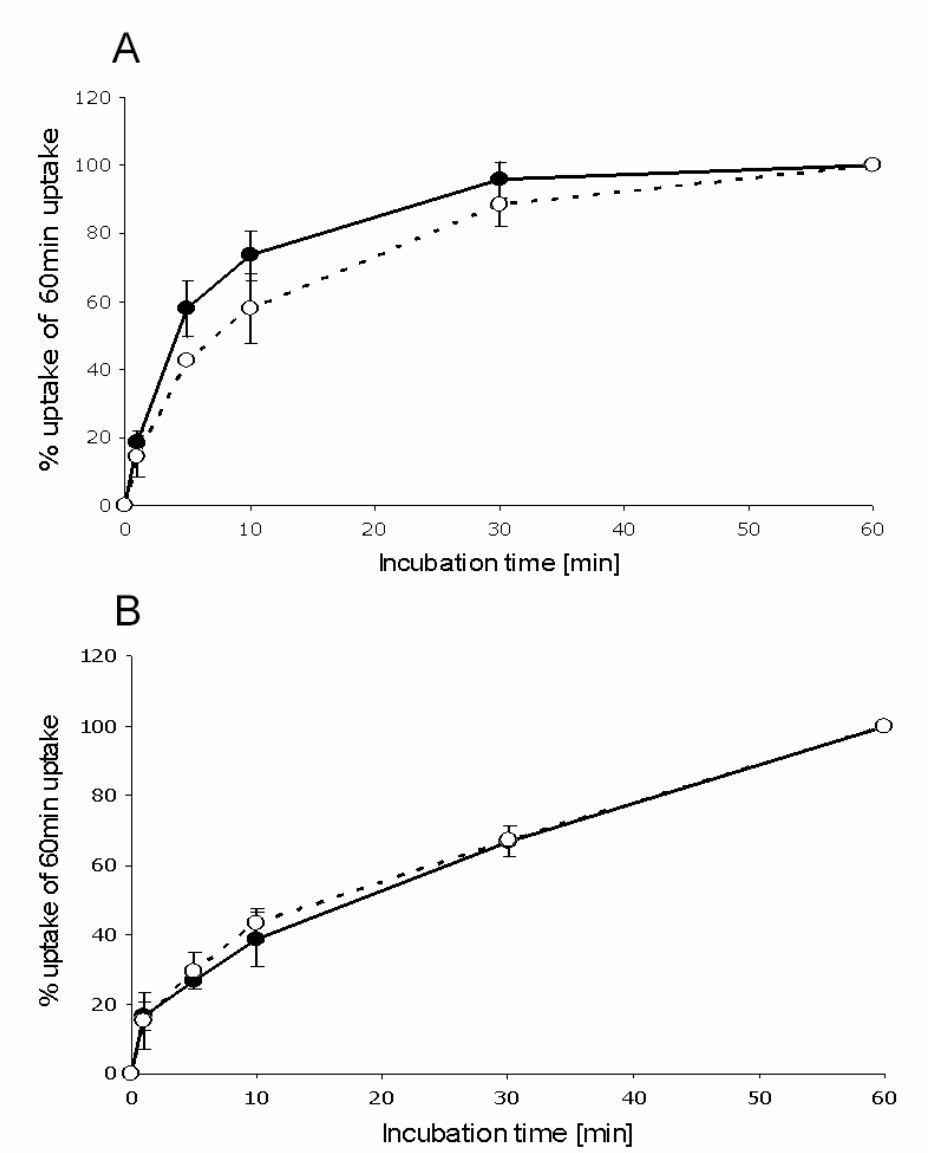

Fig.1

Time course of taurocholate (A) and phalloidin (B) transport into skate hepatocytes I Skate hepatocytes were incubated in elasmobranch Ringer buffer with 10 μM taurocholate (A) or 1 μM demethylphalloin (B). The incubation buffer contained either 270 mM sodium (●) or 270 mM choline (○) to determine the portion of sodium-independent transport. Substrate uptake was determined at the time intervals indicated and presented as % of total uptake at 60 min. Values represent the means ± SE of duplicate measurements in three separate cell preparations.

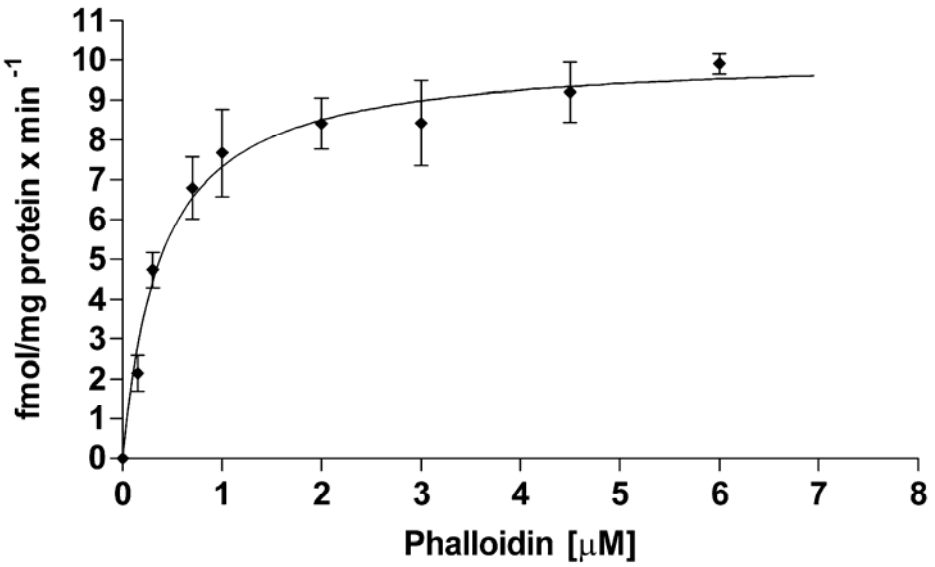

Fig. 2

Saturation kinetics of phalloidin transport into skate hepatocytes I Skate hepatocytes were incubated in standard elasmobranch Ringer buffer supplemented with increasing concentrations of phalloidin (0.15 – 6 μM). Initial linear transport was determined at 1 min. Values represent the means ± SE of quadruplicate measurements in two separate cell preparations. Values were fitted to Michaelis-Menten equation using nonlinear regression analysis to obtain the kinetic parameters.

Inhibition studies of phalloidin transport into skate hepatocytes I Because phalloidin has been shown to be taken up into rat and human livers by members of the OATP/*SLCO* superfamily of solute carriers [1, 3, 11] and because an ancient Oatp, Oatp1d1, has been identified in skate liver [8], additional experiments examined whether an organic anion transport protein or even Oatp1d1 is involved in phalloidin transport. For this purpose, the inhibition pattern of phalloidin transport into skate hepatocytes was measured using typical substrates and potential inhibitors of mammalian liver Oatps/OATPs [1, 2]. The latter have previously been established or suggested as Oatp1d1 substrates [3, 4, 6, 8]. As illustrated in Fig. 3, the strongest inhibitor of [^{3}H]-demethylphalloin transport was unlabeled phalloidin, which is consistent with demethylphalloin being a structural and biological equivalent of phalloidin. From 40-60% inhibition of uptake was also found for the well known Oatp/OATP substrates estrone-3-sulfate, taurocholate and related bile salt derivatives, the organic dye BSP, the organic anion transport inhibitors cyclosporin A and probenecid. In contrast, digoxin and microcystin-LR at a concentration of 10 μM did not inhibit phalloidin uptake to a significant extent.

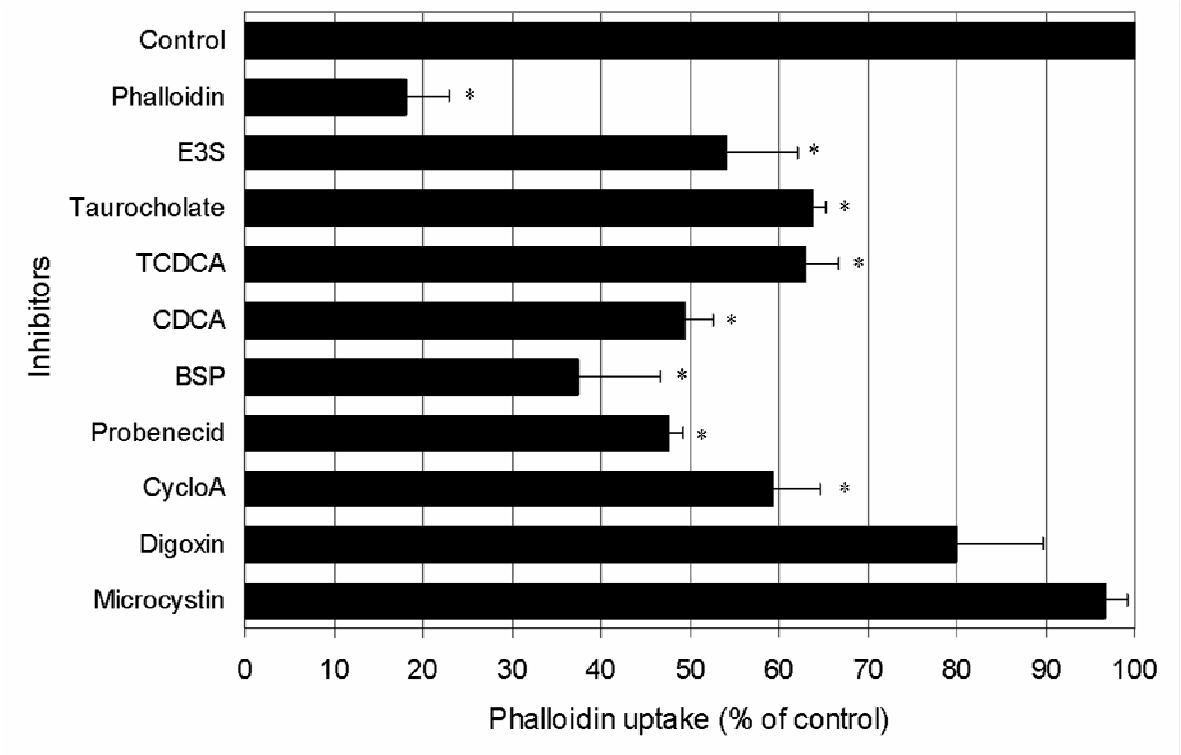

Fig. 3

***Cis*-inhibition of phalloidin transport into skate hepatocytes I** 1 μM demethylphalloin transport into skate hepatocytes at 1 min was determined in standard elasmobranch Ringer buffer in the absence (control) and presence of various inhibitors, the concentrations of which were chosen on the basis of previously estimated Km-values of Oatp-mediated substrate uptake [1, 3] and of the inhibition pattern of Oatp1d1-mediated estrone-3-sulfate uptake [8]. Inhibitor concentrations were: Phalloidin (10 μM), estrone-3-sulfate (E3S, 50 μM), taurocholate (50 μM), taurochenodeoxycholate (TCDCA, 50 μM), chenodeoxycholate (CDCA, 50 μM), bromosulfophthalein (BSP, 10 μM), probenecid (500 μM), cyclosporine A (CycloA,10 μM), digoxin (50 μM), microcystin-LR (10 μM). Results are given as percent of control uptake. Values are given as means ± SE of quadruplicate measurements in three separate cell preparations.

Because microcystin-LR has been shown to be transported by all major rat and human liver Oatps/OATPs including Oatp1b2, OATP1B1 and OATP1B3 [4], which all share an amino acid sequence identity greater than 40% with skate Oatp1d1, and because the absence of significant inhibition of demethylphalloin uptake at a concentration of 1 μM (~3 times above the Km-value) by 10 μM microcystin-LR does not exclude the possibility that microcystin-LR might represent a low affinity substrate of Oatp1d1, a more detailed analysis of the inhibition kinetics was performed. As illustrated in Fig. 4, strong *cis*-inhibition of demethylphalloin uptake was only observed if the microcystin-LR concentrations were increased well above 100 μM (estimated Ki-value ~ 150 μM). Furthermore, the Dixon-plot analysis is consistent with a competitive type of inhibition. These results support the assumption that microcystin-LR might indeed represent a low affinity substrate for the skate liver phalloidin uptake system (i.e. possibly Oatp1d1).

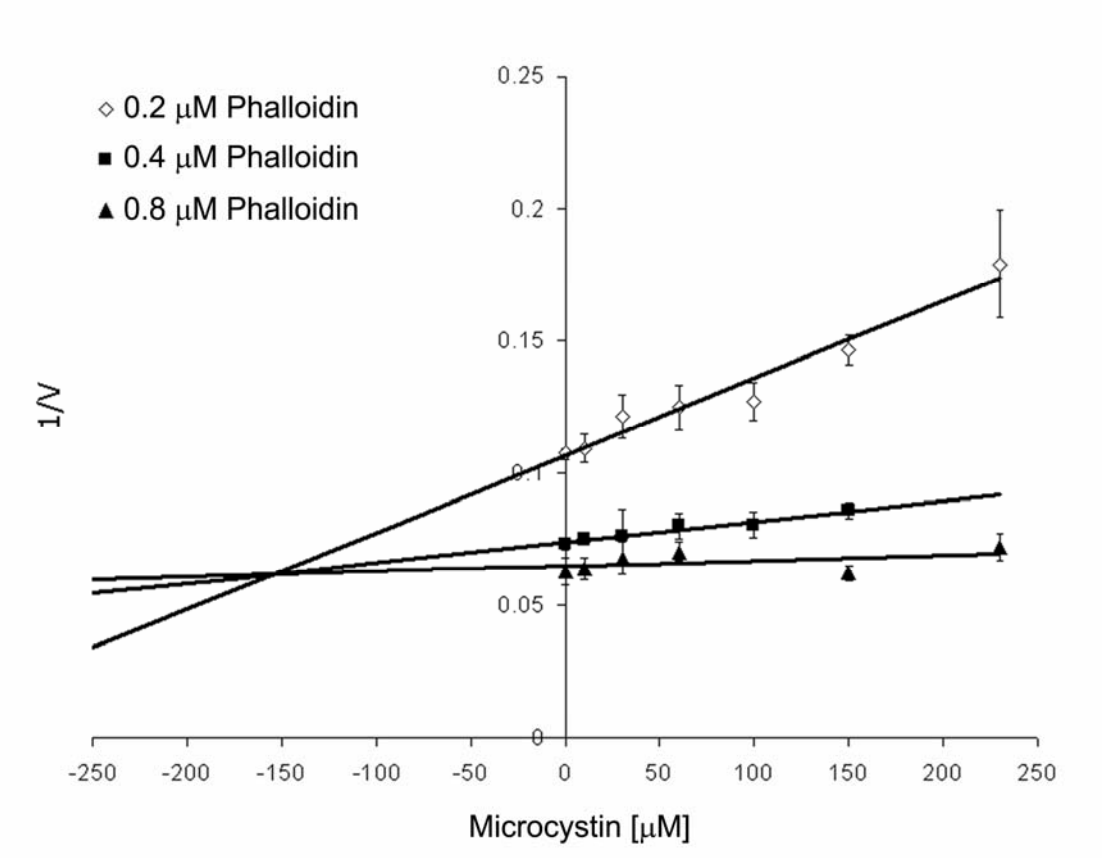

Fig. 4

Dixon plot of inhibition of phalloidin transport by microcystin-LR into skate hepatocytes I Phalloidin transport at 1 min into skate hepatocytes was determined in standard elasmobranch Ringer buffer supplemented with the indicated substrate concentrations (0.2, 0.4, 0.8 μM) in the absence or presence of increasing concentrations of microcystin-LR (10, 30, 60, 100, 150, 230 μM). Data represent the means ± SE of quadruplicate determinations in one representative out of two cell preparations. Estimated Ki-values in both experiments amounted to ~ 152 and 160 μM, respectively.

Phalloidin and microcystin-LR transport into Oatp1d1 expressing *Xenopus laevis* oocytes I To directly investigate the hypothesis that Oatp1d1 is responsible for phalloidin and microcystin-LR transport into skate hepatocytes, transport studies in cRNA injected *Xenopus laevis* oocytes were performed. Thereby, the transport properties of Oatp1d1 were compared also to the alternative skate organic anion transporter Ostα/β [17] and to the mammalian Oatp1d1 orthologue OATP1C1 [8, 9]. The organic anion estrone-3-sulfate was included as a standard substrate to control for transport competent oocytes and thyroxine served as a control substrate for OATP1C1 [9]. As summarized in Table 1, phalloidin uptake was stimulated twofold in Oatp1d1 expressing oocytes as compared to water injected oocytes. In contrast,

Ostα/β-cRNA injected oocytes exhibited virtually no increased phalloidin uptake although Ostα/β was effectively expressed at the surface of the oocytes as indicated by the markedly increased uptake of estrone-3-sulfate. Also, no increased phalloidin uptake was found in OATP1C1 expressing oocytes despite an approximately 8-fold stimulation of the control substrate thyroxine (Table 1). In addition to phalloidin, Oatp1d1-expressing oocytes also showed an approximately 3-fold stimulation of microcystin-LR uptake, whereas microcystin-LR was less well transported by Ostα/β (Table 1). These results demonstrate that phalloidin and microcystin-LR are transport substrates of skate liver Oatp1d1.

Table 1

Transport of phalloidin and microcystin-LR by Oatp1d1, Ostα/β and OATP1C1 in water and cRNA-injected *Xenopus laevis* oocytes[a]

Substrates[b]	Water *(fmol/oocyte x 30 min)*	Oatp1d1 *(fmol/oocyte x 30 min)*	Ostα/β *(fmol/oocyte x 30 min)*	OATP1C1 *(fmol/oocyte x 30 min)*
Phalloidin (4μM)	60.2 ± 5.8	122.1± 16.7*	72.5 ± 6.1	60.3 ± 5.3
Microcystin-LR (4μM)	3.8 ± 0.3	9.9 ± 2.4*	6.0 ± 2.3*	
Thyroxine (5 nM)	1.1 ± 0.1			8.9 ± 1.3*
Estrone-3-Sulfate (50 nM)	1.3 ± 0.2	16.9 ± 5.2*	46.2 ± 14.3*	2.1 ± 0.2*
Estrone-3-Sulfate (500nM)	5.7 ± 1.0	47.6 ± 11.6*	342.0 ± 47.9*	

[a]Oocytes were injected with water, 5 ng Oatp1d1-cRNA, 2 ng Ostα/β-cRNA or 5 ng OATP1C1-cRNA. Substrate uptake was measured at 30 min in10-40 oocytes in two separate experiments.

[b]Thyroxine was included as a control substrate for OATP1C1 (10). Estrone-3-sulfate served as control for functionally competent transporter expression levels. * Significantly different from water-injected oocytes ($p < 0.05$).

Finally, saturation kinetics analysis of Oatp1d1 mediated phalloidin and microcystin-LR transport was performed in cRNA-injected *X. laevis* oocytes. Because preliminary experiments demonstrated that initial transport rates for both cyclic oligopeptides increased linearly over at least 45 min (results not shown), uptake rates were measured at 30 min for all kinetic experiments. As indicated in Fig. 5, Oatp1d1 mediated uptake of increasing concentrations of phalloidin up to 10 μM exhibited saturability with an apparent Km-value of 2.2 ± 0.8 μM (Fig. 5A) and an apparent Vmax of 0.5 ± 0.1 fmol/oocyte per min. Furthermore, apparent saturation kinetics was also found for initial uptake rates of microcystin-LR, where the apparent Km-value amounted to 26.9 ± 9.9 μM (Fig. 5B) and the Vmax to 0.9 ± 0.2 fmol/oocyte per min. Hence, the affinity of Oatp1d1 for microcystin-LR is approximately 10-fold lower than its affinity for phalloidin, which provides an explanation for the failure of 10 μM microcystin-LR to inhibit the uptake of 1 μM phalloidin in skate hepatocytes (see Fig. 3). These results strongly support the hypothesis that Oatp1d1 is responsible for uptake of both phalloidin and microcystin-LR into skate hepatocytes.

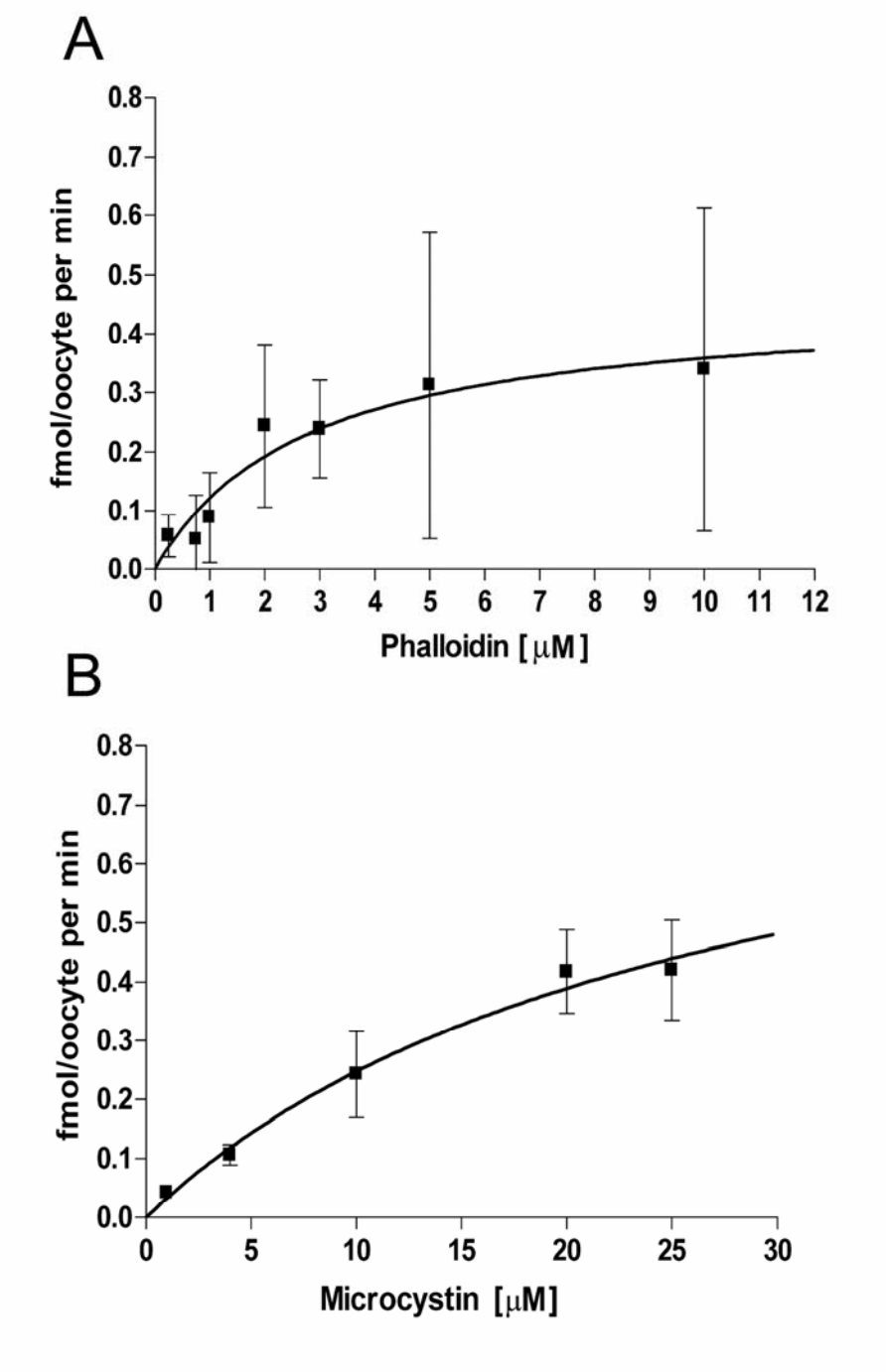

Fig. 5

Saturation kinetics of phalloidin (A) and microcystin-LR (B) uptakes into *Xenopus laevis* oocytes I Oocytes were injected with 5 nl water or 5 ng Oatp1d1 cRNA. After three days in culture, transport was determined over the initial 30-min period at increasing concentrations of phalloidin or microcystin-LR, respectively. Measurements were performed at 25 °C in two separate oocyte preparations (9-12 oocytes). Data represent the means ± SE. Values were fitted to Michaelis-Menten using nonlinear regression analysis to obtain the kinetic parameters.

3. 5 Discussion

The present study provides direct evidence that Oatp1d1 mediates phalloidin and microcystin-LR uptake into skate liver. This conclusion is derived from the following observations: 1) Isolated skate hepatocytes exhibited high affinity uptake of phalloidin with an apparent Km of ~ 0.4 μM (Fig. 2). 2) Phalloidin uptake into skate hepatocytes could be inhibited by typical Oatp/OATP substrates (Fig. 3) and in an apparent competitive manner, also by high concentrations of microcystin-LR (Fig. 4). 3) Oatp1d1 expressing oocytes exhibited high affinity phalloidin (apparent Km ~ 2.2 μM) and lower affinity microcystin-LR (apparent Km ~ 27 μM) uptake (Fig. 5). And 4) Ostα/β, the second so far identified organic anion transporter of skate hepatocytes, did not show phalloidin and only minor microcystin-LR transport, when expressed in *X. laevis* oocytes (Table 1). Hence, Oatp1d1 mirrors the oligopeptide transport properties of the mammalian liver Oatps/OATPs, supporting the notion that Oatp1d1 represents an evolutionarily ancient precursor of the mammalian liver transporters [8]. In mammalian liver, phalloidin uptake has been shown to be mediated by Oatp1b2 in the rat [3] and by OATP1B1 and to a lesser degree also by OATP1B3 in man [3, 11]. In contrast, no phalloidin transport has been observed with Oatp1a1, Oatp1a4, OATP1A2 and OATP2B1 [3]. Hence, only the liver specific transporters of the OATP1B subfamily [18] exhibited phalloidin transport in mammalian species, whereas the more widely expressed members of the OATP1A and OATP2B subfamilies [18] did not accept phalloidin as a transport substrate. The affinities (Km-values) of the mammalian transporters for phalloidin have been reported to be 5.7 μM (Oatp1b2), 7.5 μM (OATP1B3) and 17 μM (OATP1B1) [3]. This study demonstrates that even skate hepatocytes exhibit high affinity phalloidin uptake although phallotoxins do not represent typical water borne organic substances. However, as a cyclic oligopeptide phalloidin belongs to the Oatp/OATP substrates [3, 11], and skate hepatocytes express the evolutionarily ancient Oatp1d1 [8], which mediated phalloidin uptake when expressed in *Xenopus laevis* oocytes (Table 1, Fig. 5). These findings indicate that Oatp1d1 is responsible for the phalloidin uptake activity of skate hepatocytes, although the approximately 5-fold difference in the apparent Km-values between phalloidin uptake into hepatocytes (~ 0.4 μM, Fig. 2) and Oatp1d1 expressing oocytes (~ 2.2 μM, Fig. 5) cannot exclude the possible involvement of additional, so far unidentified transport systems. The only other so far

known multispecific organic anion transporter of skate hepatocytes, Ostα/β, did not exhibit any phalloidin transport activity when expressed in *X. laevis* oocytes (Table 1). Interestingly, OATP1C1, which is predominantly expressed in human brain and testis [9] and which shares the highest overall amino acid sequence identity with the skate liver Oatp1d1 [8] , did also not show any phalloidin transport activity (Table 1). Hence, phalloidin transport appears to be a characteristic feature of liver specific Oatps/OATPs in both mammalian as well as in skate livers.

In addition to phalloidin, Oatp1d1 also transports the water borne cyclic oligopeptide microcystin-LR (Table 1, Fig. 5). This protein phosphatase inhibitor has been previously shown to be transported into skate liver by a multispecific organic substrate transporter that can be inhibited by a wide range of organic anions such as bromosulfophthalein (BSP), bile salts (e.g. cholate, taurocholate), rifampicin, rifamycin B, rose bengal and trypan blue [6]. These latter compounds are typical Oatp/OATP substrates and many of them also inhibit Oatp1d1 [8]. Hence, the previous studies are consistent with Oatp1d1 being responsible for microcystin uptake into skate liver, although the affinity of Oatp1d1 for microcystin was found to be approximately 10-fold lower (Km ~27 μM, Fig. 5) as compared to its affinity for phalloidin (Km ~2.2 μM, Fig. 5). Furthermore, in skate hepatocytes microcystin inhibited phalloidin uptake with a Ki-value of approximately 150 μM (Fig. 4), which further supports the relatively low affinity of Oatp1d1 for microcystin-LR. With respect to the discrepancy between the Km- and Ki-values, it has to be noted that the experimental validation of the transport kinetics were hampered by the considerable oocyte toxicity of microcystin-LR above concentrations of 25 μM [4]. Nevertheless, the Km-value of Oatp1d1 for microcystin (~27μM) compares well with the corresponding Km-values of the human transporters OATP1B1 (~7 μM), OATP1B3 (~9 μM) and OATP1A2 (~20 μM) [4]. In addition, it is consistent with the observation that 100 μM taurocholate ($Km_{Oatp1d1}$ ~85 μM; [8]) inhibits microcystin-LR (10 μM) uptake into skate hepatocytes by approximately 50 % [6]. Hence, low affinity uptake of microcystin-LR into skate liver can explain the high sensitivity of microcystin induced hepatotoxicity to inhibition of hepatocellular uptake by a variety of Oatp/OATP substrates [6]. In fact, the broad substrate specificity of skate and mammalian hepatic Oatps/OATPs offers the opportunity to prevent and/or antagonize microcystin induced liver injury by parenteral administration of a variety of

organic anions including BSP, bile salts, cyclosporine A or rifampicin. A similar conclusion has been reached recently also with respect to amatoxin induced liver injury, as the main poison of the green death cap (*Amanita phalloides*), α-amanitin, is taken up into human liver by OATP1B3 [5]. Hence, identification and characterization of the uptake carriers involved can be of considerable importance for prevention and/or treatment of toxin induced liver injury in man as well as in various animal species. The latter also includes now the little skate *Leucoraja erinacea*, which might be subject to occasional intoxication with marine toxins such as the phosphatase inhibiting microcystins.

In conclusion, the present study identifies Oatp1d1 as the phalloidin and microcystin-LR uptake system in skate liver. Because the same cyclic oligopeptides are also transported by the liver specific Oatps/OATPs in rodents and in men, the data support the notion that Oatp1d1 represents an evolutionarily ancient precursor of the mammalian liver Oatps/OATPs. Furthermore, the present observations provide further evidence that Oatp/OATP-mediated toxin uptake is important for certain forms of toxic liver injury such as microcystin induced hepatocellular necrosis.

3.6 Acknowledgments

This study was supported in part by the Swiss National Science Foundation, Grants 31-64140.00 and 3100A0-112524/1, the National Institutes of Health Grants DK48823, and DK34989, and Grant ES03828 to the Center for Membrane Toxicity Studies at the Mount Desert Island Biological Laboratory.

3.7 References

1. Hagenbuch, B. and P.J. Meier, *Organic anion transporting polypeptides of the OATP/ SLC21 family: phylogenetic classification as OATP/ SLCO superfamily, new nomenclature and molecular/functional properties.* Pflugers Arch, 2004. 447(5): p. 653-65.
2. Hagenbuch, B. and P.J. Meier, *The superfamily of organic anion transporting polypeptides.* Biochim Biophys Acta, 2003. 1609(1): p. 1-18.
3. Meier-Abt, F., H. Faulstich, and B. Hagenbuch, *Identification of phalloidin uptake systems of rat and human liver.* Biochim Biophys Acta, 2004. 1664(1): p. 64-9.
4. Fischer, W.J., et al., *Organic anion transporting polypeptides expressed in liver and brain mediate uptake of microcystin.* Toxicol Appl Pharmacol, 2005. 203(3): p. 257-63.
5. Letschert, K., et al., *Molecular characterization and inhibition of amanitin uptake into human hepatocytes.* Toxicol Sci, 2006. 91(1): p. 140-9.
6. Runnegar, M., N. Berndt, and N. Kaplowitz, *Microcystin uptake and inhibition of protein phosphatases: effects of chemoprotectants and self-inhibition in relation to known hepatic transporters.* Toxicol Appl Pharmacol, 1995. 134(2): p. 264-72.
7. Enjalbert, F., et al., *Treatment of amatoxin poisoning: 20-year retrospective analysis.* J Toxicol Clin Toxicol, 2002. 40(6): p. 715-57.
8. Cai, S.Y., et al., *An evolutionarily ancient Oatp: insights into conserved functional domains of these proteins.* Am J Physiol Gastrointest Liver Physiol, 2002. 282(4): p. G702-10.
9. Pizzagalli, F., et al., *Identification of a novel human organic anion transporting polypeptide as a high affinity thyroxine transporter.* Mol Endocrinol, 2002. 16(10): p. 2283-96.
10. Puchinger, H. and T. Wieland, *[Search for some metabolites from poisoning by desmethylphalloin (DMP)].* Eur J Biochem, 1969. 11(1): p. 1-6.
11. Fehrenbach, T., et al., *Characterization of the transport of the bicyclic peptide phalloidin by human hepatic transport proteins.* Naunyn Schmiedebergs Arch Pharmacol, 2003. 368(5): p. 415-20.
12. Petzinger, E., *Competitive inhibition of the uptake of demethylphalloin by cholic acid in isolated hepatocytes. Evidence for a transport competition rather than a binding competition.* Naunyn Schmiedebergs Arch Pharmacol, 1981. 316(4): p. 345-9.
13. Munter, K., D. Mayer, and H. Faulstich, *Characterization of a transporting system in rat hepatocytes. Studies with competitive and non-competitive inhibitors of phalloidin transport.* Biochim Biophys Acta, 1986. 860(1): p. 91-8.
14. Meriluoto, J.A., et al., *Synthesis, organotropism and hepatocellular uptake of two tritium-labeled epimers of dihydromicrocystin-LR, a cyanobacterial peptide toxin analog.* Toxicon, 1990. 28(12): p. 1439-46.
15. Smith, D.J., et al., *Isolation and characterization of a polarized isolated hepatocyte preparation in the skate Raja erinacea.* J Exp Zool, 1987. 241(3): p. 291-6.
16. Smith, D.J., et al., *Taurocholate uptake by isolated skate hepatocytes: effect of albumin.* Am J Physiol, 1987. 252(4 Pt 1): p. G479-84.
17. Wang, W., et al., *Expression cloning of two genes that together mediate organic solute and steroid transport in the liver of a marine vertebrate.* Proc Natl Acad Sci U S A, 2001. 98(16): p. 9431-6.
18. Hagenbuch, B. and P. Dawson, *The sodium bile salt cotransport family SLC10.* Pflugers Arch, 2004. 447(5): p. 566-70.

CHAPTER 4

Identification of Amino Acid Residues Essential for Efficient Transport Mediated by Oatp1a4

A. Hammann-Hänni[1], Y. Miao[3], J. van Montfoort[1], F. Meier-Abt [1], M.G. Grütter[2], P. Meier-Abt[1] and B. Hagenbuch[3]

[1)] Division of Clinical Pharmacology and Toxicology, University Hospital Zurich, Switzerland

[2)] Department of Biochemistry, University of Zurich, Switzerland

[3)] Department of Pharmacology, Toxicology and Therapeutics, the University of Kansas Medical Centre, Kansas City, Kansas, USA

In preparation

4.1 Abstract

Many organic anion transporting polypeptides (Oatps) have overlapping substrate specificities and mediate uptake of a wide variety of structurally unrelated compounds. For certain Oatps specific substrates have been reported. Among the well characterized members of the OATP1A subfamily, Oatp1a4 is a high affinity digoxin transporter while Oatp1a1 does not transport digoxin. To identify amino acids that are important for Oatp1a4-mediated transport, we expressed chimeras between Oatp1a4 and Oatp1a1 in *Xenopus laevis* oocytes and used digoxin transport as a functional tool. Based on the results with these chimeras we performed site-directed mutagenesis and identified three amino acid residues (F328, S334 and M361) that when mutated to the residues found in Oatp1a1, resulted in reduced digoxin transport. Kinetic analysis revealed that these mutations reduced the apparent affinity of Oatp1a4 to digoxin. We then measured uptake of the general Oatp substrates taurocholate, estradiol-17β-glucuronide and D-penicillamine^{2,5}-enkephalin (DPDPE) in oocytes as well as in HeLa cells expressing the mutant proteins. Consistent with our hypothesis that the mutated amino acid residues are important for overall Oatp1a4-mediated uptake, transport of all tested substrates was reduced in both expression systems. Furthermore, similar as for digoxin, the affinity for DPDPE was also reduced. In summary, we have identified three amino acid residues, F328, S334 and M361, which are essential for transport mediated by Oatp1a4. However, we do not yet know whether these amino acid residues are directly involved in substrate binding or whether they affect the three-dimensional structure of the transporter.

4.2 Introduction

Organic anion transporting polypeptides (animals: Oatps; human: OATPs) form a superfamily of 12 transmembrane helices (TMH) proteins that can currently be subdivided into 6 mammalian families (≥ 40 % amino acid sequence identities, OATP1-6) and 13 subfamilies (≥ 60 % amino acid sequence identities) [1]. The OATP1 family comprises the rodent Oatp1a1 (gene symbol *Slco1a1*), Oatp1a3 (*Slco1a3*), Oatp1a4 (*Slco1a4*), Oatp1a5, (*Slco1a5*), Oatp1a6 (*Slco1a6*), Oatp1b2 (*Slco1b2*), as well as the human OATP1A2 (*SLCO1A2*), OATP1B1 (*SLCO1B1*), OATP1B3 (*SLCO1B3*) and OATP1C1 (*SLCO1C1*). Most of these are multispecific carriers that accept a variety of amphipathic organic compounds including bile salts, organic anionic dyes, steroid conjugates, thyroid hormones, prostaglandins, anionic oligopeptides, numerous drugs and other xenobiotics [2]. Members of other families, such as the prostaglandin transporters (PGTs) of the OATP2 family which transport only eicosanoids or OATP2B1 which mainly transports the steroid-conjugates estrone-3-sulfate and dehydroepiandrosterone sulfate, have a much narrower substrate specificity [3, 4]. Characterization of single Oatps/OATPs so far has concentrated on functional aspects of the multispecificity, i.e. on apparent affinity constants and on *cis*-inhibition patterns of the different substrates [2, 3, 5]. Such inhibition experiments performed with Oatp1a4 suggested that there might be different substrate recognition sites for digoxin and estradiol-17β-glucuronide [6].

Only a few studies have been reported investigating the molecular basis of the substrate specificity for members of the OATP-gene superfamily and identified structural elements involved in substrate binding and/or transport. Experiments with the PGTs from human, rat and mouse and some of their chimeras suggested that the C-terminal half of the protein is important for the apparent affinity of prostaglandin E_2 [7]. Using cysteine-scanning mutagenesis the same group mapped the substrate-binding site of the rat PGT to TMH 10 [8] and identified conserved cationic amino acids important for prostaglandin transport [9]. However, no such studies have been performed for the multispecific Oatps such as rat Oatp1a1, Oatp1a4 and Oatp1a5.

Besides common substrates such as the bile salt taurocholate, the steroid–conjugate estradiol-17β-glucuronide, and the opioid peptide D-penicillamine^{2,5} enkephalin (DPDPE) [10, 11] there are specific compounds that can be used to distinguish between Oatp1a1, Oatp1a4 and Oatp1a5 on a functional level. Bromosulfophthalein

is a good substrate for Oatp1a1 and Oatp1a5 but is not transported by Oatp1a4. On the other hand, digoxin is a high affinity substrate for Oatp1a4 (Km ~ 0.24 μM) and is also transported by Oatp1a5 but is not a substrate for Oatp1a1 [11].

Based on these substrate differences and the overall high amino acid sequence identity of 77%, we hypothesized that digoxin transport in combination with chimeras between Oatp1a1 and Oatp1a4 and site-directed mutagenesis should allow us to identify distinct regions and/or individual amino acids that are important for Oatp1a4-mediated substrate recognition and transport.

4.3 Materials and Methods

Animals I Female *Xenopus laevis* were purchased from the African Xenopus facility c.c., Noordoek, South Africa. The frogs were maintained and treated according to NIH guidelines.

Materials I All oligonucleotides were ordered from Microsynth (Balgach, Switzerland). Cell culture media and reagents were obtained from Invitrogen (Groningen, The Netherlands). Radiolabeled [^{3}H]-digoxin (9.0 Ci/mmol), [estradiol-6,2-^{3}H]-estradiol-17β-D-glucuronide (45.0 Ci/mmol) and [tyrosyl-2,6-^{3}H(N)]-D-penicillamine^{2,5} enkephalin (DPDPE; 40.0 Ci/mmol) were purchased from PerkinElmer Life Sciences (Boston, MA). [^{3}H]-Taurocholic acid was obtained from American Radiolabeled Chemicals Inc. (St. Louis, MO). Unlabeled DPDPE was obtained from BACHEM (Bubendorf, Switzerland).
Unless stated otherwise, all other chemicals were provided in the highest degree of purification available from Sigma (St. Louis, MO) or Fluka (Buchs, Switzerland).

Construction of chimeras and mutants I In order to avoid problems with different RNA stabilities due to different 3' untranslated regions, all the constructs were cloned into the so-called Oatp1a1 backbone. This Oatp1a1 backbone was constructed as follows: The Oatp1a1 cDNA (GenBank accession number NM_017111) in the pSPORT1 vector [12] was cut with the restriction enzymes *Nco*I and *Bsm*I. The resulting overhangs were filled in with Klenow enzyme (Amersham Biosciences, Buckinghamshire HP7 9NA, England) and after dephosphorylation with calf intestinal alkaline phosphatase (Promega, Madison, WI, U.S.A.), the Oatp1a1 backbone was gel purified. This vector allowed cloning of blunt ended cDNAs between bases 89 and 2142 of the original Oatp1a1 construct resulting in identical 3' and 5' untranslated sequences. To be able to detect all constructs with the same antibody, a 6-His tag was attached to the Oatp1a1 and Oatp1a4 open reading frame (ORF) by PCR amplification with the primers Oatp1a1f90 and Oatp1a1rHis for Oatp1a1 and Oatp1a4f122 and Oatp1a4rHis for Oatp1a4 (Table 1). To reduce PCR related mutations, all amplifications were performed with the proofreading enzyme *Pfu Turbo* DNA polymerase (Stratagene, La Jolla, CA, U.S.A.). After amplification of the His-tagged Oatp1a1 and Oatp1a4 ORFs, they were cloned into the Oatp1a1 backbone. The correct orientation and sequence were confirmed by sequencing of both strands

on an ABI PRISM® 310 Genetic Analyzer (Applied Biosystems, Foster City, CA, U.S.A.). In functional assays with *X. laevis* oocytes, the His-tagged constructs could not be distinguished from the normal proteins.

For the construction of the chimeras, an overlap PCR approach was used. In a first round of PCR, two overlapping fragments (chimf and chimr primers are at the same position on the two cDNA strands and thus overlap) were produced with templates and primers according to Tables 1 and 2. After gel-purification of the amplification products, they were used as templates for a second round of PCR using the flanking primers (reverse and universal, Tables 1 and 2). These final amplicons contained the multiple cloning site of the original pSPORT1 vector and therefore were cut with the restriction enzymes *Sal*I and *Not*I. After gel-purification of the digested fragments they were directionally cloned into a *Sal*I-*Not*I cut pSPORT1 vector and their correct sequence was verified by sequencing both strands.

To introduce single amino acid mutations a similar overlap PCR approach was used. The middle primers (Table 2) contained the desired mutation and together with the flanking “reverse” and “universal” primers the mutation was introduced after two rounds of PCR. All constructs were verified by sequencing both strands.

Table 1

Primers used to prepare the different chimeras and mutants

Primer	Sequence (5' to 3')	
	Primers to introduce the His tag	
Oatp1a1f90	GAAGAAACAGAGAAAAAGATTGCA	
Oatp1a1rHis	TTAATGGTGATGGTGATGATGCAGCTTCGTTTTCAGTTCTCC	
Oatp1a4f122	GGAAAATCTGAGAAAAGGGTTGCA	
Oatp1a4rHis	TCAATGGTGATGGTGATGATGGTCCTCCGTCACTTTCGACCT	
	Primers for chimeras	Chimera
Reverse	CAGGAAACAGCTATGAC	All
Universal	TGTAAAACGACGGCCAGT	All
Chim1f	ATTTACATGCTTTTCATCCTTA	1/2
Chim1r	TAAGGATGAAAAGCATGTAAAT	1/2
Chim1af	TTACTGTCAAGAAAGCTGCA	3
Chim1ar	TGCAGCTTTCTTGACAGTAA	3
	Primers for mutations	Mutation[1]
Mut1for	AGTGTTCTCCAGGTGAATGCATTTATC	F328V
Mut1rev	GATAAATGCATTCACCTGGAGAACACT	F328V
Mut2for	CTCCAGTTCAATGGCTTTATCAATTCA	A330G
Mut2rev	TGAATTGATAAAGCCATTGAACTGGAG	A330G
Mut3for	GCATTTATCAATAAATTTACCTTCATG	S334K
Mut3rev	CATGAAGGTAAATTTATTGATAAATGC	S334K
Mut4for	TCCACTGCTGAGGCAGTCTTCCTTATG	V353A
Mut4rev	CATAAGGAAGACTGCCTCAGCAGTGGA	V353A
Mut5for	ACTGCTGAGGTAATATTCCTTATGGGT	V354I
Mut5rev	ACCCATAAGGAATATTACCTCAGCAGT	V354I
Mut6for	ATGGGTCTTTATAGCTTACCTCCAATA	M361S
Mut6rev	TATTGGAGGTAAGCTATAAAGACCCAT	M361S

[1] F328V means that the Phe-328 was replaced by a valine and so on.

Table 2

Templates and primers used to construct the different chimeras

Chimera	Template[1]	Forward primer 1st PCR	Reverse primer 1st PCR	Template 2nd PCR	Forward primer 2nd PCR	Reverse primer 2nd PCR
1	Oatp1a1 Oatp1a4	Reverse Chim1f	Chim1r Universal	Amplification product of 1st PCR	Reverse	Universal
2	Oatp1a4 Oatp1a1	Reverse Chim1f	Chim1r Universal	Amplification product of 1st PCR	Reverse	Universal
3	Oatp1a1 Oatp1a4	Reverse Chim1af	Chim1ar Universal	Amplification product of 1st PCR	Reverse	Universal

[1] The Oatp1a1 and Oatp1a4 templates were the His-tagged constructs described in the Materials and Methods section.

Functional characterization in *Xenopus laevis* oocytes I For *in vitro* synthesis of cRNA, the cDNA clones were linearized with *Not*I and capped cRNA was synthesized using the mMESSAGE mMACHINE T7 kit (Ambion, Austin, TX, U.S.A.). Oocytes were prepared and handled as described previously [13] and after an overnight incubation at 18 °C, healthy oocytes were injected with 50 nl water or 5 ng of the respective cRNA. After 3 days in culture, transport of radiolabeled substrates was measured at 25 °C in a medium containing 100 mM choline chloride, 2 mM KCl, 1 mM $CaCl_2$, 1 mM $MgCl_2$ and 10 mM HEPES/Tris, pH 7.5, as described previously [14]. Kinetics were determined at 15 minutes which was within the initial linear range (not shown). The obtained values, corrected with the values measured with water-injected oocytes, were fitted to the Michaelis-Menten equation using nonlinear regression analysis to obtain kinetic parameters.

Immunodetection of His-tagged proteins I Oocytes were injected with either 50 nl of water or with 5 ng of the respective cRNAs. After three days in culture they were fixed with 3 % paraformaldehyde in phosphate buffered saline (PBS) and after two washes with PBS frozen in Tissue Freezing Medium (Electron Microscopy Sciences, Fort Washington, PA, U.S.A.). Sections (10 μm) immobilized on gelatine coated slides were washed three times for 30 seconds with PBS, incubated for 5 minutes with 0.25 % Triton X-100 in PBS, and then washed three times for 30 seconds with PBS. Afterwards, the sections were blocked for one hour in 5 % normal goat serum and 0.1 % Triton X-100 in PBS. Following a wash step (3 times 10 minutes PBS), the sections were incubated for one hour with the Penta-His Antibody (QIAGEN GmbH, Hilden, Germany) at a 1:25 dilution in 2 % normal goat serum, 0.1 % Triton X-100 in PBS. After a wash step (three times 10 minutes PBS), the sections were incubated with a monoclonal Cy3 labeled goat-anti-mouse antibody (Jackson ImmunoResearch Laboratories, West Grove, PA, U.S.A.) at a 1:300 dilution in 2 % normal goat serum, 0.1 % Triton X-100 in PBS. After a final wash step (four times 10 minutes PBS) the sections were mounted and pictures were taken with a Zeiss Axiovert 25 (Karl Zeiss AG, Feldbach, Switzerland).

Cell culture and preparation of vaccinia virus I All cells were grown in monolayer cultures in a humidified incubator at 37 °C, in an atmosphere of 5 % CO_2. For the vaccinia viral stock preparation, BHK-21 cells (European Collection of Cell Culture, Wiltshire, UK) were used while transport studies were undertaken with HeLa cells (European Collection of Cell Culture, Wiltshire, UK). BHK-21 cells were maintained in Eagle's Minimal Essential medium supplemented with 2 mM L-glutamine, 1 mM sodium pyruvate, 0.1 mM non essential amino acids, 10% fetal bovine serum and 1% penicillin/streptomycin. High titer stocks of the modified vaccinia virus Ankara expressing the bacteriophage T7 RNA polymerase (MVA-T7pol, kindly provided by G. Sutter, Paul-Ehrlich-Institute, Langen, Germany) were obtained by infecting BHK-21 cells grown to subconfluence in 75 cm^2 culture flasks with virus (reconstituted from the stock obtained from G. Sutter) in 3 ml of medium for 1 hour at 37 °C [15]. The virus was then removed and replaced by fresh medium. Infected cells were incubated for 2 days at 37 °C. Cells were harvested in 5 ml fresh medium and underwent three rounds of freeze-thaw, first in dry ice/ethanol, then in a 37 °C bath. Before storage at -70 °C the virus solution was sonicated for 1 minute. To increase

the virus titer, BHK-21 cells were grown in 175 cm^2 flasks and infected with 2 ml of the 1st passage virus for 1 hour, for subsequent virus passages only 1 ml was used. After this, 30 ml of medium were added and the cells were cultured for 2 days before they were harvested in 15 ml medium and processed as described above. For the final amplification the harvested cells were centrifuged for 10 minutes at 1000 x g (IEC Centra-8R, International Equipment company, NEEDHAM HTS, MA) and the resulting pellet was resuspended in 1 ml 10 mM Tris (pH 9) per 175 cm^2 flask of infected cells and then underwent three rounds of freeze-thaw before 1 min of sonification. Before using these viral preparations in transport studies with HeLa cells, they were titrated by X-Gal staining as described [16] on 6-well plates.

Functional characterization using recombinant vaccinia virus-infected HeLa cells I HeLa cells were maintained in Eagle's Minimal Essential medium supplemented with 2 mM L-glutamine, 0.1 mM non essential amino acids, 10 % fetal bovine serum and 1% penicillin/streptomycin. Exponentially growing HeLa cells were harvested by trypsinisation and re-plated at a density of 1 x 10^5 in 1 ml growth medium in 24-well-plates twenty-four hours before virus adsorption and transfection.
Adsorption and infection with the MVA-T7pol virus for transient expression was done as follows. The vaccinia virus was thawed on ice and after 1 min of sonification, cells were infected with 10 pfu/cell in serum-free OptiMEM I medium. The vaccinia virus was allowed to adsorb for 60 minutes at 37 °C. Preliminary studies where HeLa cells were infected with increasing pfu/cell (not shown) demonstrated that 10 pfu/cell resulted in maximal transport rates. The virus-containing medium was removed after 60 minutes and, after washing the cells once, replaced by growth medium and transfection mixture. The transfection mixture consisted of 0.4 μg of expressing plasmid (the same cDNA used to prepare cRNA) or empty pSPORT1 as a control and 1 μl of the cationic lipid agent Lipofectamine™ 2000 (Invitrogen, Groningen, The Netherlands). The transfected cells were then incubated for 17 to 19 hours at 37 °C. After washing the cells three times with prewarmed (37 °C) uptake buffer (100 mM NaCl, 2 mM KCl, 1 mM $CaCl_2$, 1 mM $MgCl_2$ and 10 mM HEPES/Tris, pH 7.4) transport was initiated by adding 200 μl uptake buffer containing 0.4 – 0.7 μCi radiolabeled substrate with sufficient unlabeled compound to achieve the indicated concentration. Transport was terminated at designated times by four washes with

ice-cold uptake buffer. Cells were lysed with 250 μl 1 % Triton X-100. Cell associated radioactivity was measured by scintillation counting (PerkinElmer Life Sciences, Boston, MA) and the protein concentration was determined using the bicinchoninic acid protein assay kit (Pierce, Rockford,IL) [17]. Transport in transiently transfected HeLa cells with radiolabeled digoxin (0.25 μM), estradiol-17β-glucuronide (1 μM), DPDPE (0.1 μM) and taurocholate (20 μM) was measured in triplicates over the initial 2-minute-period. Kinetics for digoxin and DPDPE were determined at 30 seconds and 2 minutes respectively, which was within the linear range (not shown). Passive diffusion was determined by carrying out parallel experiments using the empty pSPORT1 vector, and this value was subtracted from the total transport determined in the presence of transporter DNA. Michaelis-Menten-type nonlinear curve fitting was carried out to obtain estimates of the maximal uptake rate (Vmax) and the apparent affinity constant (Km) (Sigmaplot for Windows 5.0, SPSS Inc., Chicago, IL and SYSTAT for Windows 8.0). All experiments were performed at least three times.

Statistical analysis I Data are presented as means ± S.E. Wildtype Oatp1a4 and the three mutants were analyzed using ANOVA (analysis of variance) for one-way analysis. As a post test, Bonferroni's Multiple Comparison Test was performed if overall $p<0.05$, which is taken as the limit denoting significant differences.

4.4 Results

Digoxin transport with chimeras between Oatp1a1 and Oatp1a4 I To examine the structural requirements for Oatp1a4-mediated transport, we produced chimeras between Oatp1a1, which does not transport digoxin, and Oatp1a4, which represents a high affinity digoxin transporter. Chimeras (Fig. 1) were prepared based on the high nucleotide sequence identity with primers that were identical for Oatp1a1 and Oatp1a4 (Tables 1 and 2) using an overlap PCR approach. Chimera 1 and 2 were constructed as mirror images containing TMH 1-7 of Oatp1a1 followed by the C-terminal TMH 8-12 of Oatp1a4 and TMH 1-7 of Oatp1a4 followed by the rest of Oatp1a1, respectively. Together with His-tagged wildtype Oatp1a1 and Oatp1a4 they were expressed in *X. laevis* oocytes. Initial uptake rates for digoxin were determined and expressed in percent of the uptake obtained for wildtype Oatp1a4-injected oocytes. Preliminary experiments revealed that the His-tagged Oatps transported typical substrates at the same rates as the wildtype Oatps (data not shown). Compared to Oatp1a4, only chimera 1 was able to mediate significant transport of digoxin (Fig. 1). Since this construct contained the C-terminal TMH 8-12 of Oatp1a4 and the reverse chimera 2 did not mediate digoxin transport, we concluded that TMH 8-12 are essential for Oatp1a4-mediated transport.

To further investigate how much of this C-terminal part of Oatp1a4 is needed for digoxin transport, an additional chimera was produced (chimera 3) and functionally tested in oocytes. In comparison to chimera 1, one additional TMH and some connecting amino acids, a total of 64 amino acids from Oatp1a1, were sufficient to completely abolish digoxin transport mediated by this chimeric protein in *X. laevis* oocytes (Fig. 1). Therefore, we concluded that this stretch of 64 amino acids from position 324 to 387 of Oatp1a4, is required for substrate transport and we further analyzed it in comparison to Oatp1a1 and Oatp1a5.

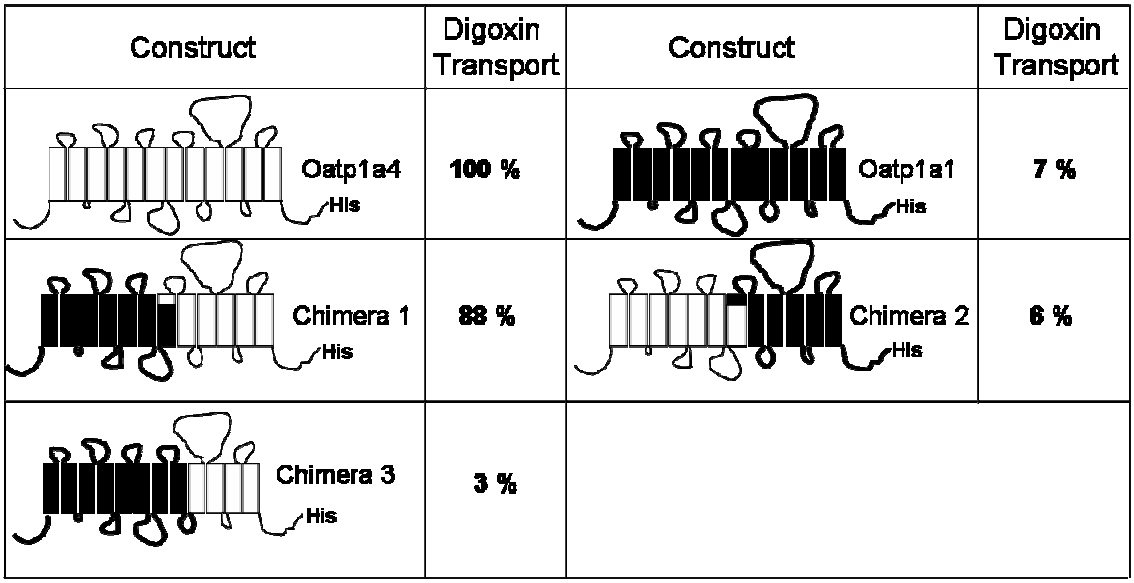

Fig. 1

Digoxin transport by wildtype and chimeric Oatp1a1 and Oatp1a4 constructs into *Xenopus laevis* oocytes I Oocytes were injected with 50 nl water or 5 ng cRNA of the respective His-tagged constructs and after three days in culture transport of 0.5 μM [^{3}H]-digoxin was determined at 25 °C with 9-12 oocytes per condition. Black boxes and thick lines represent Oatp1a1, white boxes and thin lines Oatp1a4. Values are given as percent of the initial transport rates obtained for wildtype Oatp1a4-injected oocytes and correspond to the mean of three (one for chimera 3) independent experiments.

Comparison of amino acids 324 to 387 of Oatp1a4 with Oatp1a1 and Oatp1a5 I

In order to identify single amino acids that are important for Oatp1a4-mediated substrate binding and/or transport, the 64 amino acids of Oatp1a4 were compared to the corresponding amino acids of Oatp1a1 and Oatp1a5 (Fig. 2A). The multiple alignment of both Oatp1a4 and Oatp1a5 with Oatp1a1 revealed that there are only 6 amino acid positions that differ in the digoxin transporters, Oatp1a4 and Oatp1a5, compared with Oatp1a1, the non-digoxin transporter (Fig. 2A, boxed). F328 of Oatp1a4 corresponds to a valine in Oatp1a1, A330 to a glycine, S334 to a positively charged lysine, V353 to an alanine, V354 to an isoleucine and M361 to a serine. As shown in Fig. 2B, these six amino acid residues are all located close to the extracellular border of TMH 7 and 8 in the predicted membrane topology of Oatp1a4.

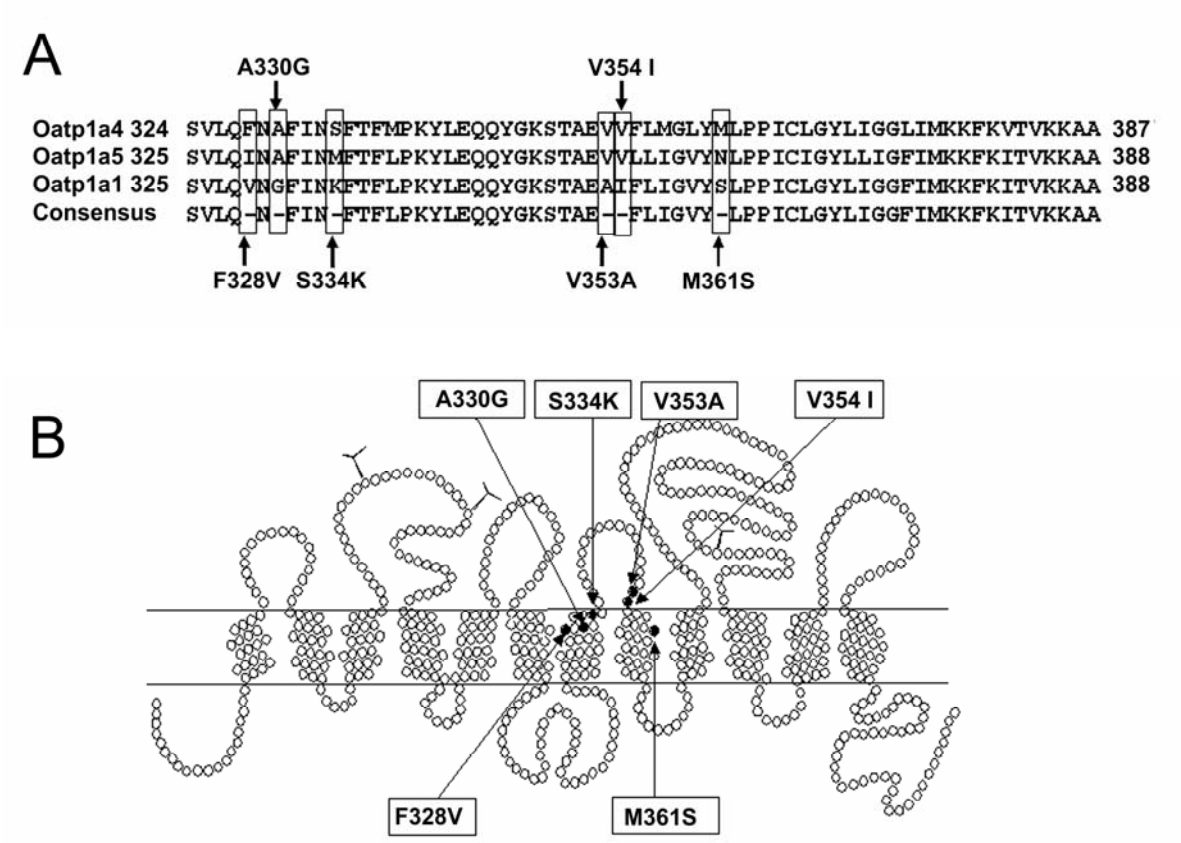

Fig. 2

Partial amino acid sequence alignment of rat Oatp1a4, Oatp1a5 and Oatp1a1 around TMH 7 and 8 (A) and location in the predicted membrane topology of Oatp1a4 based on hydrophobicity analysis (B) I (A), The 64 amino acids that were replaced from chimera 1 to chimera 3 (Fig. 1) are shown and the amino acid residues that differ between Oatp1a1 and both Oatp1a4 and Oatp1a5 are boxed and labeled. (B), Location of the six amino acid residues in the predicted membrane topology of Oatp1a4.

Site-directed mutagenesis of Oatp1a4 and functional characterization of Oatp1a4 mutants in *Xenopus laevis* oocytes I Because any of the identified amino acid residues could be important for Oatp1a4-mediated substrate transport, each of the six residues was changed individually in His-tagged Oatp1a4 to its counterpart amino acid residue in Oatp1a1 (Fig. 2, Table 1). The resulting mutant Oatp1a4 proteins were expressed in oocytes and digoxin transport was reapplied as a functional tool in order to compare initial rates of digoxin transport of the mutants to wildtype Oatp1a4.

As shown in Fig. 3, digoxin transport rates of mutants A330G, V353A and V354I were comparable to wildtype Oatp1a4. On the other hand, digoxin transport rates obtained with mutants F328V, S334K and M361S were clearly reduced when compared to wildtype Oatp1a4.

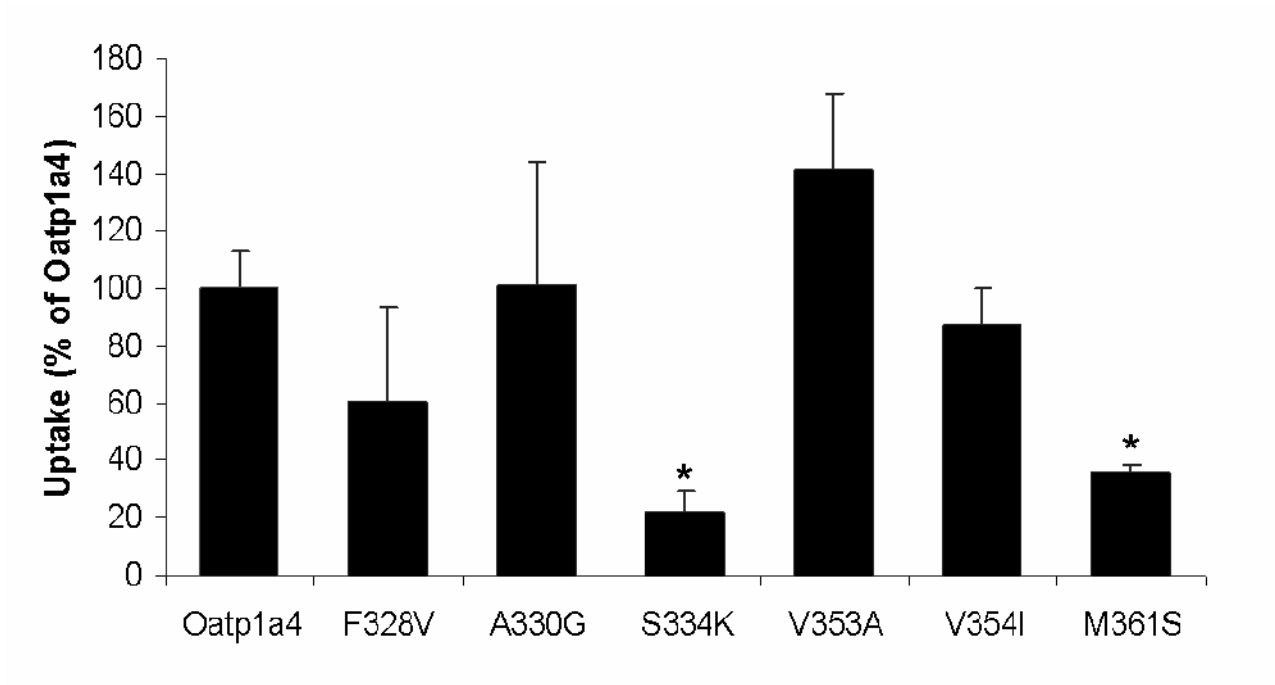

Fig. 3

Digoxin transport by wildtype and mutated Oatp1a4 into *Xenopus laevis* oocytes I Oocytes were injected with 50 nl water or 5 ng cRNA of the respective constructs and after three days in culture transport of 0.5 μM [^{3}H]-digoxin was determined at 25 °C with 9-12 oocytes per condition. Values represent the means ± SE of three independent experiments and are given as percent of the initial transport rates obtained for wildtype Oatp1a4-injected oocytes. * $p < 0.05$ compared to Oatp1a4.

Expression in *Xenopus laevis* oocytes and kinetic analysis of Oatp1a4 mutants F328V, S334K and M361S I Reduced digoxin uptake could be due to altered protein expression or translocation to the plasma membrane, a lowered binding affinity for digoxin (apparent *K*m) or a reduced maximal transport rate (Vmax). Therefore, we first tested the expression of the different mutants at the oocyte plasma membranes. Immunostaining of oocytes expressing the respective His-tagged constructs with an anti-His antibody is displayed in Fig. 4. In water-injected oocytes no fluorescence signal was obtained (Fig. 4A, B) while in oocytes expressing Oatp1a4 (Fig. 4C), or any one of the mutants F328V (Fig. 4D), S334K (Fig. 4E) and M361S (Fig. 4F) a clear fluorescence signal was observed in the plasma membrane indicating that the mutants were expressed at the membrane with no dramatic changes in protein expression and translocation.

To confirm these results, we performed kinetic analysis and determined the apparent Km values for digoxin uptake mediated by wildtype Oatp1a4 and the three mutants. The results are summarized in Table 3 and revealed that the apparent Km values for the mutant proteins were between 6 and 45 fold higher as compared to wildtype Oatp1a4, which means that the affinities for digoxin were 6- to 45- fold lower for the mutants. The order of affinity from high to low (Oatp1a4 > F328V > M361S > S334K) is the same as the transport rates shown in Fig. 3 and thus suggests that determination of a single uptake point in the linear portion of the uptake rate in oocytes is a valid means to test for potential mutations before doing time consuming kinetics.

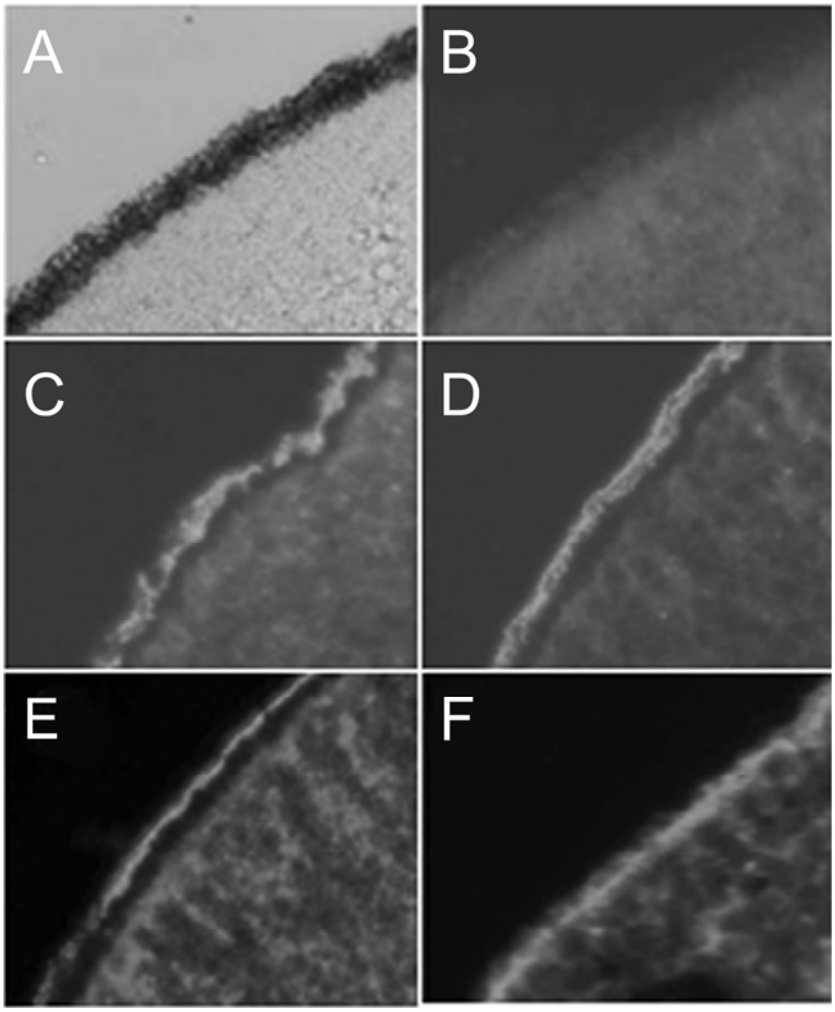

Fig. 4

Expression of wildtype and mutated Oatp1a4 in *Xenopus laevis* oocytes I Oocytes were injected with 50 nl water or 5 ng cRNA of His-tagged wildtype or mutated Oatp1a4. After three days in culture oocytes were fixed and cut as described in the Materials and Methods section. Immunodetection with a monoclonal anti-His antibody revealed a sign at the plasma membrane whereas fluorescence was absent in oocytes injected with water. (A) water-injected light microscopy control; (B) water-injected; (C) Oatp1a4; (D) F328V; (E) S334K; and (F) M361S.

Table 3

Apparent Km values for digoxin uptake mediated by wildtype Oatp1a4 and the three mutants

Construct	apparent Km (μM)
Oatp1a4	0.3 ± 0.3
F328V	1.7 ± 0.2
S334K	13.4 ± 1.6
M361S	8.8 ± 1.6

Initial (15 minutes) digoxin transport rates at increasing concentrations were determined at 25 °C in cRNA injected *X. laevis* oocytes after three days in culture. Transport values of two independent experiments were corrected with values obtained from water-injected control oocytes and the resulting net carrier-mediated uptake values were fitted by nonlinear regression analysis to the Michaelis-Menten equation.

Taurocholate and estradiol-17β-glucuronide transport by wildtype and mutated Oatp1a4 in *Xenopus laevis* oocytes I In order to test whether the observed functional effects are indeed a general phenomenon for Oatp1a4-mediated substrate uptake, initial transport rates were measured for two well known Oatp substrates, taurocholate and estradiol-17β-glucuronide.

Similarly to digoxin, we found that all three mutant proteins transported the two common substrates with strongly reduced transport rates when compared to wildtype Oatp1a4 (Fig. 5A and 5B) suggesting that the identified amino acid residues are important for overall Oatp1a4-mediated substrate transport.

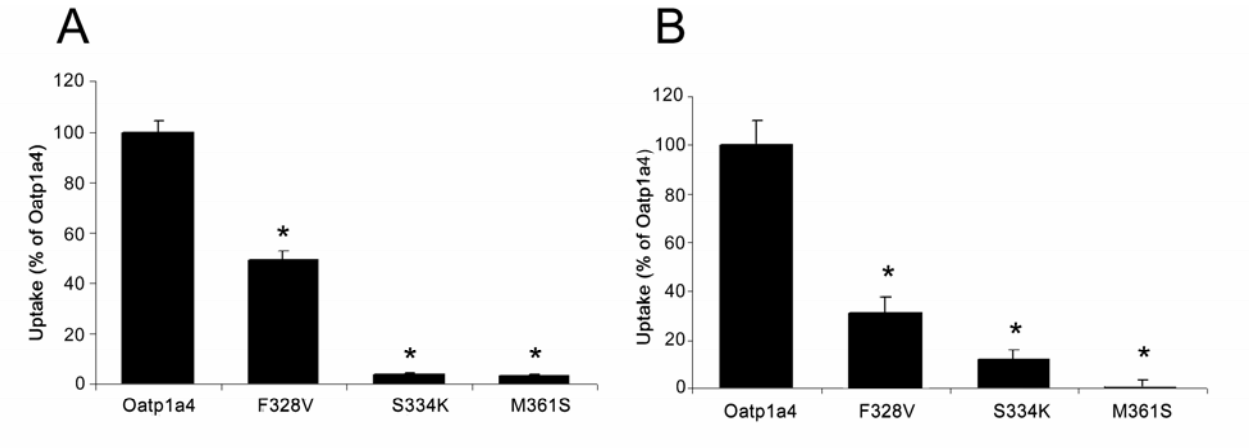

Fig. 5

Taurocholate (A) and estradiol-17β-glucuronide (B) transport by wildtype and mutated Oatp1a4 into *Xenopus laevis* oocytes I Oocytes were injected with 50 nl water or 5 ng cRNA of wildtype or mutated Oatp1a4. After three days in culture transport of [2-^{3}H]-taurocholic acid (20 μM) and [estradiol-6,2-^{3}H]-estradiol-17β-glucuronide (0.5 μM) were determined at 25 °C with 9-12 oocytes per condition. Values represent the means ± SE and are given as percent of the initial transport rates obtained for wildtype Oatp1a4-injected oocytes. *p<0.05 compared to Oatp1a4.

Substrate specificities of wildtype and mutated Oatp1a4 in HeLa cells I To validate the results obtained with the *X. laevis* oocytes system in a mammalian expression system, we used the vaccinia virus system to transiently express Oatp1a4 and the mutant proteins in HeLa cells. We first determined the kinetic parameters for Oatp1a4-mediated digoxin transport to compare them to the results obtained in oocytes. Digoxin transport in Oatp1a4-expressing HeLa cells was saturable with an apparent Km value of 0.6 ± 0.2 μM and a Vmax value of 2.9 ± 0.5 pmol/mg protein x min^{-1} (data not shown). This apparent Km value for Oatp1a4-mediated digoxin transport is very similar to the one obtained in oocytes (Table 3), which displayed that the two systems should yield similar results. Therefore, we determined initial transport rates for the Oatp1a4-specific substrate digoxin and estradiol-17β-glucuronide, taurocholate as well as DPDPE, substrates common to several Oatps, in HeLa cells transiently expressing either Oatp1a4 or one of the three mutant transporters. Transient expression of Oatp1a4 in HeLa cells resulted in only about twofold increase of digoxin, estradiol-17β-glucuronide and taurocholate transport rates. However, the induction of DPDPE transport was 3- to 5-fold higher in

HeLa cells transfected with Oatp1a4 as compared to cells transfected with the parental plasmid (not shown). The results in pmol/mg protein are summarized in Table 4 and show clearly that transport rates of the mutants are consistently lower than of wildtype Oatp1a4 for all the tested substrates, confirming the previous results obtained with oocytes expressing the transport proteins.

Table 4

Substrate specificity of Oatp1a4 and three mutants in HeLa cells

	Digoxin (0.25 μM)	Estradiol-17β-Glucuronide (1 μM)	DPDPE (0.1 μM)	Taurocholate (5 μM)
Oatp1a4	3.2 ± 0.4	2.3 ± 0.7	1.2 ± 0.3	7.6 ± 0.7
F328V	1.3 ± 0.7	1.3 ± 0.6	0.4 ± 0.1*	4.7 ± 1.4
S334K	2.0 ± 0.8	1.1 ± 0.2	0.4 ± 0.1*	5.3 ± 0.5
M361S	0.3 ± 0.3*	0 ± 0.4*	0.1 ± 0*	0.4 ± 0.2*

Oatp1a4, F328V, S334K and M361S were transiently expressed in HeLa cells and transport of [^{3}H]-digoxin, [estradiol-6,2-^{3}H]-estradiol-17β-glucuronide (0.5 μM), [Tyrosyl-2,6-^{3}H(N)]-D-Penicillamine-2,5 enkephalin (0.1 μM) and [2-^{3}H]-taurocholic acid (20 μM) was measured over an initial 2-min period. The values obtained in parallel experiments using the parental plasmid were subtracted from the total transport rates. Means ± SE of three independent experiments are given in pmol/mg protein.

* $p<0.05$ vs. wildtype Oatp1a4

Kinetic analysis of wildtype Oatp1a4 and the mutants F328V and S334K in HeLa cells I Because DPDPE transport rates for the mutants F328V and S334K were high enough, we performed kinetic analysis. As shown in Fig. 6 transport of increasing concentrations of DPDPE was measured and kinetic constants were calculated for wildtype Oatp1a4 (Fig. 6A), F328V (Fig. 6B) and S334K (Fig. 6C). The apparent Km value of 32 ± 17 μM for Oatp1a4 is in the same range as published earlier with oocytes by Gao et al. [18] and the Vmax value was 252.1 ± 48.6 pmol/mg protein x min^{-1} in our transient expression system. Consistent with the results for digoxin transport in oocytes, the apparent Km values for DPDPE transport mediated by the mutant proteins were approximately 5-fold higher than for wildtype Oatp1a4. Similarly, the maximal transport rates (Vmax values) were the same in test of significance for all tested constructs confirming the qualitative results obtained in oocytes.

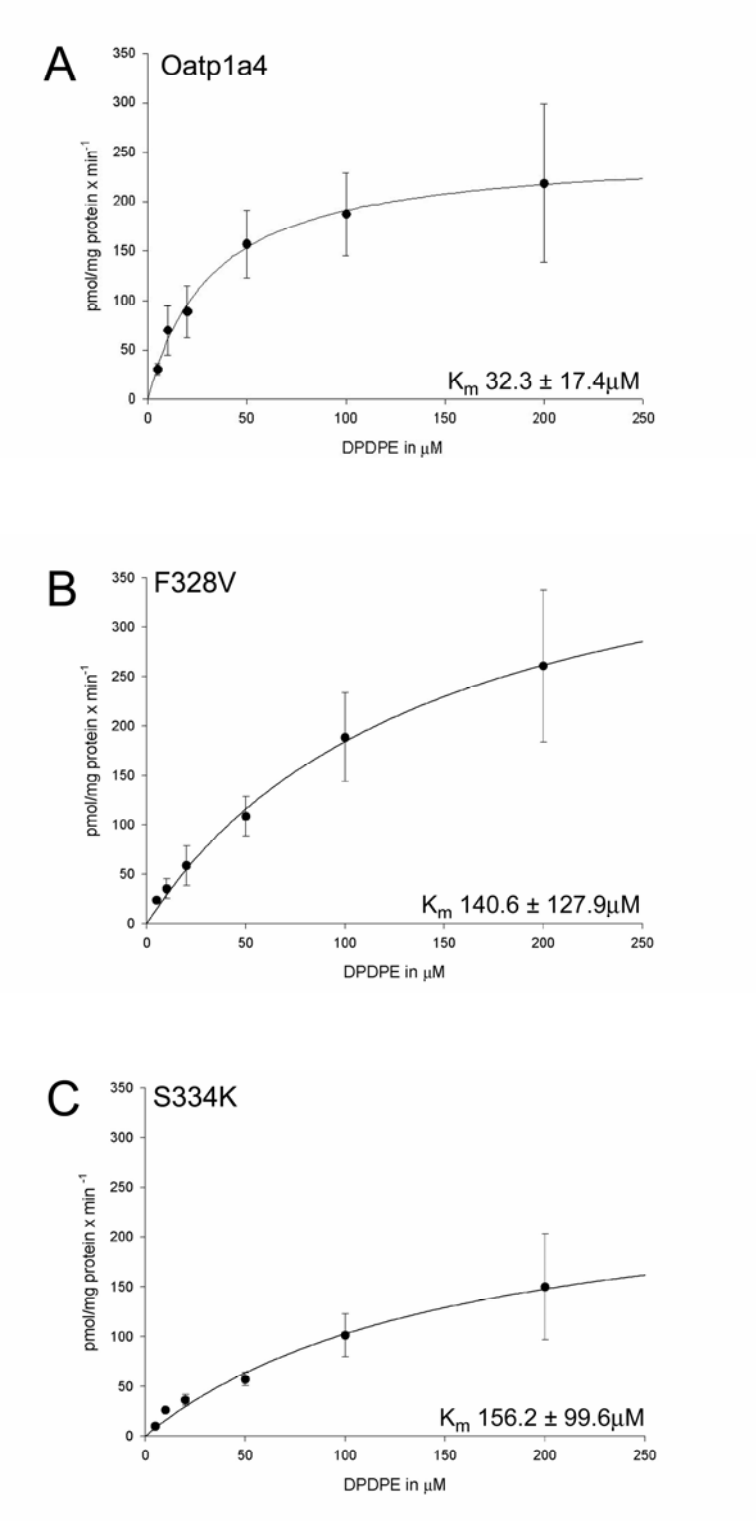

Fig. 6

Kinetics of DPDPE transport by wildtype and mutated Oatp1a4 in HeLa cells I Oatp1a4 (A), F328V (B) and S334K (C) were transiently expressed in HeLa cells and transport at increasing concentrations of DPDPE was determined over the initial 2-min period. Data are shown as the means ± SE of three or more independent experiments. Values were fitted to Michaelis-Menten equation using nonlinear regression analysis in order to obtain the kinetic parameters.

4.5 Discussion

In order to determine amino acids which are essential for Oatp1a4-mediated substrate recognition and transport, we constructed chimeras between Oatp1a4 and Oatp1a1 and used site-directed mutagenesis to replace individual amino acids in Oatp1a4 to the corresponding amino acids of Oatp1a1. We hypothesized, that using digoxin transport as a functional tool to distinguish between Oatp1a1 and Oatp1a4 function, we should be able to identify amino acid residues at or close to the Oatp1a4 substrate binding and/or transport site. The presented results obtained with chimeric constructs and mutated Oatp1a4 allowed us to identify three individual Oatp1a4 amino acids, F328, S334 and M361 that, when mutated to the corresponding amino acids found in Oatp1a1, resulted in a drastically compromised digoxin transport. Furthermore, using substrates that are transported by both, Oatp1a4 and Oatp1a1, we could demonstrate that these three amino acids also affect transport of common Oatp substrates such as DPDPE, taurocholate and estradiol-17β-glucuronide and therefore we conclude that they are important for overall Oatp1a4-mediated transport.

As a first step towards the elucidation of the substrate binding and transport site in Oatp1a4, we used the high amino acid sequence identity between Oatp1a1 and Oatp1a4 to prepare strategic chimeras and characterized them with respect to digoxin transport. The initial transport rates with these chimeric proteins revealed that the region around TMH 7 and TMH 8 is essential for Oatp1a4-mediated transport, since replacing it with the sequence from Oatp1a1 abolished transport completely. Thus, construction of chimeras between proteins of similar amino acid sequences can help to narrow down important protein parts to a few amino acids as has previously been shown for other transport proteins such as e.g. the Na^+/dicarboxylate and Na^+/sulfate cotransporters and the peptide transporters Pept1 and Pept2 [19, 20]. Upon closer inspection and comparison of the Oatp1a4 amino acid sequence with the sequences of both Oatp1a1 and Oatp1a5 in the region around TMH 7 and 8, six amino acid residues were identified, that could be crucial for Oatp1a4-mediated transport. However, only three amino acid residues were important for high affinity digoxin transport since the initial transport rate was clearly decreased only for the Oatp1a4 mutants F328V, S334K and M361S.

Mutations and polymorphisms often result in impaired membrane localization of transport proteins which could explain reduced transport rates [21, 22]. However, our

immunofluorescence data and mainly the kinetic results obtained with transfected HeLa cells indicated that this is not the case for the mutations we investigated and displayed that the kinetics of uptake were altered. Indeed, the apparent Km values for the three variants of Oatp1a4 were several fold higher than the ones of wildtype Oatp1a4, suggesting that the identified amino acid residues are directly involved in substrate binding or are important to keep the protein in an optimal structure for high affinity substrate binding. In a previous study, we identified and characterized the mouse orthologue of rat Oatp1a4 [23] and found an amino acid replacement in mouse Oatp1a4 which corresponds to the F328V mutation characterized in this study. Interestingly, the mouse Oatp1a4 mediates digoxin uptake with a much lower affinity (Km ~ 5.7 μM) as compared to rat Oatp1a4 [23] which supports our current findings that F328 plays an important role in high affinity substrate binding and/or transport.

Polymorphisms that do not affect protein expression have also been described and characterized in human OATP1B1 another multispecific member of the OATP1 family of transporters [24]. One of the identified polymorphisms led to an amino acid change of isoleucine at position 353 to threonine near TMH 7 and 8. The resulting mutant OATP1B1 had a 5-fold lower affinity for estrone-3-sulfate transport as compared to wildtype OATP1B1, suggesting that for the OATP1 family members the region around TMH 7 and 8 is important for substrate binding and/or transport unlike TMH 10 which has been reported to be important for substrate recognition in the OATP2A subfamily [8].

In order to extend the studies beyond digoxin transport and test whether the identified amino acid residues indeed affect overall Oatp1a4-mediated substrate transport, we tested uptake of additional typical Oatp substrates estradiol-17-β-glucuronide, taurocholate and DPDPE. The results clearly demonstrate that the three amino acid residues identified affected not only high affinity digoxin transport but also transport of substrates that are known as good substrates of Oatp1a1. Thus our prediction that using a chimera approach with digoxin to distinguish between Oatp1a1 and Oatp1a4 would allow us to identify amino acid residues that are important for overall Oatp1a4-mediated transport was confirmed.

We do not know at the moment whether these amino acid residues are important for the three-dimensional structure of Oatp1a4 or are directly involved in substrate recognition. The bulkiness of the side chains e.g. in the amino acid residues

methionine at position 361 (M361) and phenylalanine at position 328 (F328) could be important to maintain the protein in a conformation optimal for high affinity substrate transport. Its loss would then lead to altered affinities as also suggested in an earlier chimeric analysis of the glucose transporters Hxt1 and Hxt2 in yeast [25]. That the changed amino acids rather change the overall conformation of Oatp1a4 and not directly interact with substrate binding is also supported by kinetic and inhibition studies performed with Oatp1a4 which suggest that estradiol-17-β-glucuronide interacts at a recognition site different from that for taurocholate and digoxin [6].

Concomitant studies aiming at the generation of a theoretical structural model of representative OATP/SLCO superfamily members [26] emerged with some remarkable consideration concerning the location of the individual amino acids identified in our study. Analysis of the conservation pattern of representative OATPs identified the presence of a central pore that might be functionally significant. Measuring the electrostatic potential on the surface of the protein model showed that the putative pore was positive. This is consistent with a pore that is exposed to the aqueous phase and binding and transporting negatively charged compounds. The four sites F328V, S334, M361S and V354, face the pore in the theoretical models and may thus be expected to affect transport activity directly. Our findings with the oocytes expression system displayed affected transport efficiency after mutation for the former three sites as seen in Fig. 3. Moreover, A330G and V353A which have clearly no impact on transport efficiency, if mutated, are assumed to be buried in the models and are hence not expected to affect transport activity directly.

In summary, we have identified three amino acids which are essential for Oatp1a4-mediated transport. Mutations to the corresponding residue of Oatp1a1 decreased the apparent affinities for digoxin and DPDPE transport explaining the reduced transport rates. To further characterize and explain the underlying molecular mechanisms, additional experiments including crystallization of the substrate-transporter complexes in combination with functional characterization of point mutations of critical residues are required.

4.6 Acknowledgments

We thank Vasilije Vranic and Danielle Dres-Villard for their expert technical assistance.

4.7 References

1. Hagenbuch, B. and P.J. Meier, *Organic anion transporting polypeptides of the OATP/ SLC21 family: phylogenetic classification as OATP/ SLCO superfamily, new nomenclature and molecular/functional properties.* Pflugers Arch, 2004. 447(5): p. 653-65.
2. Hagenbuch, B. and P.J. Meier, *The superfamily of organic anion transporting polypeptides.* Biochim Biophys Acta, 2003. 1609(1): p. 1-18.
3. Kullak-Ublick, G.A., et al., *Organic anion-transporting polypeptide B (OATP-B) and its functional comparison with three other OATPs of human liver.* Gastroenterology, 2001. 120(2): p. 525-33.
4. Schuster, V.L., *Molecular mechanisms of prostaglandin transport.* Annu Rev Physiol, 1998. 60: p. 221-42.
5. Meier, P.J., et al., *Substrate specificity of sinusoidal bile acid and organic anion uptake systems in rat and human liver.* Hepatology, 1997. 26(6): p. 1667-77.
6. Sugiyama, D., et al., *Effect of 17 beta-estradiol-D-17 beta-glucuronide on the rat organic anion transporting polypeptide 2-mediated transport differs depending on substrates.* Drug Metab Dispos, 2002. 30(2): p. 220-3.
7. Pucci, M.L., et al., *Cloning of mouse prostaglandin transporter PGT cDNA: species-specific substrate affinities.* Am J Physiol, 1999. 277(3 Pt 2): p. R734-41.
8. Chan, B.S., J.A. Satriano, and V.L. Schuster, *Mapping the substrate binding site of the prostaglandin transporter PGT by cysteine scanning mutagenesis.* J Biol Chem, 1999. 274(36): p. 25564-70.
9. Chan, B.S., Y. Bao, and V.L. Schuster, *Role of conserved transmembrane cationic amino acids in the prostaglandin transporter PGT.* Biochemistry, 2002. 41(29): p. 9215-21.
10. Reichel, C., et al., *Localization and function of the organic anion-transporting polypeptide Oatp2 in rat liver.* Gastroenterology, 1999. 117(3): p. 688-95.
11. Cattori, V., et al., *Localization of organic anion transporting polypeptide 4 (Oatp4) in rat liver and comparison of its substrate specificity with Oatp1, Oatp2 and Oatp3.* Pflugers Arch, 2001. 443(2): p. 188-95.
12. Jacquemin, E., et al., *Expression cloning of a rat liver Na(+)-independent organic anion transporter.* Proc Natl Acad Sci U S A, 1994. 91(1): p. 133-7.
13. Hagenbuch, B., B.F. Scharschmidt, and P.J. Meier, *Effect of antisense oligonucleotides on the expression of hepatocellular bile acid and organic anion uptake systems in Xenopus laevis oocytes.* Biochem J, 1996. 316 (Pt 3): p. 901-4.
14. Hagenbuch, B., et al., *Functional expression cloning and characterization of the hepatocyte Na+/bile acid cotransport system.* Proc Natl Acad Sci U S A, 1991. 88(23): p. 10629-33.
15. Sutter, G., M. Ohlmann, and V. Erfle, *Non-replicating vaccinia vector efficiently expresses bacteriophage T7 RNA polymerase.* FEBS Lett, 1995. 371(1): p. 9-12.
16. Drexler, I., et al., *Highly attenuated modified vaccinia virus Ankara replicates in baby hamster kidney cells, a potential host for virus propagation, but not in various human transformed and primary cells.* J Gen Virol, 1998. 79 (Pt 2): p. 347-52.
17. Smith, P.K., et al., *Measurement of protein using bicinchoninic acid.* Anal Biochem, 1985. 150(1): p. 76-85.
18. Gao, B., et al., *Organic anion-transporting polypeptides mediate transport of opioid peptides across blood-brain barrier.* J Pharmacol Exp Ther, 2000. 294(1): p. 73-9.
19. Doring, F., et al., *Importance of a small N-terminal region in mammalian peptide transporters for substrate affinity and function.* J Membr Biol, 2002. 186(2): p. 55-62.
20. Pajor, A.M., et al., *The substrate recognition domain in the Na+/dicarboxylate and Na+/sulfate cotransporters is located in the carboxy-terminal portion of the protein.* Biochim Biophys Acta, 1998. 1370(1): p. 98-106.
21. Kameyama, Y., et al., *Functional characterization of SLCO1B1 (OATP-C) variants, SLCO1B1*5, SLCO1B1*15 and SLCO1B1*15+C1007G, by using transient expression systems of HeLa and HEK293 cells.* Pharmacogenet Genomics, 2005. 15(7): p. 513-22.
22. Michalski, C., et al., *A naturally occurring mutation in the SLC21A6 gene causing impaired membrane localization of the hepatocyte uptake transporter.* J Biol Chem, 2002. 277(45): p. 43058-63.
23. van Montfoort, J.E., et al., *Functional characterization of the mouse organic-anion-transporting polypeptide 2.* Biochim Biophys Acta, 2002. 1564(1): p. 183-8.

24. Tirona, R.G., et al., *Polymorphisms in OATP-C: identification of multiple allelic variants associated with altered transport activity among European- and African-Americans.* J Biol Chem, 2001. 276(38): p. 35669-75.
25. Kasahara, T., M. Ishiguro, and M. Kasahara, *Comprehensive chimeric analysis of amino acid residues critical for high affinity glucose transport by Hxt2 of Saccharomyces cerevisiae.* J Biol Chem, 2004. 279(29): p. 30274-8.
26. Meier-Abt, F., Y. Mokrab, and K. Mizuguchi, *Organic anion transporting polypeptides of the OATP/SLCO superfamily: identification of new members in nonmammalian species, comparative modeling and a potential transport mode.* J Membr Biol, 2005. 208(3): p. 213-27.

CHAPTER 5

Functional Expression of Rat Oatp1a1 and Rat Ntcp in Sf9 Cells and Functional Reconstitution of Solubilized Rat Ntcp

5.1 Abstract

Multispecific rat Oatp1a1 (*Slco1a1*) and the rat Na^+/bile salt cotransporter Ntcp (*Slc10a1*) were expressed in Sf9 insect cells using the baculovirus expression system. Western blot analysis confirmed expression of the two transport proteins. Sf9 cells infected with Oatp1a1 and Ntcp recombinant baculoviruses clearly exhibited substrate uptake, while wildtype-infected Sf9 cells did not accumulated any substrate investigated. Unexpectedly, Oatp1a1-mediated transport could not be confirmed with Oatp1a1 Sf9 membrane vesicles. An exterior pH 6, applying an inwardly directed H^+-gradient, did not stimulate estrone-3-sulfate uptake into Sf9 vesicles, although a pH-dependent transport mechanism of Oatp1a1 has been proposed by other research groups. However, in Sf9 membrane vesicles isolated from Ntcp-expressing cells Ntcp successfully accumulated taurocholate in a sodium-dependent manner. Focus was therefore laid on the cotransporter Ntcp. Suitable conditions for direct solubilization were obtained with 0.4% of the detergent FOS-choline-16. Highest Ntcp-recovery turned out to be at ~ 1.8 mg protein of Ntcp Sf9 membrane vesicles per ml. Functional activity of solubilized Ntcp was proven with subsequent reconstitution into artificial liposomes. These proteoliposomes accumulated taurocholate sodium-dependently in the same range as shown with Ntcp Sf9 membrane vesicles. It is therefore assumed that the conformation of Ntcp found in Sf9 membrane vesicles and after reconstitution is similar to conformation in intact liver cells.

With these studies an expression system has been established which allows readily solubilization of functional Ntcp. For future isolation of purified Ntcp this system will enable analyses required to investigate the transport-competent protein structure of Ntcp.

5.2 Introduction

Rat organic anion transporting polypeptide 1a1 (Oatp1a1, *Slco1a1*) and the Na^+/taurocholate cotransporting polypeptide (Ntcp, *Slc10a1*) are both expressed in rat liver at the basolateral membrane of hepatocytes. Oatp1a1 is multispecific and mediates transmembrane transport of a wide range of endogenous and exogenous organic compounds (see also Introduction Chapter 1, Table 1). Ntcp, on the other hand, has much narrower substrate specificity. Principally Ntcp is responsible for transport of unconjugated and conjugated bile salts into hepatocytes [1].

Knowledge about the transport mechanism of Oatp1a1-mediated transport is moderate. It is well established that Oatps/OATPs act in a sodium-independent manner and are capable of mediating anion exchange [2, 3]. Investigations with Oatp1a1 expressed in *Xenopus laevis* oocytes, in HeLa cells and in CHO cells suggested HCO_3^-, GSH or glutathione-S-conjugates as an anion being exchanged [4, 5]. Different research groups pursued the investigation of the transport mode and suggested a pH-dependent transport mechanism [6, 7]. According to Satlin and co-workers an inwardly directed H^+-gradient stimulated taurocholate (TC) transport into HeLa cells expressing Oatp1a1 (pHi>pHo) [8]. Furthermore unpublished data from our laboratory suggest as well that Oatp/OATP-mediated uptake is either mediated with OH^-- (HCO_3^-) exchange or H^+-cotransport (see ETH PhD Thesis Nr.17208, Simone Leuthold). This hypothesis is based on investigations of Oatp1a1 and several other members of the OATP1 family upon the effect of the extra cellular pH on Oatp-mediated substrate transport. With reference to transport mechanism Ntcp is well-defined as a Na^+/bile salt cotransporter. Thus driving force is an inwardly directed electrochemical Na^+-gradient. This gradient is maintained by the basolateral Na^+/K^+-ATPase as well as the negative intracellular potential [9, 10].

Most membrane transport proteins are present at low concentrations in their native tissue. Their overexpression is a requirement for direct solubilization and reconstitution. Sf9 cells are used as a high-level expression system and several mammalian membrane transport proteins have been successfully expressed and were functionally characterized in cells or in isolated membrane vesicles, amongst others rabbit Na^+/Glucose cotransporter [11], rat renal Na^+/Phosphate and Na^+/Sulfate cotransporters [12] and several ATP binding cassette (ABC) transporters [13-15]. For our investigations Oatp1a1 and Ntcp were expressed in Sf9 cells using recombinant baculoviruses.

Solubilization is one of the first steps towards isolation of a membrane transport protein. Full isolation of a purified transport protein is a still prerequisite for characterization of structural properties and necessary for a complete molecular description of the function of transport-competent protein. The main problem associated with the functional isolation stems from the instability of the transport protein towards the harsh conditions during the processing for purification. Therefore the determination of the proper conditions for solubilization and reconstitution into an environment approximately the native membrane is an important first part of the strategy. Starting material originating from a high-yield expression system with large quantities is required. Effective solubilization of membrane proteins requires both, the selection of a detergent and appropriate solubilization conditions [16-18].

It is of capital importance that the detergent does affect neither secondary nor tertiary structure of the protein irreversibly, as this might impact functionality. Subsequent reconstitution enables measurement of functional activity. In case of membrane transport proteins the maintenance of functional activity can be conveniently followed by substrate transport into vesicles. As a reconstituted transporter is isolated in an artificial lipid bilayer, functional studies are easily possible. No complications from other membrane components occur, as it might be in a viable cell. To our knowledge rat Oatp1a1 and Ntcp have neither been isolated before from their natural lipidic environment nor from any heterologous expression system.

With this study we pursued two objectives: The first aim was to establish standard methods for functional expression of Oatp1a1 and Ntcp in Sf9 cells. Secondly, we determined suitable conditions for direct solubilization of Ntcp Sf9 membrane vesicles with subsequent functional reconstitution into artificial liposomes.

.

5.3 Materials and Methods

Materials I Radiolabelled [^{3}H]-taurocholate (1.2 Ci/mmol) and [^{3}H]-estrone-3-sulfate (57.3 Ci/mmol) were purchased from Perkin Elmer Life Sciences (Boston, MA, USA). The sodium salt of taurocholic acid and soya-bean asolectin were obtained from Fluka Chemie (Buchs, Switzerland). Cholesterol was from SIGMA (St.Louis, MO, USA) and the detergents used for solubilization were acquired as follows: n-octyl-β-D-glucopyranoside (OG), n-dodecyl-β-D-maltopyranoside (DDM) and FOS-choline-16 (FOS-16) from Anatrace (Maumee, OH, USA) and CHAPS from Applichem (Darmstadt, Germany). Cell culture media and reagents were purchased from Invitrogen (Groningen, The Netherlands) and BD Biosciences (Eremodegem, Belgium). Sf9 insect cells were obtained from BD Biosciences. All other chemicals were of the highest purity available from commercial sources.

Expression of rat Ntcp and Oatp1a1 in Sf9 insect cells I Sf9 (*Spodoptera frugiperda*) insect cells were maintained in Grace's insect cell culture medium supplemented with 10% foetal bovine serum (heat-inactivated) and 1 % penicillin/streptomycin and were grown as a monolayer culture in a humidified incubator at 27 °C. Recombinant wildtype (WT) baculovirus and baculoviruses carrying Ntcp and Oatp1a1 used for Sf9 cell infections had been generated in our laboratory prior to this study using the Bac-to-Bac® Baculovirus Expression System (Invitrogen) (data not shown). The viral titers were determined by serial dilutions, investigating its effect on the viability of Sf9 cells. A tetrazolium salt, MTT dye [19], was utilized giving a quantifiable colorimetric reaction assessing the virus's effect in accordance with the virus titer.

5 x 10^6 Sf9 cells per 10 cm dish or 55 x 10^6 Sf9 cells per 24.5 x 24.5 cm square plate were infected with recombinant viruses. Before adding the virus, Sf9 cells were routinely seeded and allowed to attach for one hour. Infections with WT control baculoviruses were performed at a multiplicity of infection (MOI) of 5, whereas infections with Ntcp baculoviruses were performed at a MOI of 20 and with the Oatp1a1 baculoviruses at a MOI of 7. Cells were harvested three days after infections and used for transport studies either in suspension or after the isolation of membrane vesicles.

Transport studies with Sf9 cells I To confirm the functionality of rat Ntcp and Oatp1a1 expressed in insect cells, transport studies with Sf9 cells in suspension were performed. 1 x 10^6 cells were washed twice with 1 ml Grace's insect medium supplemented with 1 % penicillin/streptomycin, with centrifugation steps in between for 2 min at 1000 x g. Ntcp-expressing cells were then resuspended in 250 µl uptake buffer, which consisted of 5 mM D-glucose, 5 mM $MgCl_2$, 3 mM $CaCl_2$, 122 mM NaCl or CholineCl and 10 mM MES/Tris, pH 6.5 supplemented with 10 µM [^{3}H]-taurocholate. The uptake buffer for cells expressing Oatp1a1 consisted of 5 mM D-glucose, 5 mM $MgCl_2$, 3 mM $CaCl_2$, 122 mM NaCl and 10 mM MES/Tris, pH 6.0 or 10 mM HEPES/Tris, pH 7.5 supplemented with 10 µM [^{3}H]-taurocholate or 0.5 µM [^{3}H]-estrone-3-sulfate. Transport was allowed to take place for 15 min at 25°C and was then stopped by adding 1 ml uptake buffer containing 1 mM taurocholate and 122 mM CholineCl. Cells were lysed with 1% Triton X-100 and the retained radioactivity determined by liquid scintillation counting (PerkinElmer Life Sciences, Boston, MA, USA). Protein concentrations were measured using the bicinchoninic acid (BCA) protein assay kit (Pierce, Rockford, IL, USA) [20].

Isolation of Sf9 membrane vesicles I Isolation of membrane vesicles from virus-infected Sf9 cells was performed as described by Gerloff and co-workers [21]. In brief, Sf9 cells were scraped from culture dishes, centrifuged for 10 min at 1400 x g at 4°C and homogenized with 20 strokes with a glass-Teflon tissue homogenizer in 50 mM mannitol, 2 mM EGTA, 50 mM Tris/HCl, pH 7.0, 1 µg/ml leupeptin/antipain and 0.5 mM phenylmethylsulfonyl fluoride. Undisrupted cells, nuclear debris, and large mitochondria were then pelleted at 500 x g for 10 min at 4°C. The supernatants were centrifuged for 1 hour at 100 000 x g. The resulting pellets containing membrane vesicles were resuspended by repeated syringing (20 times) through 25-gauge needles in 250 mM sucrose, 0.2 mM $CaCl_2$, 20 mM HEPES/Tris, pH 7.5 for Ntcp Sf9 vesicles. This medium had been prefiltered through 0.45 µm cellulose nitrate filters and will be referred to as SMS (standard membrane suspension buffer) throughout this chapter. For the Oatp1a1-expressing Sf9 vesicles the SMS consisted of 250 mM sucrose, 0.2 mM $CaCl_2$, 100 mM NaCl and 20 mM HEPES/Tris, pH 7.5. Total protein concentrations were determined using the BCA protein assay kit. Vesicles were snap-frozen in liquid nitrogen and stored until required for transport studies.

Transport studies with Sf9 membrane vesicles I Transport into freshly thawed Sf9 vesicles isolated from WT-infected, Ntcp- or Oatp1a1-expressing Sf9 cells was determined by a rapid filtration assay as described before [21, 22]. All solutions for the Ntcp Sf9 vesicle uptake were prepared with reference to transport studies with basolateral rat liver plasma membrane vesicles in Zimmerli et al [22]. For transport studies, Sf9 vesicle suspensions were diluted with SMS to the desired protein concentration (3.5 μg/μl) and Sf9 vesicles were then incubated at 37 °C in the uptake buffer. The latter had been prefiltered through 0.45 μm cellulose nitrate filters and consisted of 62.5 mM sucrose, 0.2 mM $CaCl_2$, 6.25 mM $MgCl_2$, 125 mM NaCl or KCl and 20 mM HEPES/Tris, pH 7.5 supplemented with 1 μM [^{3}H]-taurocholate for Ntcp Sf9 vesicles. The uptake buffer for Oatp1a1 Sf9 vesicles contained 250 mM sucrose, 0.2 mM $CaCl_2$, 6.25 mM $MgCl_2$, 100 mM NaCl and 50 mM MES/Tris, pH 6.0 and was supplemented with 0.5 μM [^{3}H]-estrone-3-sulfate. Transport studies were carried out by adding 80 μl of the uptake buffer to 20 μl of vesicle suspension (70 μg protein/uptake), which had been preincubated in a tube at 37°C for 1 min. The tube was mixed vigorously and returned to a water bath for varying times. After the time periods indicated, uptake was terminated by addition of 3 ml ice-cold stop solution containing 100 mM sucrose, 5 mM $MgCl_2$, 0.2 mM $CaCl_2$, 100 mM KCl and 20mM HEPES/Tris, pH 7.5 for Ntcp Sf9 vesicles and 50 mM sucrose, 5 mM $MgCl_2$, 0.2 mM $CaCl_2$, 100 mM NaCl and 50 mM MES/Tris, pH 6.0, for Oatp1a1 Sf9 vesicles. Mixtures were vacuum-filtered rapidly through 0.45 μm cellulose nitrate filters (Sartorius AG, Goettingen, Germany), which had been pre-soaked in cold deionized water. In case of taurocholate transport studies the filters had been additionally rinsed with 2 ml of 1 mM unlabelled taurocholate, in order to reduce adherence of the bile acid to the filter. The test tubes were rinsed twice with additional 3 ml of the stop solution and the filter was then washed with a final 3 ml of stop solution. Vesicle-associated radioactivity retained on the filters was determined by liquid scintillation counting. All Sf9 vesicle determinations were corrected for a 0-time-point at which addition of radio labelled substrate was followed immediately by 3 ml of ice-cold stop solution with subsequent washing-steps described above. Measurements were performed in triplicates and were confirmed with at least two separate membrane preparations.

Western blotting I Proteins in the Sf9 membrane vesicles (50-70 μg of total protein) or fractions of soluble and insoluble proteins were resolved by electrophoresis on an 8 % (w/v) sodium dodecyl sulfate polyacrylamide gel. Protein samples were mixed with Lämmli's sample buffer, with bromphenol blue as a tracking dye [23] and were then boiled for 1 min for complete denaturation. Following gel electrophoresis, proteins were transferred electrophoretically onto nitrocellulose membranes (Amersham Biosciences, Otelfingen, Switzerland) according to standard procedures [24]. After blocking hydrophobic and non-specific binding sites of the membranes with 5% milk (BIORAD, Reinach, Switzerland) diluted in Tris-buffered saline containing 0.2% Tween 20, the blots were probed with Ntcp and Oatp1a1 antibodies. The rabbit polyclonal Ntcp and Oatp1a1 antibodies raised against the C-terminal ends of Ntcp and Oatp1a1, had been previously generated in our laboratory [25, 26] and served as primary antibodies. Specificities of the Ntcp and Oatp1a1 antisera were tested with isolated basolateral rat liver plasma membranes [25, 27] (data not shown). The membranes were incubated for 2 hours with the Ntcp antibody at a dilution of 1:6000, while the Oatp1a1 antibody was at a 1:1000 dilution. Subsequently, the secondary antibody, a commercially available horse-radish peroxidase-conjugated goat anti-rabbit antibody (Amersham Biosciences, Otelfingen, Switzerland), was used at a dilution of 1:30000. Bound antibodies were visualized with Uptilight HRP blotting chemiluminescent substrate (Interchim, Montluçon Cedex, France) and subsequent autoradiography on a KODAK image station 2000MM analyzer (Eastman Kodak Co., Rochester, NY, USA).

Detergent solubilization of Ntcp Sf9 membrane vesicles and reconstitution of Ntcp in proteoliposomes I Solubilization of Sf9 vesicles was performed either in a final volume of 200 μl or for subsequent reconstitution experiments in a final volume of up to 7ml (≤ 30% of the void volume of the used gel filtration column, see below). Thus Sf9 vesicles were diluted with ice-cold solubilization buffer containing 100 mM KCl and 20 mM Tris/HCl, pH 7.5, supplemented with the respective detergents at the concentration indicated. Optimal solubilization conditions were determined as described in the results section. The solubilization reactions were vortexed several times during 1 hour incubation on ice. Insoluble material was collected as a pellet after centrifugation at 100 000 x g for 1 hour. The soluble and insoluble fractions

were assayed for protein concentrations; and in equal aliquots the presence of Ntcp was assessed by Western blot analysis using the Ntcp antiserum as described above. The clear supernatants will be referred to as the fraction of soluble proteins "Sol", while the fraction of insoluble proteins is abbreviated "Insol".

Reconstitution was performed by reincorporation of the solubilized Ntcp into the lipid bilayer of liposomes, followed by rapid removal of the detergents using gel filtration. For this purpose 4 - 6 mg soya-bean asolectin with membrane stabilizing cholesterol (m/m ratio 9:1) [28, 29] was dissolved in diethylether and the samples were evaporated to dryness under a gentle stream of nitrogen gas. In order to ensure total removal of the organic solvent, the round bottom flask with lipids was vacuum dried for 1 hour. The thin film of lipids was dispersed with the clear solubilizate containing Ntcp, derived from the solubilization described above. The mixture was then allowed to form proteoliposomes with slight shaking for 1 hour at 4°C.

Removing the FOS-choline-16 from the mixed micellar solutions was performed by gel filtration by means of a Sephadex G-50 (fine) column (1 x 30 cm, BIORAD, Reinach, Switzerland). The column was pre-equilibrated and eluted at a rate of 0.75 ml/min with solubilization buffer. Fractions of 1.5 ml containing proteoliposomes were collected, as determined by turbidity measurements at 280nm, and pooled. The presence of Ntcp was confirmed by Western blotting. Proteoliposomes with incorporated Ntcp were then harvested by high-speed centrifugation at 290 000 x g for 1.5 hours. Recovered proteoliposomes were immediately resuspended in SMS, and homogenized by 20 passages through a 25-gauge needle. After protein determination with a BCA assay the proteoliposomes were kept on ice until used for taurocholate uptake by the rapid filtration assay.

Transport studies into proteoliposomes I In order to test functionality of the reconstituted Ntcp, uptake measurements into proteoliposomes was performed. These uptake measurements were carried out with reference to Sf9 membrane vesicles transport studies. Proteoliposome suspension was used in 20 µl aliquots (each containing 40-70µg protein) and mixed with 80 µl of Ntcp uptake buffer containing 125 mM NaCl or CholineCl and supplemented with 1µM or 10µM [^{3}H]-taurocholate. Timed uptake reactions were terminated with ice-cold stop solution as described before for transport studies with Sf9 membrane vesicles. Radioactivity associated with proteoliposomes was determined by liquid scintillation counting. All determinations were corrected for a 0-time-point.

5.4 Results

Oatp1a1 expression and functional characterization in Sf9 insect cells I Prior to functional studies, recombinant baculovirus infection conditions were optimized, i.e. maximal Oatp1a1 expression with minimal MOI was investigated by Western blot analysis. Varying the MOI from 5 up to 15 revealed that expression did not accumulate past 7 MOI 3 days post-infection (data not shown). Thereafter we routinely infected Sf9 cells with Oatp1a1 baculovirus at a MOI of 7 pfu and harvested cells after 3 days. In Fig. 1 Sf9 cells infected with Oatp1a1 baculovirus were monitored by the use of a polyclonal antiserum [26] and showed expression of the protein. 70μg of total protein, the amount used for aliquots doing later transport studies with Sf9 membrane vesicles, was loaded onto the gel. As evident in Fig. 1 proteins migrate as two broad bands at ~ 80kD and at ~ 55kD, respectively. No bands are present in WT-infected control cells, when using the same Oatp1a1 antiserum. Using isolated basolateral rat liver plasma membranes, mature *N*-glycosilated Oatp1a1 migrates as one broad band at ~ 86 ± 6 kDa [26, 30].

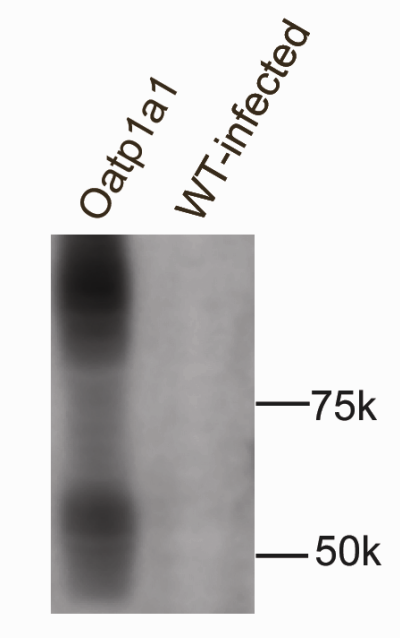

Fig. 1

Expression of Oatp1a1 in baculovirus-infected Sf9 insect cells I Western blot analysis of membrane vesicles isolated from Oatp1a1-expressing and wildtype (WT)-infected Sf9 cells (70μg of protein/lane). Sf9 cells were infected with Oatp1a1 recombinant baculovirus at a MOI 7 and with control WT baculovirus at a MOI of 5, both for 3 days. Molecular weight markers are indicated in kilodaltons.

The Oatp1a1 protein synthesis in Sf9 cells has been clearly demonstrated. However, we wished to measure transport function in these cells. For this purpose two well-established Oatp1a1 substrates were chosen: Estrone-3-sulfate (E3S) and the bile acid taurocholate (TC). Transport into Oatp1a1-expressing Sf9 cells was measured. In order to investigate a possible pH-gradient dependent transport mechanism we carried out Sf9 cell transport studies with an inwardly directed H^+-gradient. E3S transport was investigated with external pH (pHo) 7.5 as well as with pHo 6.0. Oatp1a1-infected Sf9 cells, pHo 7.5, incorporated more than twofold more E3S than WT-infected Sf9 cells (Fig. 2). Acidification with pHo 6.0 increased E3S uptake even more during the whole time course.

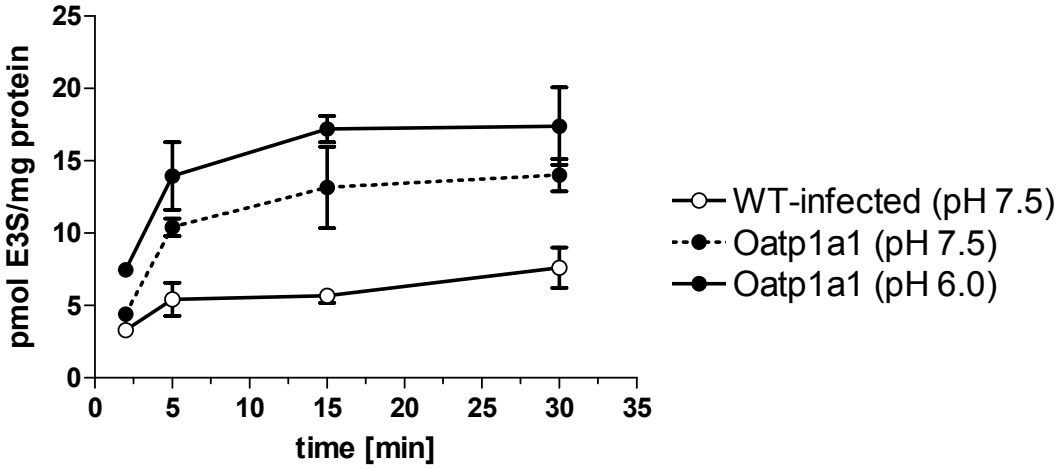

Fig. 2

Time course of estrone-3-sulfate transport into Oatp1a1-expressing Sf9 cells I Transport of [^{3}H]-estrone-3-sulfate (0.5 μmol/l) was determined 3 days after infection in Oatp1a1-expressing and WT-infected cells at 25°C for 15 min. Uptake buffers were of pH 6.0 or 7.5. Data represent the means ± SD of triplicate determinations from at least two infections.

The second substrate investigated showed the same phenomenon as found for E3S. As evident from the results in Fig. 3 taurocholate transport into Oatp1a1-expressing Sf9 cells is clearly higher than into WT-infected cells during the whole time course up to 30 min. This stimulation of TC transport can be associated with Oatp1a1.

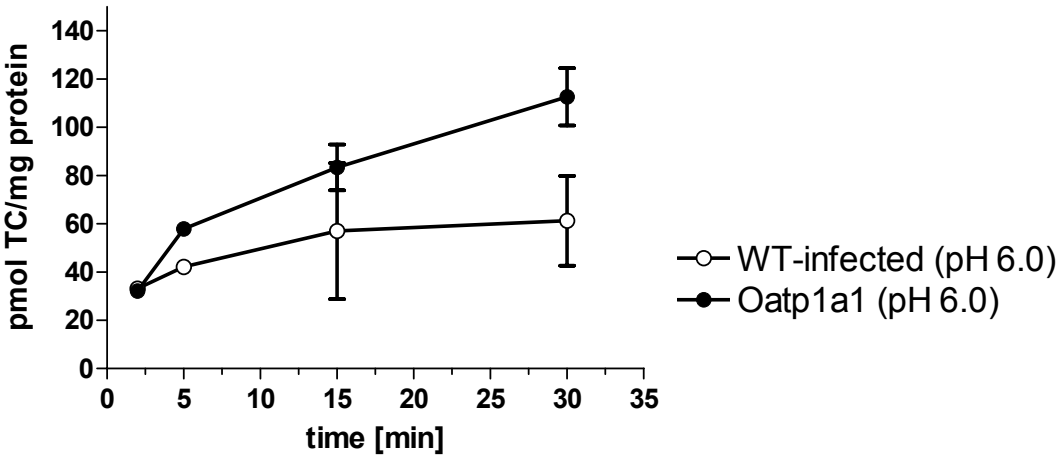

Fig. 3

Time course of taurocholate transport into Oatp1a1-expressing (●) and WT-infected (○) Sf9 cells I Transport of [^{3}H]-taurocholate (10 μmol/l) was determined 3 days after infection at 25°C for 15 min in uptake buffer with pH 6.0. Data represent the means ± SD of triplicate determinations from at least two infections. Some variability is smaller than the symbols.

Functional characterization of Oatp1a1 in Sf9 membrane vesicles I The uptake conditions from transport studies in Sf9 cells, namely the acidic pHo 6.0, were transferred to transport studies with Sf9 membrane vesicles isolated from Oatp1a1-expressing Sf9 cells. Sf9 membrane vesicles allow the variability of pHi and pHo, a requirement for further studies on the pH-gradient as a possible driving force of Oatp1a1. The experiments with Oatp1a1 Sf9 vesicles with pHi/pHo 7.5/6.0 revealed unexpected results. E3S transport can not be associated with Oatp1a1 function. In Fig. 4 the time courses for E3S uptake look the same and are not distinguishable, whether Sf9 cells expressed Oatp1a1 or were infected with WT baculovirus.

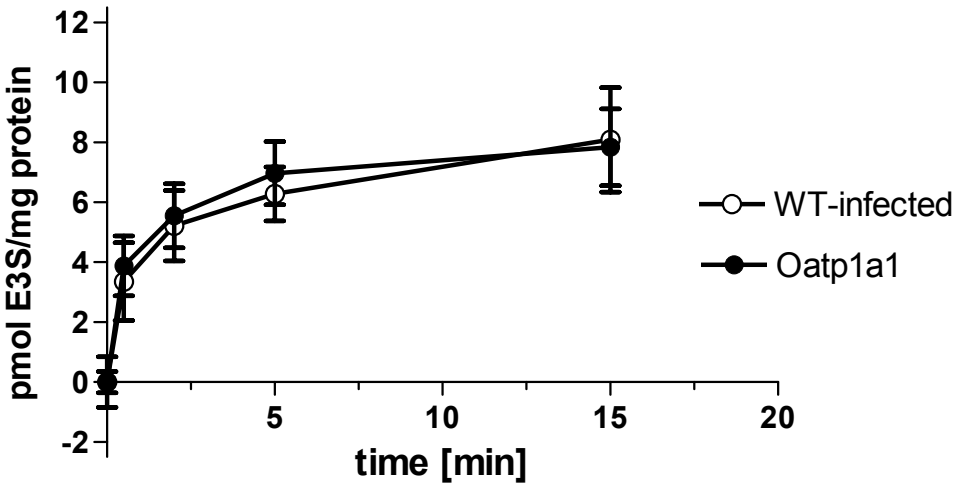

Fig. 4

Time course of estrone-3-sulfate transport into membrane vesicles isolated from Oatp1a1-expressing (●) and WT-infected (○) Sf9 cells I Transport of [^{3}H]-estrone-3-sulfate (0.5 μmol/L) was determined at pHi/pHo 6.0/7.5 as described in Material and Methods. Data represent the means ± SD of triplicate determinations of two separate membrane preparations.

Ntcp expression and functional characterization in Sf9 insect cells I As described for Oatp1a1 baculovirus, routine infection was optimized beforehand, determining lowest MOI which leads to roughly constant Ntcp expression levels after 3 days of infection. Infection was accomplished routinely at 20 MOI. Expression of the cotransporter Ntcp in Sf9 cells was first analyzed by immunoblotting. With the Ntcp antiserum proteins of approximately 30-35 kDa and ~55 kDa, respectively, were detected (Fig 5). Several weak bands were observed with WT-infected Sf9 cells, likely originating from Sf9 cell proteins, which are bound unspecifically by the polyclonal anti-Ntcp antibody.

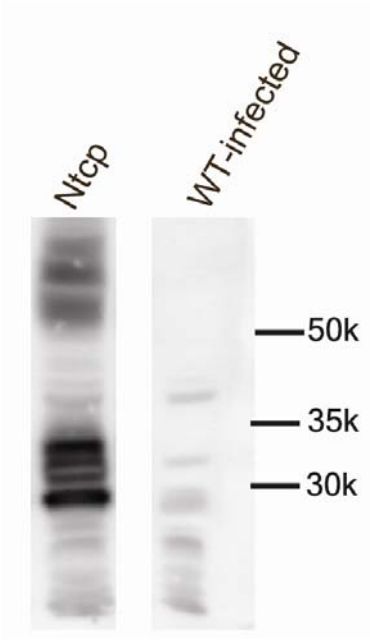

Fig. 5

Expression of Ntcp in baculovirus-infected Sf9 insect cells I Western blot analysis of membrane vesicles isolated from Ntcp-expressing and WT-infected Sf9 cells (70μg of protein/lane). Sf9 cells were infected with Ntcp recombinant baculovirus at a MOI of 20 and WT-infected Sf9 cells at a MOI 5, both for 3 days.

In order to determine if Ntcp, when expressed in Sf9 cells, is functional, i.e. stimulates TC transport sodium-dependently, transport studies were carried out in Sf9 cells as well as in membrane vesicles isolated from Ntcp-expressing Sf9 cells. As illustrated in Fig. 6 Ntcp-expressing Sf9 cells exhibit a dramatically elevated level of TC. In the presence of sodium TC uptake was stimulated 26-fold. Without sodium no TC was incorporated in the cells, as also seen in WT-infected control cells, suggesting no endogenous Na^+-dependent TC transporter in Sf9 cells.

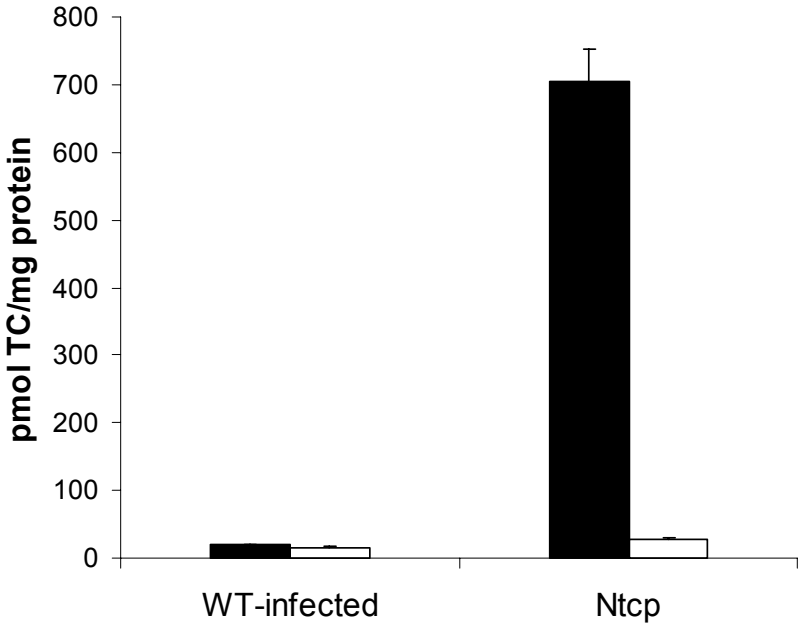

Fig. 6

Ntcp expressed in Sf9 cells mediates taurocholate uptake in a sodium-dependent manner I Transport of [^{3}H]-taurocholate (10μmol/l) was determined in Ntcp-expressing and WT-infected cells 3 days after infection at 25°C for 15 min either in the presence (filled bars) or in the absence (open bars) of sodium. Data are given as the mean ± SE of triplicate determinations from one single infection.

Functional characterization of Ntcp in Sf9 membrane vesicles I As illustrated in Fig. 7A, Ntcp Sf9 membrane vesicles demonstrate clearly higher TC uptake in the presence of sodium than in its absence; however, to a lower extent than first shown with Ntcp-expressing Sf9 cells. After reaching a peak, TC transport reverses slowly coming to equilibrium after 60 min. At this point, endogenous TC uptake in the absence of sodium and the TC uptake in the presence of sodium are at equilibrium across the vesicle membrane. The value is higher than the initial value but lower than the peak. In comparison vesicles of WT-infected Sf9 cells do not show a sodium-dependent TC transport confirming the lack of an endogenous sodium-dependent TC transporter in Sf9 cells (Fig. 7B).

Taken together transport studies in cells and membrane vesicles displayed Ntcp functionality in the Sf9 expression system. Sf9 membrane vesicles with operating Na^+/TC cotransporter were thereupon used as starting material for solubilization.

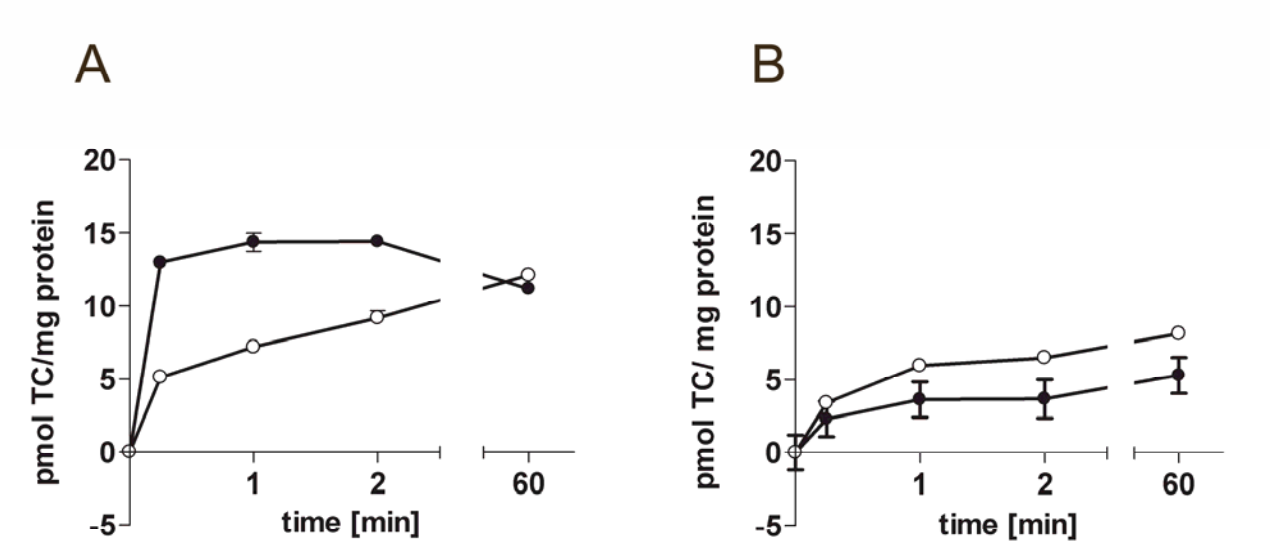

Fig. 7

Sodium-dependent time course of taurocholate transport into membrane vesicles isolated from Ntcp-expressing (A) and WT-infected (B) Sf9 cells I Transport of [^{3}H]-taurocholate (1μmol/l) in the presence (●) and absence (○) of sodium was performed as described in the Material and Methods section. Data represent the means ± SE of triplicate determinations of two separate membrane preparations. The control experiment with WT-infected Sf9 vesicles was performed with three determinations of one membrane preparation. Some variability is smaller than the symbols.

Detergent solubilization of Ntcp Sf9 membrane vesicles I Detergents are central to the isolation and solubilization of membrane proteins and the selection of a suitable detergent(s) is an important aspect of successful functional membrane solubilization and possible future purification. The choice of detergents was motivated by differences in head groups and hydrophobic regions. With the choice three main classes of detergents were covered. The non-ionic sugar-based detergents DDM and OG, the zwitterionic detergent CHAPS and FOS-choline-16, which is lipid-like, were used. Non-ionic detergents have been described as mild and

non-denaturing, but with short chains deactivation might occur. Zwitterionic detergents are generally more deactivating, for structural studies; however, they are commonly used [31].

After the provided functionality of Ntcp in Sf9 membrane vesicles the latter were used for direct solubilization. In order to compare the differences of each detergent, identical amounts of membrane vesicles were utilized. Complete and stable solubilization of membrane proteins generally occurs above the detergent critical micelle concentration (CMC). Here, we tested the solubilization of 2 mg of total membrane protein with the four detergents at concentrations specified in Table 1. 1% CHAPS was included in our studies with reference to Keller and co-workers, who used the zwitterionic detergent for solubilization and further purification of human OCT1 (*SLC22A1*) [32].

Table 1

CMC and concentrations of detergents used for the solubilization of Ntcp Sf9 membrane vesicles

	CMC (w/v)	concentrations used	in % (w/v)
FOS-16	0.00053%	80xCMC	0.4%
		8xCMC	0.04%
DDM	0.0087%	80xCMC	0.7%
		5xCMC	0.04%
OG	0.53%	15xCMC	8%
		5xCMC	2.5%
CHAPS	0.49%	50xCMC	25%
		2xCMC	1%

Solubilization was carried out as described in the Material and Method section. After high-speed centrifugation, the effectiveness of solubilization was analyzed in the supernatants. Using equal volumes of the supernatant (Sol) and of the fraction with insoluble proteins (Insol), Ntcp recovery was determined with Western blot analysis. Fig. 8 gives evidence for 0.4% FOS-16 (upper panel) and 8% OG (lower panel) being most effective in solubilizing Ntcp. For both detergents the fractions of soluble

proteins give clearly darker and bigger bands for Ntcp than found for the neighbouring lane loaded with the fractions of insoluble proteins. Solubilization with the other detergents demonstrated very similar bands for fractions of soluble and insoluble proteins or a weaker signal for Ntcp recovery in the supernatant. So, these results identified two candidate detergents for further characterization of Ntcp.

However, further work with 8% OG for Ntcp solubilization revealed difficulties in its removal with subsequent gel filtration. Detergent originated foam was found in the collected fractions from gel filtration and was still visible after centrifugation to gain proteoliposomes. Incomplete Ntcp reconstitution possibly because of not tight proteoliposomes hindered transport studies (data not shown).

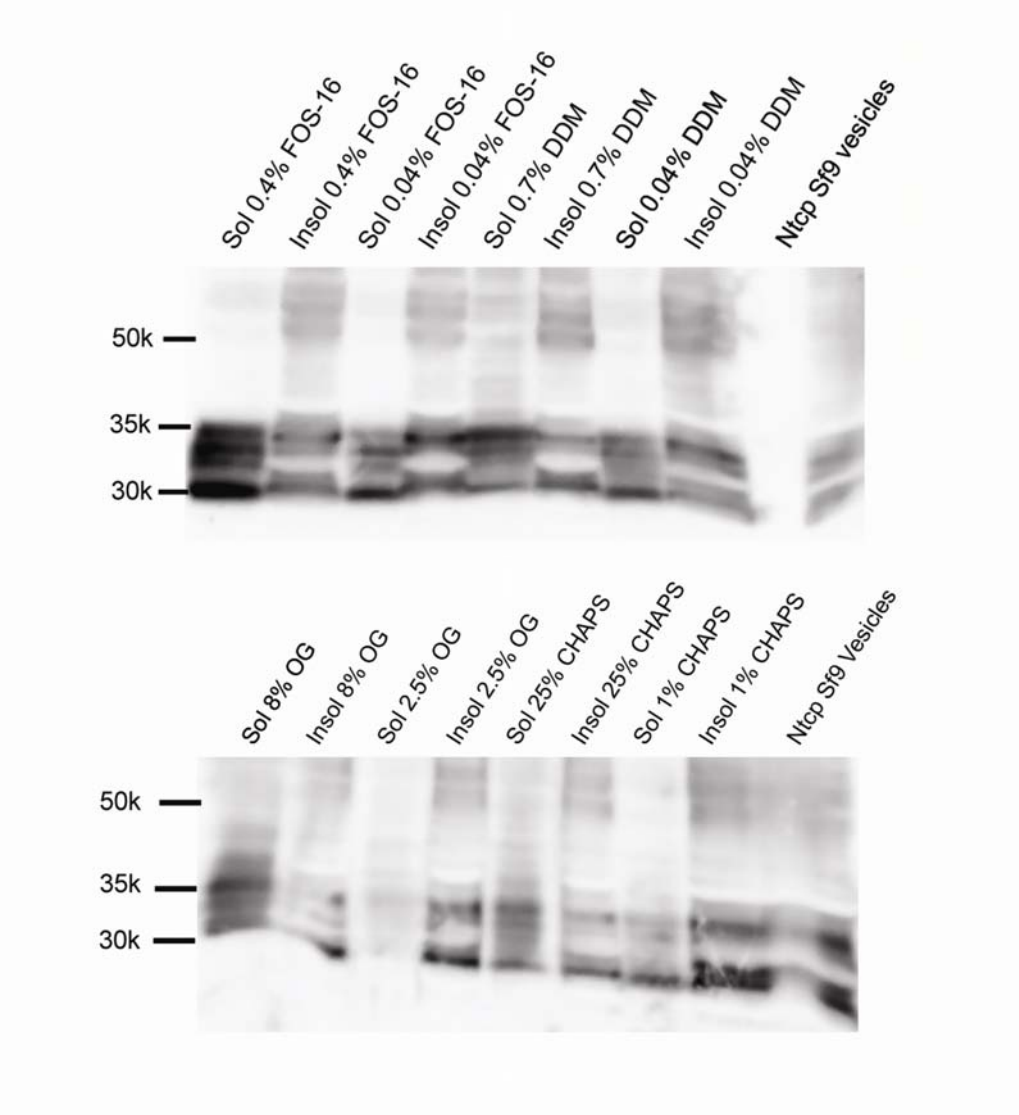

Fig. 8

Solubilization of Ntcp Sf9 membrane vesicles with different detergents I 2 mg of total protein were solubilized as described in Material and Methods in the presence of the detergents indicated, each at concentrations described in Table 1. Identical aliquots of the supernatants with soluble proteins (Sol) and of the resuspended pellets with insoluble proteins (Insol) were probed for Ntcp by Western blotting.

Optimization of Ntcp solubility with FOS-Choline-16 I Further investigation with 0.4% FOS-16 revealed an influence on detergent to membrane protein ratio on Ntcp recovery. An additional screen after solubilizing with 0.4% FOS-16 varying the amount of total protein of Ntcp Sf9 membrane vesicles was performed. Scanning results determining solubilities are shown in Fig. 9. When solubilizing 350 μg per 200 μl, 0.4% FOS-16 dissolves Ntcp most, approximately 54% determined with scanning densiometry. With provided conditions only about 30% of total protein was extracted. After treatment with 0.4% FOS-16 the yield in solubilization of total protein was only 20% for 600 μg and 15% for 850 μg of Ntcp Sf9 membrane vesicles. Consequently, further solubilization was carried out with 350 μg per 200μl, which comes to 1.8 mg of total protein of Ntcp vesicles per ml solubilization reaction. The resulting supernatant containing Ntcp was then subjected to reconstitution.

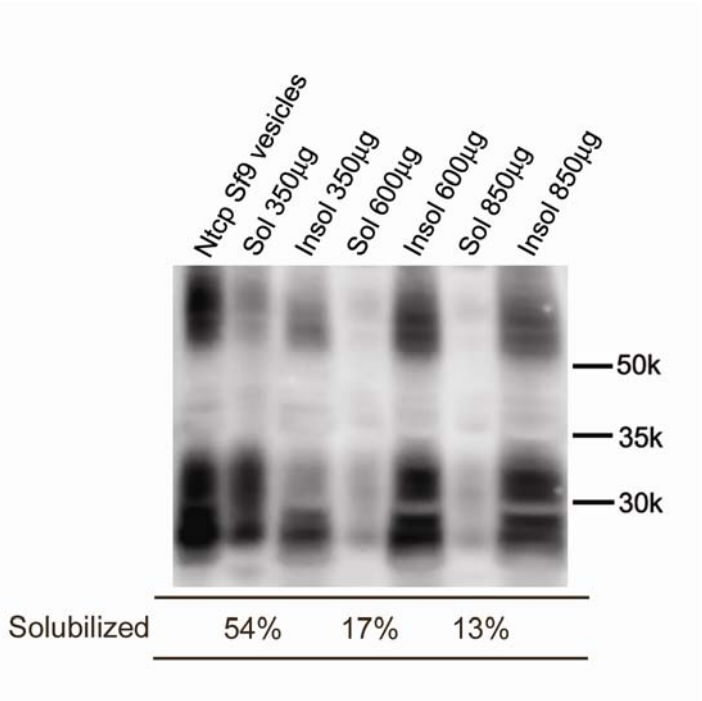

Fig. 9

Optimization of solubilization of Ntcp Sf9 membrane vesicles with 0.4% FOS-choline-16 at different detergent/membrane protein ratios I Total protein amount, indicated in μg, was solubilized in 200 μl as described in Material and Methods. Identical aliquots of the fractions with soluble and insoluble proteins were probed for Ntcp by Western blotting. The first lane was loaded with Ntcp Sf9 membranes (50 μg of total protein). Scanning densiometry was performed on a KODAK Image station 2000MM analyzer (Eastman Kodak Co., Rochester, NY, USA).

Sodium-dependent taurocholate transport into proteoliposomes containing Ntcp I Besides functional results Fig. 10A shows the assessment of Ntcp in different steps during solubilization and reconstitution of Ntcp with 0.4% FOS-16. Fraction #9 is one of the fractions, which were proceeded with in the pool used for the last high-speed centrifugation step to harvest proteoliposomes. On the other hand a late collected fraction (Fraction #32) was included in the analysis. Fraction #9, the pool #4-15 and prominently proteoliposomes are demonstrated to contain Ntcp as the immunoreactive pattern of Ntcp is identical to the pattern observed in Ntcp Sf9 membrane vesicles.

Functional studies with 1 μM TC, determined with the freshly resuspended pellet containing Ntcp proteoliposomes, are given in Fig 10B. At both time points investigated sodium-dependent TC transport is demonstrated. After 5 min a 1.7- fold signal for TC uptake is found. At 10 min only 1.2-fold more TC is accumulated in the presence of sodium than in its absence. Adjusting the transport conditions to shorter time points and augmentation of TC concentration from 1μM to 10μM gave results shown in Fig. 11. The insert proves reconstituted Ntcp in the associated Western blot. Sodium-dependent TC uptake was just below 2-fold after 1 min.

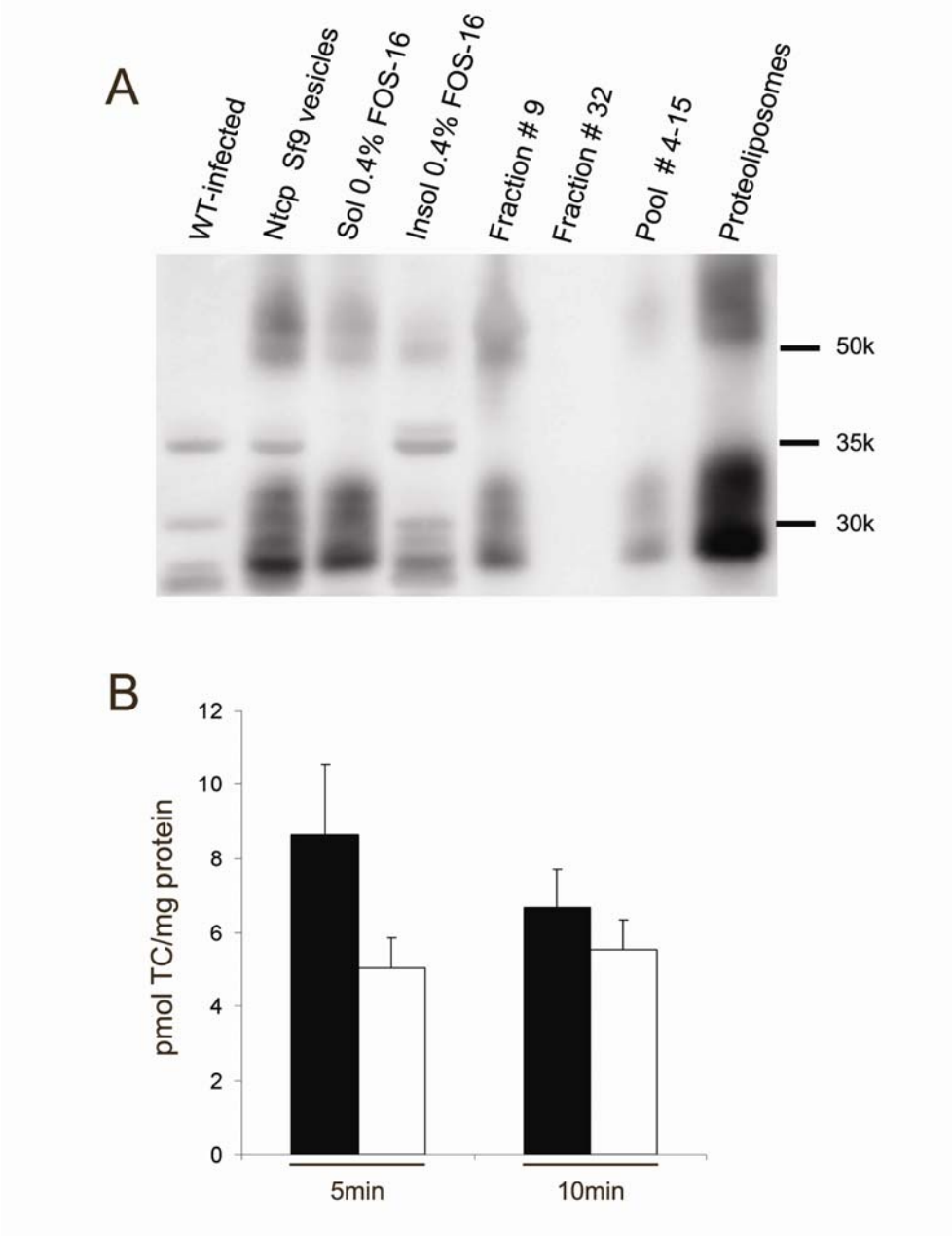

Fig. 10

Western blot analysis of fractions collected during solubilization and reconstitution of Ntcp (A) and sodium-dependent transport of taurocholate into proteoliposomes gained with gel filtration (B) I In (A) Ntcp and WT-infected Sf9 vesicles were used as controls at 50 μg of total protein per lane. Transport of [^{3}H]-taurocholate (1 μmol/l) in the presence (filled bars) and absence (open bars) of sodium was performed as described in the Material and Methods section. Data represent the means ± SE

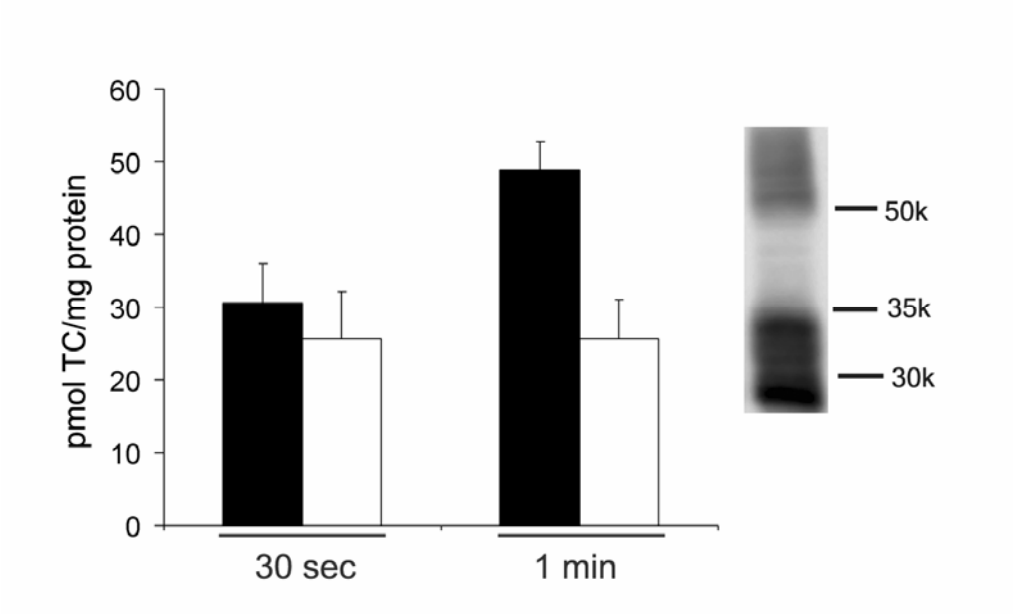

Fig. 11

Sodium-dependent transport of taurocholate into proteoliposomes gained with gel filtration I

Transport of [^{3}H]-taurocholate (10 μmol/l) in the presence (filled bars) and absence (open bars) of sodium was performed as described in the Material and Methods section. Data represent the means ± SE. Insert shows Ntcp determined in proteoliposomes with Western blot analysis.

5.5 Discussion

In the present study a high-level expression system for Oatp1a1 and Ntcp was established. Expression in Sf9 cells was suitable for transport studies with the two membrane transport proteins. Functional prove for Ntcp is obtained not only in Sf9 cells but also in Sf9 membrane vesicles, secondly, suitable conditions were determined for direct solubilization of Ntcp. After solubilization with 0.4% (w/v) of the phospholipid analogue FOS-choline-16, initial attempts demonstrated that it is feasible to functionally reconstitute Ntcp into artificial liposomes.

Both membrane transport proteins Oatp1a1 and Ntcp have been cloned and functionally expressed in *Xenopus laevis* oocytes and in mammalian cell lines [1, 2, 26, 33]. However, they have not been expressed in a system from which they could be readily solubilized. The Sf9 insect cell line is as an expression system preferable to that of a prokaryote such as *Escherichia coli* because it is known that posttranslational modification of proteins is different in a bacterial system than in a eukaryotic expression system [34]. There is evidence that insect cells can perform most of the processing steps occurring in mammalian cells. As a consequence, there is a greater probability that a protein expressed in insect cells will have normal biological activity [35].

Expression of Oatp1a1 and Ntcp in Sf9 cells was monitored by Western blot. Results revealed that protein sizes determined (Fig. 1 and 5) diverge from published molecular weight of 86 kDa (Oatp1a1, [25, 26]) and 51 kDa (Ntcp, [25]) in isolated basolateral rat liver plasma membranes. Besides bands similar to published protein size, additional bands were detected at a lower molecular weight for both proteins. It can be speculated that the discrepancy between the molecular mass of the expressed Oatp1a1 and Ntcp and the mass observed in isolated basolateral rat liver plasma membranes might be explained by the lack of or by an incomplete glycosilation. Under-glycosilation in Sf9 cells has been shown for some transport proteins before. Many transport proteins have been, however, functionally expressed in Sf9 cells: Human and rat MRP1 (previously called MRP) were successfully investigated for substrate specificity in Sf9 cells, although shorter proteins were measured presumably due to lower degree of glycosilation [36]. Under-glycosilation of rabbit Na^+/glucose cotransporter in Sf9 cells was described as well as not critical for function [11].

Concerning Oatp1a1 one study investigated the functional role of *N*-glycosilation in *X. laevis* oocytes [30]. The results suggested that Oatp1a1 is dependent on *N*-glycosilation as function is impaired when expressing Oatp1a1 in *S. serevisiae*, which has limited ability to carry out certain posttranslational modifications, including glycosilation. However, the precise role that glycosilation plays in the functional expression stayed unknown. Deglycosilation experiments done with Ntcp in isolated basolateral rat liver plasma membranes [25] decreased the molecular weight from 51 to 33.5 kDa, which is in agreement with the lower bands found in our immunoblots. We do not know if glycosilation is incomplete or not. Since functional activity in Sf9 cells for both transport proteins can be associated with the respective transporter (Fig. 2, 3 and 6), it is suggested that the conformation of Oatp1a1 and Ntcp in Sf9 cells is similar to that in intact host tissue.

Further functional characterization was carried out with transport studies using Sf9 membrane vesicles expressing Oatp1a1 or Ntcp. An advantage of membrane vesicles to cells is methodically full access to intracellular and extra cellular conditions. Transport studies with pHi>pHo in Oatp1a1 Sf9 membrane vesicles were unexpected (Fig. 4). The inwardly directed H^+-gradient did not activate E3S transport into vesicles, when comparing to endogenous E3S uptake into Sf9 membrane vesicles isolated from WT-infected cells. With this expression system we could not confirm in vesicles what was found in Oatp1a1-expressing HeLa cells, namely the H^+-gradient as a possible driving force [8] of the transport protein. It is possible that after exterior acidification the H^+-gradient was less sustainable with the buffer capacity of membrane vesicles than with viable cells.

In contrast, the activity of Ntcp in Sf9 membrane vesicles could be shown. The Na^+/TC cotransport is reflective for functional activity, known in hepatocytes (Fig. 7) and is reasonable in agreement with former studies carried out with isolated basolateral rat liver membrane vesicles. Within 1 min TC uptake was stimulated 3-5 times [22], while Ntcp Sf9 membrane vesicles incorporated after the same time more than 2 times more TC in the presence of sodium than it its absence. In comparison this sodium-dependent signal is much lower than the signal found in Ntcp-expressing Sf9 cells. In Sf9 cells the accumulation was 26-fold in the presence of sodium. A possible explanation is altered orientation of the cotransporter after isolation of membrane vesicles. Moreover the lack of Na^+/K^+ ATPase after homogenizing and isolating membrane vesicles compared to fully functional cells might have an impact

on stability of the Na^+-gradient applied. Former transport experiments with primary cultured rat hepatocytes [37] compared to studies with isolated basolateral rat liver membrane vesicles [22] displayed a 2-3-fold loss in sodium-dependent TC incorporation. This complies with the loss of TC uptake into Sf9 cells to TC uptake into Sf9 membrane vesicles, both expressing rat Ntcp.

With sodium-dependent TC uptake into Ntcp Sf9 membrane vesicles functionality is provided. Solubilization conditions were established. Detergents from three main classes were used. In a first screen, moderate solubility of Ntcp excluded the sugar-based detergent DDM and CHAPS, a zwitterionic surfactant, from further use (Fig. 8). Subsequent studies with the second sugar-based detergent OG revealed its impracticality. Removal of OG was incomplete after detergent dilution and subsequent gel filtration. Optimal solubilization conditions with 0.4% FOS-choline-16 turned out to be at 1.8 mg protein of membrane vesicles/ml.

In order to evidence solubilization of functionally active Ntcp, reconstitution into artificial liposomes was carried out promptly. Throughout solubilization and subsequent reconstitution Ntcp was monitored by Western blot analysis. The determined protein pattern of reconstituted Ntcp (Fig. 10A) was as shown before in Ntcp Sf9 membrane vesicles, implying neither degradation nor any harsh impact on the cotransporter during isolation. It was more crucial to demonstrate functionality. Since 1μM TC transport after 5 min was higher in the presence of sodium than in its absence, reconstituted Ntcp reveals functional activity. The signal at a later time point, namely 10 min, is moderate (Fig. 10B).

Using our reconstitution system, the orientation in the proteoliposomes has not been defined. To overcome possible forfeit of outside-in Ntcp and in order to aim at a better TC signal, 10 times higher concentration of TC was used for uptake studies into proteoliposomes. 10μM is still below the published Km value for TC mediated by rat Ntcp. The Km has been consistently determined at 25 μM, in *X. laevis* oocytes [33], in hepatocytes [38] as well as in isolated basolateral rat liver plasma membrane vesicles [22]. After 1 min the highest sodium-dependent TC uptake was determined. This signal of reconstituted and functional active Ntcp is in the same range as was found for Ntcp Sf9 membrane vesicles. As it may be, it is the qualitative similarity between native Ntcp in Sf9 vesicles and reconstituted Ntcp transport properties

rather than the quantitative increase in specific transport activity that essentially proves transport function of Ntcp.

The research presented provides results on functional expression and isolation of Ntcp from its lipidic environment using the baculovirus/Sf9 cell-based expression system. Furthermore Ntcp was reconstituted into an analogous milieu that mimics the lipid bilayer; where Na^+/ TC cotransport was proven.
This system will be useful for future studies aimed at structural determinations. The method of reconstitution will serve for purification and will be of use to monitor the transport activity of Ntcp during each step of purification. Future isolation of purified Ntcp will enable analyses required to investigate the transport-active form of Ntcp. In case of clarity upon driving force(s) of Oatps/OATPs these procedures established should be useful for isolating members of the OATP superfamily.

5.6 References

1. Schroeder, A., et al., *Substrate specificity of the rat liver Na(+)-bile salt cotransporter in Xenopus laevis oocytes and in CHO cells.* Am J Physiol, 1998. 274(2 Pt 1): p. G370-5.
2. Jacquemin, E., et al., *Expression cloning of a rat liver Na(+)-independent organic anion transporter.* Proc Natl Acad Sci U S A, 1994. 91(1): p. 133-7.
3. Shi, X., et al., *Stable inducible expression of a functional rat liver organic anion transport protein in HeLa cells.* J Biol Chem, 1995. 270(43): p. 25591-5.
4. Li, L., et al., *Identification of glutathione as a driving force and leukotriene C4 as a substrate for oatp1, the hepatic sinusoidal organic solute transporter.* J Biol Chem, 1998. 273(26): p. 16184-91.
5. Marin, J.J., et al., *Sensitivity of bile acid transport by organic anion-transporting polypeptides to intracellular pH.* Biochim Biophys Acta, 2003. 1611(1-2): p. 249-57.
6. Kobayashi, D., et al., *Involvement of human organic anion transporting polypeptide OATP-B (SLC21A9) in pH-dependent transport across intestinal apical membrane.* J Pharmacol Exp Ther, 2003. 306(2): p. 703-8.
7. Nozawa, T., et al., *Functional characterization of pH-sensitive organic anion transporting polypeptide OATP-B in human.* J Pharmacol Exp Ther, 2004. 308(2): p. 438-45.
8. Satlin, L.M., V. Amin, and A.W. Wolkoff, *Organic anion transporting polypeptide mediates organic anion/HCO3- exchange.* J Biol Chem, 1997. 272(42): p. 26340-5.
9. Weinman, S.A., M.W. Carruth, and P.A. Dawson, *Bile acid uptake via the human apical sodium-bile acid cotransporter is electrogenic.* J Biol Chem, 1998. 273(52): p. 34691-5.
10. Hagenbuch, B., B.F. Scharschmidt, and P.J. Meier, *Effect of antisense oligonucleotides on the expression of hepatocellular bile acid and organic anion uptake systems in Xenopus laevis oocytes.* Biochem J, 1996. 316 (Pt 3): p. 901-4.
11. Smith, C.D., B.A. Hirayama, and E.M. Wright, *Baculovirus-mediated expression of the Na+/glucose cotransporter in Sf9 cells.* Biochim Biophys Acta, 1992. 1104(1): p. 151-9.
12. Fucentese, M., et al., *Functional expression and purification of histidine-tagged rat renal Na/Phosphate (NaPi-2) and Na/Sulfate (NaSi-1) cotransporters.* J Membr Biol, 1997. 160(2): p. 111-7.
13. Akita, H., et al., *Transport activity of human MRP3 expressed in Sf9 cells: comparative studies with rat MRP3.* Pharm Res, 2002. 19(1): p. 34-41.
14. Masereeuw, R., et al., *Impaired renal secretion of substrates for the multidrug resistance protein 2 in mutant transport-deficient (TR-) rats.* J Am Soc Nephrol, 2003. 14(11): p. 2741-9.
15. Saito, H., et al., *A new strategy of high-speed screening and quantitative structure-activity relationship analysis to evaluate human ATP-binding cassette transporter ABCG2-drug interactions.* J Pharmacol Exp Ther, 2006. 317(3): p. 1114-24.
16. Hjelmeland, L.M. and A. Chrambach, *Solubilization of functional membrane proteins.* Methods Enzymol, 1984. 104: p. 305-18.
17. Hjelmeland, L.M., *Solubilization of native membrane proteins.* Methods Enzymol, 1990. 182: p. 253-64.
18. Jones, M.N., *Surfactants in membrane solubilisation.* Int J Pharm, 1999. 177(2): p. 137-59.
19. Mosmann, T., *Rapid colorimetric assay for cellular growth and survival: application to proliferation and cytotoxicity assays.* J Immunol Methods, 1983. 65(1-2): p. 55-63.
20. Smith, P.K., et al., *Measurement of protein using bicinchoninic acid.* Anal Biochem, 1985. 150(1): p. 76-85.
21. Gerloff, T., et al., *The sister of P-glycoprotein represents the canalicular bile salt export pump of mammalian liver.* J Biol Chem, 1998. 273(16): p. 10046-50.
22. Zimmerli, B., J. Valantinas, and P.J. Meier, *Multispecificity of Na+-dependent taurocholate uptake in basolateral (sinusoidal) rat liver plasma membrane vesicles.* J Pharmacol Exp Ther, 1989. 250(1): p. 301-8.
23. Laemmli, U.K., *Cleavage of structural proteins during the assembly of the head of bacteriophage T4.* Nature, 1970. 227(5259): p. 680-5.
24. Roman, L.M. and A.L. Hubbard, *A domain-specific marker for the hepatocyte plasma membrane: localization of leucine aminopeptidase to the bile canalicular domain.* J Cell Biol, 1983. 96(6): p. 1548-58.
25. Stieger, B., et al., *In situ localization of the hepatocytic Na+/Taurocholate cotransporting polypeptide in rat liver.* Gastroenterology, 1994. 107(6): p. 1781-7.

26. Eckhardt, U., et al., *Polyspecific substrate uptake by the hepatic organic anion transporter Oatp1 in stably transfected CHO cells.* Am J Physiol, 1999. 276(4 Pt 1): p. G1037-42.
27. Meier, P.J., et al., *Structural and functional polarity of canalicular and basolateral plasma membrane vesicles isolated in high yield from rat liver.* J Cell Biol, 1984. 98(3): p. 991-1000.
28. Quick, M. and E.M. Wright, *Employing Escherichia coli to functionally express, purify, and characterize a human transporter.* Proc Natl Acad Sci U S A, 2002. 99(13): p. 8597-601.
29. Panayotova-Heiermann, M., et al., *Purification and functional reconstitution of a truncated human Na(+)/glucose cotransporter (SGLT1) expressed in E. coli.* FEBS Lett, 1999. 459(3): p. 386-90.
30. Lee, T.K., et al., *N-glycosylation controls functional activity of Oatp1, an organic anion transporter.* Am J Physiol Gastrointest Liver Physiol, 2003. 285(2): p. G371-81.
31. Seddon, A.M., P. Curnow, and P.J. Booth, *Membrane proteins, lipids and detergents: not just a soap opera.* Biochim Biophys Acta, 2004. 1666(1-2): p. 105-17.
32. Keller, T., et al., *Purification and functional reconstitution of the rat organic cation transporter OCT1.* Biochemistry, 2005. 44(36): p. 12253-63.
33. Hagenbuch, B., et al., *Functional expression cloning and characterization of the hepatocyte Na+/bile acid cotransport system.* Proc Natl Acad Sci U S A, 1991. 88(23): p. 10629-33.
34. Luckow, V.A. and M.D. Summers, *Signals important for high-level expression of foreign genes in Autographa californica nuclear polyhedrosis virus expression vectors.* Virology, 1988. 167(1): p. 56-71.
35. Altmann, F., et al., *Insect cells as hosts for the expression of recombinant glycoproteins.* Glycoconj J, 1999. 16(2): p. 109-23.
36. Bakos, E., et al., *Membrane topology and glycosylation of the human multidrug resistance-associated protein.* J Biol Chem, 1996. 271(21): p. 12322-6.
37. Rippin, S.J., et al., *Cholestatic expression pattern of sinusoidal and canalicular organic anion transport systems in primary cultured rat hepatocytes.* Hepatology, 2001. 33(4): p. 776-82.
38. Frimmer, M. and K. Ziegler, *The transport of bile acids in liver cells.* Biochim Biophys Acta, 1988. 947(1): p. 75-99.

CHAPTER 6

General Discussion and Perspectives

Studies with individual members of the OATP superfamily have concentrated on aspects of their multispecificity, i.e. the apparent affinity constants (Km) and *cis*-inhibition pattern of different endogenous and exogenous substrates. The remarkably extensive work done with OATP1 family members led to the investigations in line with this PhD thesis. Functional determinants for transport activity of members of the OATP1 family have been outlined.

In our first study we examined an evolutionarily ancient Oatp found in skate liver, Oatp1d1 [1]. It was of interest to examine whether Oatp1d1 as an evolutionary precursor shares transport of the toxins phalloidin and microcystin with mammalian liver Oatps/OATPs. Oatp1d1 indeed mirrors the toxin transport properties of the more evolved mammalian Oatps/OATPs. The closest mammalian Oatp1d1 orthologue OATP1C1 did not share the phalloidin transport activity. The two transporting polypeptides exhibit only 50.4% amino acid sequence identity, which in this case is assumed to be not sufficient for comparable substrate specificity.

It remains to be investigated also with closer related orthologs and/or paralogs whether there are evolutionarily conserved structural determinants that account for overlapping substrate profiles. Meier-Abt et al identified novel Oatps in other evolutionarily ancient animals with database search [2]. Oatps have been identified in zebra fish, frog, fruit fly and worm; all these animals are in representative positions in animal evolution and their genomes have been fully sequenced. In assumption of their future expression cloning, these less evolved Oatps could be used in comparative functional genomic studies with well-investigated more evolved Oatps/OATPs.

In connection with the characterization of Oatp1d1 two aspects of importance for future functional characterization of Oatps/OATPs have to be addressed: In this first study inhibition studies with common Oatp/OATP-substrates were carried out with isolated skate hepatocytes expressing Oatp1d1. Such experiments address the great interest in specific inhibitors for transport proteins such as Oatps/OATPs. Screening experiments on a large scale would possibly succeed in identification of specific inhibitors. Such specific inhibitors would ease matters for further more detailed functional characterization in cells where multiple Oatps/OATPs are expressed. Moreover, such inhibitors could be developed into drugs to treat toxin-induced liver injury.

The second aspect addresses substrates ideal for functional characterization. Other exogenous or endogenous compounds of the multispecific Oatps/OATPs than toxins would be preferable for possible future comparative transport studies. Research work with the toxins such as microcystin used as a substrate turned out not to be very practical, as they are toxic for amphibian and mammalian cells required for transport studies. As many Oatps/OATPs are found to be low affinity toxin transporters, see Table below (for references see Introduction Chapter 1, Table 1), it is necessary to work with higher concentrations, which in turn leads to severe cytotoxic effects.
Either way Oatp/OATP-mediated toxin transport could be demonstrated for various members of the OATP1 family. Substrate specificity includes ochratoxin A, α-amanitin, phalloidin and microcystin.

Apparent affinity for toxins of OATP1 family members

Oatp/OATP	Toxin	Km [μM]
Oatp1a1	Ochratoxin A	17-29
OATP1A2	Microcystin	20
Oatp1a3	Ochratoxin A	6-17
Oatp1B1	Microcystin Phalloidin	7 17-39
Oatp1b2	Microcystin	6
Oatp1B1	Microcystin Phalloidin α-Amanitin	4 8 9

The fact that OATP1 family members transport several toxins suggest a certain physiological role, namely their involvement in elimination and detoxification processes in the tissues where they are expressed.

The interest for more comparative functional genomics in assessing important structural determinants among the OATP superfamily underlies the second study. In comparison to skate Oatp1d1 and human OATP1C1 with 50.4% amino acid sequence identity, the two rat paralogs, Oatp1a4 and Oatp1a1, exhibit more than 77% amino acid sequence identity. They clearly show different substrate specificity regarding digoxin transport. On this basis chimeric constructs and single Oatp1a4 mutants were generated. Three amino acids were identified in Oatp1a4 with this

approach. When mutated to amino acids of Oatp1a1, digoxin and overall Oatp1a4-mediated transport properties were affected. Kinetics for Digoxin and DPDPE investigated was altered with decreased apparent affinities (Km). The underlying mechanism for these results remains unclear. We do not know whether the conformation of the transporting polypeptide changed or whether the amino acids are directly involved in substrate binding. The theoretical model of human OATP1B3 as generated by Meier-Abt and co-workers [2] bears novel questions. Some conserved amino acid residues have been postulated to be exposed to the pore (i.e. solvent-exposed and responsible for the positive potential) others to be buried in the model. Moreover, conserved amino acids have been identified as being involved in hydrogen-bonds conserved throughout the OATP1 family. And several amino acid residues were localized in the theoretical model in positions necessary for breaks and bends of the TMHs. Taken together site-directed mutagenesis and functional characterization of the residues in question would provide further information on the exact role of these amino acid residues. As a theoretical model was generated with human OATP1B3, the track could be followed with this human liver OATP. Of course, a chimera approach would be applicable onto other closely related Oatps/OATPs which exhibit differences in substrate specificity.

For complete molecular description of function and of the transport mechanism(s) further work is necessary. Functional experiments with site-directed mutagenesis of critical residues are one approach. On the other hand, functional isolation of the purified transport protein would enable biophysical studies, e.g. to determine the oligomeric state, and would be a first step towards determining protein structure. Initial work towards the isolation of a membrane transport protein were carried out in our third investigation with Oatp1a1 and Ntcp. The initial knowledge with reference to transport mechanism for Oatp1a1 and Ntcp was, however, not comparable. Transport mode of Oatps/OATPs has not been fully described. Using the baculovirus/Sf9-cell based expression system a possible pH-gradient dependent transport mode of Oatp1a1 was pursued. Studies with Oatp1a1 Sf9 membrane vesicles, however, were without success, because measured transport was not different from WT Sf9 membrane vesicles. We included Ntcp in this study, as the transport mode is clearly described as a Na^+/bile salt cotransport. With the established expression system it was feasible to determine optimal solubilization

conditions for functional Ntcp. Further reconstitution into artificial liposomes enabled proves of the transport-competent conformation of Ntcp.

So, first steps were undertaken for isolation of a mammalian membrane transport protein. A necessity for subsequent steps would be scaling up the amount of solubilized Ntcp. Crystallization requires pure protein in the range of mg amounts. After direct solubilization of Ntcp-expressing Sf9 membrane vesicles pure protein could be obtained with a high affinity ideally monoclonal antibody. Otherwise tagged Ntcp-constructs, e.g. His-tagged Ntcp, would facilitate later purification with metal-affinity chromatography.

Despite the novel insights into structure-function relationship of Oatps/OATPs outlined above, there are still open questions in relation to more complete understanding of Oatps/OATPs.

Firstly, with reference to the role of membrane transport proteins in drug disposition the functional and physiological importance of Oatps/OATPs is still to be described in more detail. Investigations should include profound determination of tissue distribution and detailed functional characterization. A big aid would be the determination of specific Oatps/OATPs inhibitors. Taken together this might lead to understanding the clinical importance of Oatp/OATPs.

Secondly, concerning the molecular description of Oatps/OATPs knowledge is still scarce. The detailed 3D-structure of Oatps/OATPs is not solved up to date. Crystallographic structure determinations of mammalian membrane proteins are rare and difficult to obtain. Several procedures are available, though. They allow at least partial prediction of the protein structure. These methods include computational analysis or NMR investigations of soluble domains of Oatps/OATPs. In addition, aggregates and clusters, which are formed in the plasma membrane with Oatps/OATPs are highly overexpressed in mammalian cells, could help to clarify the protein structure using electron microscopy or 2D crystallography.

References

1. Cai, S.Y., et al., *An evolutionarily ancient Oatp: insights into conserved functional domains of these proteins.* Am J Physiol Gastrointest Liver Physiol, 2002. 282(4): p. G702-10.
2. Meier-Abt, F., Y. Mokrab, and K. Mizuguchi, *Organic anion transporting polypeptides of the OATP/SLCO superfamily: identification of new members in nonmammalian species, comparative modeling and a potential transport mode.* J Membr Biol, 2005. 208(3): p. 213-27.

I would like to thank Prof. Markus Grütter for engaging me as an external PhD student at the Department of Biochemistry. I appreciated his interest in my work, his encouraging guidance and support, especially during my last years.
The collaboration awakened my interest for structural approaches in biochemistry, focusing on protein crystallography, and broadened considerably my knowledge in biochemistry.

I am very grateful to Prof. Peter Meier-Abt who gave me the possibility to do my PhD thesis in the interdisciplinary context of the Division of Clinical Pharmacology and Toxicology. I appreciated him introducing me into an exciting field and I greatly benefited from his expertise.

Special thanks go to Prof. Bruno Stieger being of constancy during the entire time of my thesis work. His help in setting up new laboratory techniques and valuable methodical suggestions helped to accomplish my studies. I am very thankful for his sustained interest and his critical remarks during the writing of this manuscript.

I greatly value Prof. Raimund Dutzler's acceptance of being co-examiner. My thanks also go to Prof. Gerd Kullak-Ublick, the clinical director of the Division of Clinical Pharmacology and Toxicology now, who gave me the possibility to finalise my research work.

I owe particular thanks to Prof. Bruno Hagenbuch for his supervision during the first years of my PhD thesis. I thank him for having introduced me to work within the pleasant and stimulating atmosphere of SHO2. I enjoyed the steady exchange, the enriching discussions and I thank him for the ongoing support, also morally, - this across the big pond during the last two years.

Likewise, I would like to express my thanks to many former members of our research group. In kind memories, I think of joyful lunch breaks with Carmen, Anne, Emanuel and Isabel. The immense moral support from Simi with her never-ending high spirits meant a lot to me - including all these chatty and fun conversations together with Melissa in the office of SHO2. Additional thanks go to Melissa for reading carefully parts of my manuscript

Of course, I thank all the current members of the group, bringing in a very cheerful and pleasant atmosphere. Particularly: Christelle, Krasimira, Danielle and Stéphi in SHO2. Stéphi and Danielle I thank very much for being of constant support throughout my thesis and for introducing me to many lab techniques I have applied during my studies. I thank Uta for her many advices, support and fun chats in between. I am grateful for Jyrki's help, as a source of advice during writing my manuscript.

All non-explicitly mentioned former and current members, also from the clinical group of our department, I thank for being around and for support in many different ways.

I express my sincere thanks to my parents, who supported me with understanding and encouragement throughout the years. The fact that I can always count on them is of immense value to me. My (girl-) friends in and around Zurich were a big moral support, being there for joyful evenings and fruitful discussions, glasses of wine and motivating words, with (and without scientific content). It was precious to me and a great back up!

My most deep thanks go to Georg, my dear husband, who supported me in every single way and is a never ending source of patience, strength, humour and joy. Thanks a thousand!

since 2003-Nov	**PhD thesis** Division of Clinical Pharmacology and Toxicology, University Hospital Zurich, Prof. Dr. P. Meier-Abt (since 9/2006 Prof. Dr. G. Kullak-Ublick) External PhD student at the University of Zurich, Department of Biochemistry, Prof. M. Grütter
2003	**Employment** as a pharmacist, Morgental Apotheke, Zürich-Wollishofen, substitution as a part-time pharmacist until 12/2006
2002-Dec	**Graduation** as a federal qualified pharmacist (Eidg. Staatsexamen)
2000	4 months practical training, Technical Research and Development, Novartis Pharma AG, Basel
1998-1999	compulsory practical training Rosen Apotheke, Basel Hospital pharmacy, Inselspital, Bern
1996-2002	**Studies of pharmacy** Pharmacenter, University of Basel **Diploma thesis** Department of Clinical Pharmacology, University of Basel Prof. Dr. S. Krähenbühl „Toxicity of Benzarone/Benzbromarone and Analogues on Isolated Rat Liver Mitochondria”
1995-Dec	**Matura** (Typus B, Latin) Gymnasium Oberwil, Baselland, Switzerland
1983-1995	Schools in Baselland, Switzerland
1980-1983	Deutsche Schule, Durban, South Africa
1976	**Born** 13th of August 1976 in Basel, Switzerland

Publications

F. Meier-Abt*, **A. Hammann-Hänni***, B. Stieger, N. Ballatori and J.L. Boyer
The Organic Anion Tranport Polypeptide 1d1 (Oatp1d1) Mediates Hepatocellular Uptake of Phalloidin and Microcystin into Skate Liver; Toxicology and Applied Pharmacology 218 (2007): 274-79
*) These authors contributed equally to this work

P. Kaufmann, M. Török, **A. Hänni**, P. Roberts, R. Gasser and S. Krähenbühl; Mechanisms of Benzarone and Benzbromarone-induced Hepatic Toxicity; Hepatology; 2005, April, 41 (4): 925-35

Posters

Pharma-Posterday, 20th September 2007, Campus Irchel, Zurich

3rd Symposium of the Zurich Center for Integrative Human Physiology, 31st August 2007, University Hospital Zurich

Biomedical Transporters 2007, 12th – 16th August 2007, Berne

5th Day of Clincal Research, 23th-24th March 2006, ZKF, University Hospital Zurich

Biomedical Transporters 2005, 14th – 18th August 2005, St. Gallen

Pharma-Day '05,10th-11th March 2005, Pharmacenter Basel-Zürich, University of Basel

Oral Presentation

The Organic Anion Transport Polypeptide 1d1 (Oatp1d1) Mediates Hepatocellular Uptake of Phalloidin and Microcystin into Skate Liver

6th annual Meeting of the center for Xenobiotic and
Environmental Risk Reasearch (XERR), 24th November 2005,
University of Zurich, Irchel Campus